Evaluation of Erosion and Sediment Control Technologies and Development of Design Tools

by

Caroline Grace Harrison

A thesis submitted to the Graduate Faculty of
Auburn University
in partial fulfillment of the
requirements for the Degree of
Master of Science

Auburn, Alabama
August 8, 2026

Keywords: Floating Surface Skimmer, Roadside Channel Stabilization, Sediment Control, Erosion Control, Construction Stormwater

Approved by

Michael A. Perez, Chair, Associate Professor of Civil and Environmental Engineering
Wesley N. Donald, Research Fellow of Civil and Environmental Engineering
Jack Montgomery, Associate Professor of Civil and Environmental Engineering

Abstract

The rise in urbanization has increased pollutant loading in vulnerable receiving water bodies, attributable to impervious surfaces and construction sites. Impervious surfaces increase runoff volume and velocity and promote the accumulation of pollutants in stormwater runoff. Likewise, earthmoving activities across construction sites leave bare soil susceptible to erosive forces. Under the United States Environmental Protection Agency's National Pollutant Discharge Elimination System (NPDES), stormwater control measures can be used for both active construction and post-construction applications through the Construction General Permit and municipal separate storm sewer system permit. With these, the use of stormwater control measures is necessary to manage stormwater runoff before it enters waterways.

Sediment basins are used on construction sites to capture and detain sediment-laden runoff, allowing sedimentation to occur. Floating surface skimmers are used to dewater sediment basins by discharging from the water surface, the least turbid section of the water column. There is also an opportunity for their use in post-construction detention basins. Throughout this study, thirteen floating surface skimmers, eight designed for sediment basins and five designed for post-construction detention basins, were evaluated. Testing took place in the skimmer evaluation apparatus at the Auburn University-Stormwater Research Facility. Each skimmer was assessed across several configurations for its hydraulic performance and discharge rates. For each configuration, models were developed using various methods to predict flow rates across depths below 7 ft (2.1 m). The sediment basin skimmers were found to have average flow rates ranging as high as 92,585 ft^3/d (2,622 m^3/d) on the 8 in. (20.3 cm) skimmer set to 100%

open to as low as 981 ft^3/d (28 m^3/d) on the 1.5 in. (3.8 cm) skimmer set to 50% open. Likewise, the maximum observed flow rates for the post-construction skimmers ranged as high as 2.984 ft^3/s (0.085 m^3/s) on the 8 in. (20.3 cm) skimmer, 100% open, unvented configuration, to as low as 0.045 ft^3/s (0.001 m^3/s) on the 1.5 in. (3.8 cm) skimmer, 50% open. Once all flow rate models were developed, two skimmer sizing tools were constructed for the sediment basin skimmers and the post-construction skimmers: an engineer's calculator and an estimator's calculator. The engineer's calculator describes the stage-storage relationship as the skimmer dewaters a given basin. This calculator provides flow rate information and dewatering time. The estimator's calculator provides the user with a skimmer and associated characteristics based on the basin volume and time. The user can enter a known basin volume or calculate volume from geometric parameters.

Roadside conveyance channels are used to direct runoff away from the road's right-of-way and to protect the integrity of the road. Low-volume roads in rural areas often lack adequate stabilization measures, leading to erosion and damage to infrastructure and the surrounding environment. An outline of various channel stabilization practices was developed to provide a foundation for future testing efforts. Design concepts were typically described using the permissible tractive force method, as recommended by leading existing roadside channel design guidance. Stabilization practices highlighted throughout this study include bare channels, grass linings, rolled erosion control products, geosynthetics, riprap, concrete linings, and check dams. Using the design concepts reviewed for each practice, a preliminary draft of a channel stabilization design tool was developed. This design tool consists of two main parts:

determining peak flow rates and designing an appropriate channel armoring practice. Peak flow rates are computed using site-specific characteristics, such as rainfall type and land cover, with the TR-55 method. Designing a channel stabilization practice is based on permissible shear stress concepts. The user may select a bare soil, vegetated lining, vegetated TRM, or unvegetated TRM condition to determine an appropriate stabilization technique using channel geometry parameters.

These findings indicate that hydraulic performance and associated flow rates vary across different skimmer designs and configurations. Thus, users can appropriately size skimmers to meet their needs based on experimental results. Furthermore, design concepts outlined for various roadside channel stabilization measures provide a foundation for future testing efforts and implementable design guidance.

Artificial Intelligence (AI) Use Disclosure

In the preparation of this thesis, the following Artificial Intelligence (AI) tools were used: Grammarly and Microsoft Word. Grammarly was used primarily as a grammar and spelling assistant. Microsoft Word was used to assist in creating alt text for figures. The author acknowledges full responsibility for the intellectual content of this work and has ensured that all AI-assisted sections have been reviewed and revised for accuracy and appropriate academic style. All AI-generated content was reviewed and validated for relevance, appropriateness, and accuracy before incorporation into the final document to maintain scholarly integrity of this research.

Digital Accessibility Use Disclosure Statement

In the preparation of this thesis, the following digital accessibility tools were used to ensure this document complies with federal requirements: AU Libraries' Guide on Digital Accessibility for Theses & Dissertations. The author acknowledges full responsibility for the intellectual content of this work and has made a good faith effort to comply with digital accessibility requirements in publishing, wherein the nature of the content does not significantly change in order to do so. Furthermore, all content has been reviewed and revised to meet these requirements prior to final publication.

Acknowledgments

There are countless people who have supported me throughout my academic journey. I would like to thank my parents, Molly and Blain, who have given me their unwavering support throughout my education and have continued to inspire me to reach where I am today. I also want to thank my sister, Claire, for challenging me and always keeping me entertained. I especially want to thank Aidan, my significant other, for your utmost support and encouragement throughout our time at Auburn. I want to express my gratitude to Dr. Michael Perez and Dr. Wesley Donald, who have been incredible mentors and whose guidance has been invaluable throughout my graduate studies. In addition, I would like to thank Dr. Jack Montgomery for participating in my thesis defense committee. I would also like to thank Justin Lockhart, Jayden Siggers, Guy Savage, and the wonderful group of undergraduate research assistants, without whom this research would not have been completed. Finally, I would like to thank the Auburn Stormwater team for keeping me going and for the lifelong friendships.

Table of Contents

Abstract 2
Artificial Intelligence (AI) Use Disclosure 5
Digital Accessibility Use Disclosure Statement 6
Acknowledgments 7
Table of Contents 8
1 Chapter 1 Introduction 13
1.1 Background 13
1.2 Stormwater Control Measures 14
1.3 Definition and Purpose of Floating Surface Skimmers 16
1.4 Definition and Purpose of Roadside Channel Stabilization 17
1.5 Research Objectives 17
1.6 Expected Outcomes 18
1.7 Organization of Thesis 19
2 Chapter 2 Evaluation of Sediment Basin and Post-Construction Floating Surface Skimmer Flow Rates 21
2.1 Introduction 21
2.2 Literature Review 21
2.2.1 Sediment Basins 22
2.2.2 Sediment Basin Dewatering 23
2.2.3 Floating Surface Skimmers 25
2.2.4 Skimmer Selection and Sizing 27
2.2.5 Post-Construction Detention and Retention Basins 29
2.3 Means and Methods 30
2.3.1 Testing Apparatus 31
2.3.2 Floating Surface Skimmer Apparatus 33
2.3.3 Data Collection 41
2.3.4 Testing Regime 42
2.3.5 Data Analysis Methods 43
2.4 Results and Discussion 55
2.4.1 Sediment Basin Skimmer Results 55
2.4.2 Post-Construction Skimmer Results 67
2.5 Skimmer Sizing Tools 81

2.5.1 Sediment Basin Skimmer Sizing Tool 82
2.5.2 Post-Construction Skimmer Sizing Tool 89
2.6 Floating Surface Skimmer Testing Summary 94
3 Chapter 3 Roadside Channel Stabilization Measures 96
3.1 Introduction 96
3.2 Design of Roadside Channels 96
3.2.1 Flow Conditions and Design Parameters 97
3.2.2 Determining Degree of Erosion Protection 97
3.3 Channel Linings 99
3.3.1 Bare Channels 100
3.3.2 Vegetation 100
3.3.3 Rolled Erosion Control Products 104
3.3.4 Geosynthetics 107
3.3.5 Riprap 108
3.3.6 Gabion Baskets 109
3.3.7 Concrete 109
3.3.8 Articulating Concrete Block Mats 110
3.3.9 Check Dams 110
3.4 Beta Channel Stabilization Design Tool 113
3.5 Summary 119
4 Chapter 4 Conclusions and Recommendations 121
4.1 Introduction 121
4.2 Evaluation of Floating Surface Skimmer Flow Rates 122
4.3 Roadside Channel Stabilization Practices 125
4.4 Expected Benefits and Implementation 127
4.5 Future Research 128
4.6 Conclusions 129
4.7 Acknowledgements 130
5 References 131

List of Tables

Table 2.1 Sediment Basin Skimmer Barrel Specifications.......... 35
Table 2.2 Post-Construction Skimmer Barrel Specifications.......... 37
Table 2.3 Equations used for 8 in. (20.3 cm) Flow vs. Depth Model.......... 59
Table 2.4 Average Flow Rates for Each Skimmer Configuration.......... 60
Table 2.5 Average Flow Rates for Each 8 in. (20.3 cm) Skimmer Configuration Using Method 1 and Method 2.......... 67
Table 2.6 Flow Rate Model Equations on 8 in. (20.3 cm) Skimmer.......... 70
Table 2.7 Flow Rate and Statistical Comparison for Data and Model on 8 in. (20.3 cm) Skimmer.......... 71
Table 2.8 Flow Rate Model Equations on 4 in. (10.2 cm) Skimmer.......... 74
Table 2.9 Flow Rate and Statistical Comparison for Data and Model on 4 in. (10.2 cm) Skimmer.......... 75
Table 2.10 Flow Rate Model Equations on 3 in. (7.6 cm) Skimmer.......... 77
Table 2.11 Flow Rate and Statistical Comparison for Data and Model on 3 in. (7.6 cm) Skimmer.......... 78
Table 2.12 Flow Rate Model Equations on 2 in. (5.1 cm) Skimmer.......... 79
Table 2.13 Flow Rate and Statistical Comparison for Data and Model on 2 in. (5.1 cm) Skimmer.......... 79
Table 2.14 Flow Rate Model Equations on 1.5 in. (3.8 cm) Skimmer.......... 80
Table 2.15 Flow Rate and Statistical Comparison for Data and Model on 1.5 in. (3.8 cm) Skimmer.......... 81

List of Figures

Figure 2.1 Sediment Basin Design Diagram (IECA 2021) 23
Figure 2.2 Common Skimmer Types 26
Figure 2.3 Skimmer Evaluation Tank Schematic (Sharpe 2022) 32
Figure 2.4 Skimmer Evaluation Apparatus Components at AU-SRF 33
Figure 2.5 Example of Skimmer Components 34
Figure 2.6 8 in. (20.3 cm) and 1.5 in. (3.8 cm) Sediment Basin Skimmer Installed in Skimmer Evaluation Apparatus 35
Figure 2.7 Adjustable Slider Configuration Photos on 6 in. (15.2 cm) Skimmer 36
Figure 2.8 3 in. (7.6 cm) Post-Construction Skimmer Installed in the Skimmer Evaluation Tank 38
Figure 2.9 Adjustable Slider Configurations on the 3 in. (7.6 cm) Skimmer 38
Figure 2.10 Removable Plates and Inlet Openings on the 4 in. (10.2 cm) Skimmer 40
Figure 2.11 Photos of 4 in. (10.2 cm) and 8 in. (20.3 cm) Skimmers Vented and Unvented 41
Figure 2.12 Data Collection Components in the Skimmer Evaluation Tank 42
Figure 2.13. Flow Rate vs. Depth: 8 in. (20.3 cm) Skimmer, 100% Open 45
Figure 2.14 Flow Rate vs. Depth Linear Trendlines and Model: 8 in. (20.3 cm) Skimmer; 100% Open 46
Figure 2.15 Flow Rate vs. Depth Models: All 8 in. (20.3 cm) Skimmer Slider Configurations 47
Figure 2.16 Flow Rate vs. Depth Experimental Data and Two-Section Model: 4 in. (10.2 cm) Skimmer; 100% Open; Vented 49
Figure 2.17 Flow Rate vs. Depth Experimental Data, Model Overlay and Three-Section Model: 4 in. (10.2 cm) Skimmer; 30% Open; Vented 52
Figure 2.18 Flow Rate vs. Depth Experimental Data and Hill-Type Saturated Model: 4 in. (10.2 cm) Skimmer; 100% Open; Unvented 54
Figure 2.19 Flow Rate vs. Depth Model Comparisons: 4 in. (10.2 cm) Skimmer, Vented 55
Figure 2.20 Flow Rate vs. Depth Models for All Skimmer Configurations 58
Figure 2.21 Skimmer Flow Rate Overlap Chart 61
Figure 2.22 Flow Rate vs. Orifice Area Comparisons for All Skimmer Configurations 62
Figure 2.23 Depth vs. Time Charts: 8 in. (20.3 cm) Skimmer, 100% Open 64
Figure 2.24 Flow Rate vs. Depth Models: 8 in. (20.3 cm) Skimmer, 100% Open 65
Figure 2.25 Depth vs. Time Charts: 8 in. (20.3 cm) Skimmer, 100% Open 66
Figure 2.26 Flow Rate vs. Depth Model Comparisons: All 8 in. (20.3 cm) Skimmer Configurations 69
Figure 2.27 Flow Rate vs. Depth Model Comparisons: All 4 in. (10.2 cm) Skimmer Configurations 73
Figure 2.28 Flow Rate vs. Depth Model Comparisons: All 3 in. (7.6 cm) Skimmer Configurations 77
Figure 2.29 Flow Rate vs. Depth Model Comparisons: All 2 in. (5.1 cm) Skimmer Configurations 78

Figure 2.30 Flow Rate vs. Depth Model Comparisons: All 1.5 in. (3.8 cm) Skimmer Configurations ... 80
Figure 2.31 Sediment Basin Engineer's Calculator Sizing Tool ... 83
Figure 2.32 Stage-Storage Graph Based on Calculator Output ... 85
Figure 2.33 Engineer's Calculator Logic Flow Chart ... 86
Figure 2.34 Sediment Basin Estimator's Calculator Sizing Tool ... 87
Figure 2.35 Logical Flowchart for Sediment Basin Skimmer Sizing Tool Use ... 89
Figure 2.36 Post-Construction Engineer's Calculator Sizing Tool ... 91
Figure 2.37 Stage-Storage Graph Based on Calculator Output ... 92
Figure 2.38 Post-Construction Estimator's Calculator Sizing Tool ... 93
Figure 3.1 Peak Discharge Design Interface ... 114
Figure 3.2 Channel Armoring Design: No Armoring ... 116
Figure 3.3 Channel Armoring Design: Vegetation Armoring ... 117
Figure 3.4 Channel Armoring Design: TRM-Vegetated Armoring ... 118
Figure 3.5 Channel Armoring Design: TRM – Unvegetated Armoring ... 119

Chapter 1 Introduction

1.1 Background

Across the United States, heavy precipitation events have become increasingly common since the 1950s (Crimmins et al. 2023). The upward trend in these observed events is related to the growing frequency and intensity of storm events. With more frequent and intense storm events, maintaining stormwater infrastructure and protecting downstream water bodies is becoming increasingly challenging. As of 2022, approximately 50% of assessed waterbodies in the United States were designated as impaired, meaning they do not meet standards for drinking water, aquatic life, or recreation (Kelderman et al. 2022). These receiving waterways become impaired as nonpoint source pollutants, such as sediment, metals, oil and grease, nutrients, and pathogens, are intercepted by stormwater runoff and deposited into downstream waterways (United States Environmental Protection Agency [USEPA] 2026a). Pollutant loading in these waterbodies can be attributed to urbanization, which increases impervious surfaces and construction activity.

Impervious surfaces such as roadways, parking lots, buildings, and homes increase the volume and velocity of stormwater runoff, which limits infiltration capacity and increases erosion potential (USEPA 2007). In addition, stormwater runoff can accumulate pollutants as it flows across impervious surfaces. As a result, these pollutants can migrate into vulnerable receiving waterbodies. Furthermore, improperly managed stormwater runoff in urban areas poses additional challenges, such as increased flooding, streambank degradation, and diminished groundwater recharge (Arnold and Gibbons 1994).

Construction sites are particularly susceptible to erosive forces due to activities such as land grading, excavation, and the removal of existing vegetation. Construction sites discharge approximately 10 to 20 times as much sediment-laden runoff than agricultural lands and 1,000 to 2,000 times that of forested lands (USEPA 2023a). USEPA distinguishes sediment as one of the most significant pollutants of concern impacting receiving waterbodies (USEPA 2005). Exposed soil can be displaced by rainfall; dislodged soil particles can be intercepted and carried off-site by stormwater runoff. Sediment loading in receiving waterways can reduce dissolved oxygen levels, suffocate aquatic organisms, and clog stream channels (United States Department of Agriculture 2012). Additionally, several contaminants such as pesticide bifenthrin, flame retardant chemicals, polycyclic aromatic hydrocarbons, and several metals sorb to sediment, causing further damage to downstream waterbodies (Mahler 2018). An effective method in mitigating damage caused by erosive forces and ensuring compliance with environmental regulations is the implementation of stormwater control measures (SCMs).

1.2 Stormwater Control Measures

SCMs are used to protect downstream waterbodies by effectively slowing, treating, and managing runoff. SCMs can be categorized into construction and post-construction applications. SCMs for construction applications can also be known as erosion and sediment control (ESC) measures. The creation and evolution of SCMs are attributed to the Clean Water Act of 1972 (CWA). The CWA was passed by the U.S. Congress to protect and preserve waterbodies from polluted runoff. Under the CWA, the National Pollutant Discharge Elimination System (NPDES) was established to protect waterways through a permitting system (USEPA 2026b). NPDES permits are issued by the USEPA and provide specifications for acceptable levels of a pollutant that may be discharged into receiving waterways. These permits cover stormwater discharge from a variety of sources, including construction activities and municipal sources.

For construction activities, the NPDES authorizes stormwater discharge under the Construction General Permit (CGP). A CGP is required if 1 acre (0.4 ha) of land is disturbed, or if less than 1 acre is disturbed but part of a larger development that will disturb more than 1 acre in total (USEPA 2026c). Construction sites that meet the criteria for a CGP are required to develop a Stormwater Pollution Prevention Plan (SWPPP). SWPPPs are site-specific plans that identify potential sources of stormwater pollution, outline which ESC measures will be used to minimize stormwater runoff, and describe procedures to ensure the site remains in compliance with the CGP (USEPA 2007). ESC practices are typically implemented on construction sites to minimize erosion and detain suspended sediment present in runoff. Examples of ESC practices include sediment basins, sediment barriers, rolled erosion control products (RECPs), diversion swales, and others.

Stormwater discharge from municipal sources is regulated under a municipal separate storm sewer system (MS4) permit. An MS4 is a conveyance or system of conveyances that is designed to collect and transport stormwater until it is ultimately discharged into receiving waterbodies. MS4s can be classified as small, medium, or large based on population size. Small MS4s typically have general permits and are designated for urban areas with populations exceeding 50,000 (USEPA 2023b). Permittees must develop a stormwater management program that details how the MS4 will remain in compliance with NPDES requirements. Post-construction runoff control measures are one of the six components required in a stormwater management program. Post-construction SCMs are typically permanent installations and aim to reduce peak flows and treat runoff before it is discharged into waterways. Structural post-construction SCMs consist of storage, infiltration, and vegetative practices (Osouli et al. 2017). Specific examples of these practices include wet or dry detention ponds, infiltration trenches, grassed swales, and others.

1.3 Definition and Purpose of Floating Surface Skimmers

Floating surface skimmers are dewatering devices that discharge from the top of the water column, the least turbid section of a basin. Skimmers are commonly installed in sediment basins on active construction sites; however, skimmers are also an emerging technology for dewatering in post-construction retention basins. Since skimmers float at the water surface, there is increased time for suspended sediment to settle via gravity. The two primary advantages of floating surface skimmers compared to historical dewatering mechanisms include (1) they facilitate greater control of dewatering time and (2) they effectively reduce total suspended solids and turbidity of effluent (Zech et al. 2014). It is increasingly common for skimmers to have customizable inlets for even greater control of dewatering rates.

It is critical that skimmers are appropriately sized to meet basin detention requirements. Skimmer size is based on the maximum inlet size and can be calculated using the basin's required discharge volume and detention time. Skimmer dewatering rates can be determined using theoretical equations or through experimental testing. Experimental testing has been shown to be the optimal approach to verify dewatering rates, as calculated flow rates can result in errors when predicting skimmer performance (Sharpe et al. 2023). Furthermore, properly sized skimmers effectively reduce sediment discharge off-site and improve basin functionality.

1.4 Definition and Purpose of Roadside Channel Stabilization

A roadside channel is a constructed open channel conveyance system located beside a roadway, designed as the initial mechanism to collect and direct runoff away from the roadway (Alabama Department of Transportation 2022). Roadside channels collect sheet flow from roadways, which promotes erosion within the channel. Untreated erosion along roadways can degrade road infrastructure, pollute nearby waterways, and increase maintenance costs; thus, stabilization is necessary to mitigate its effects.

Rural roadways make up the majority of public road mileage in Alabama (United States Federal Highway Administration 2023). Rural roads typically have lower traffic volumes than urban roadways and often lack stabilization measures in their adjacent conveyance channels. As a result, an increasing number of roadside channels along rural roadways in Alabama are experiencing severe erosion. Therefore, there is a need to establish sustainable stabilization practices to preserve these vulnerable channels.

1.5 Research Objectives

This research was divided into two primary components, which include evaluating the performance of floating surface skimmers and reviewing roadside channel erosion control practices for implementation in rural areas:

(1) Define how various configurations influence the discharge rates of floating surface skimmers designed for use in either sediment basins or post-construction retention basins.

(2) Outline erosion control measures that are effective and feasible for implementation in roadside channels in rural areas throughout Alabama.

To accomplish these objectives, the research plan was divided into the following tasks:

(1) Conduct a comprehensive literature review on skimmers as a dewatering mechanism in active and post-construction settings, the importance of properly sizing skimmers, and previous testing assessing skimmer performance.

(2) Perform controlled testing of various floating surface skimmer configurations at the Auburn University – Stormwater Research Facility.

(3) Analyze the collected flow rate data throughout testing, and create models to predict the flow rate at given depths.

(4) Develop user-friendly skimmer sizing tools to provide guidance and simplify the process of selecting an appropriate skimmer size for proper implementation.

(5) Conduct a comprehensive literature review on which erosion control measures have historically been utilized in roadside channels, and the practicality of installing such erosion control measures in rural areas to provide informed decisions for future testing efforts.

(6) Develop a selection tool that provides guidance on selecting an appropriate stabilization practice for a given channel.

1.6 Expected Outcomes

The outcomes of this research study are intended to provide the ESC industry with guidance on floating surface skimmer performance and selecting appropriate roadside channel stabilization measures. Results from controlled testing improve understanding of skimmer performance and provide accurate dewatering rates through scientifically supported data. Flow rate models were used to develop interactive sizing tools that provide guidance on proper skimmer sizing based on basin detention requirements. A review of past literature on channel stabilization was used to develop a section tool that provides guidance on selecting and designing erosion control practices for implementation in roadside channels across rural Alabama. This study enhances guidance on improving SCM implementation and provides recommendations for future research to further expand the body of knowledge used for construction and post-construction stormwater management.

1.7 Organization of Thesis

This thesis is divided into four chapters that aim to describe the steps taken to achieve the defined research objectives. Following this chapter, Chapter Two: *Evaluation of Sediment Basin and Post-Construction Floating Surface Skimmer Flow Rates* reviews the application of floating surface skimmers as dewatering devices compared to other mechanisms, outlines the methodology used to assess the performance of skimmers designed for sediment basin and retention basin implementation, illustrates the results of experimental testing, and presents the skimmer sizing tools developed using flow rate models. Chapter Three: *Roadside Channel Stabilization Measures* outlines past research regarding the effectiveness of channel stabilization measures implemented to control erosion and presents the stabilization practice selection tool developed using the existing body of knowledge on the subject matter. Chapter Four: *Conclusions and Recommendations* summarizes major findings on floating surface skimmer performance and provides insight into which stabilization practices will be practical and effective for implementation in roadside channels for future testing. In addition, this chapter will highlight recommendations for future research to advance the body of knowledge on ESC practices.

Chapter 2 Evaluation of Sediment Basin and Post-Construction Floating Surface Skimmer Flow Rates

2.1 Introduction

Floating surface skimmers are often used as dewatering mechanisms in sediment basins on active construction sites. Skimmers are considered a sediment control measure as they facilitate sedimentation in sediment basins. Unlike traditional dewatering measures, such as perforated riser structures and auxiliary spillways, skimmers discharge from the least-turbid zone of the water column and provide additional control over dewatering rates to maintain available storage. There is also opportunity for skimmer applications in post-construction detention basins for TSS and turbidity reduction purposes. Selecting an appropriate skimmer size is critical for basin functionality. Skimmer performance can vary with factors such as design, inlet size, inlet shape, barrel length, material, and the use of a ventilation pipe, posing challenges for engineers and designers seeking to choose a skimmer that meets their site-specific needs. This chapter outlines past research on the purpose of skimmers compared to traditional dewatering mechanisms; the methodology used to determine dewatering rates and develop flow rate models; the results of skimmer performance testing; and the development of sizing tools to guide the selection of an appropriate skimmer based on basin parameters.

2.2 Literature Review

A review of past research on floating surface skimmer applications in construction and post-construction settings was conducted to assess skimmer performance and determine dewatering rates. Additionally, skimmers were evaluated for their effectiveness as dewatering mechanisms relative to traditional dewatering practices, and for how skimmer dewatering rates have historically been determined.

2.2.1 Sediment Basins

One such ESC practice used to prevent sediment-laden runoff from impacting off-site areas is a sediment basin. Sediment basins are temporary sediment control structures designed to intercept and detain stormwater runoff so that water may be treated via sedimentation (Fang et al. 2015). Sedimentation is the process by which suspended sediment particles settle to the basin floor via gravitational forces. To minimize the amount of sediment present in treated effluent, the sediment deposition efficiency of a sediment basin is influenced by several design parameters: size, geometry, sediment characteristics, energy dissipators, and dewatering mechanisms (Armstrong et al. 2023). The standard sediment basin details outlined by the International Erosion Control Association (IECA), as seen in Figure 2.1, require a minimum length-to-width (L:W) ratio of 2L:1W; a capacity to withstand a 2-yr, 24-hr storm event; a minimum of three evenly distributed rows of baffles; a surface dewatering mechanism that discharges from the top of the water column; and an auxiliary spillway designed to handle peak flow rates from a 10-yr, 24-hr storm event (IECA 2021).

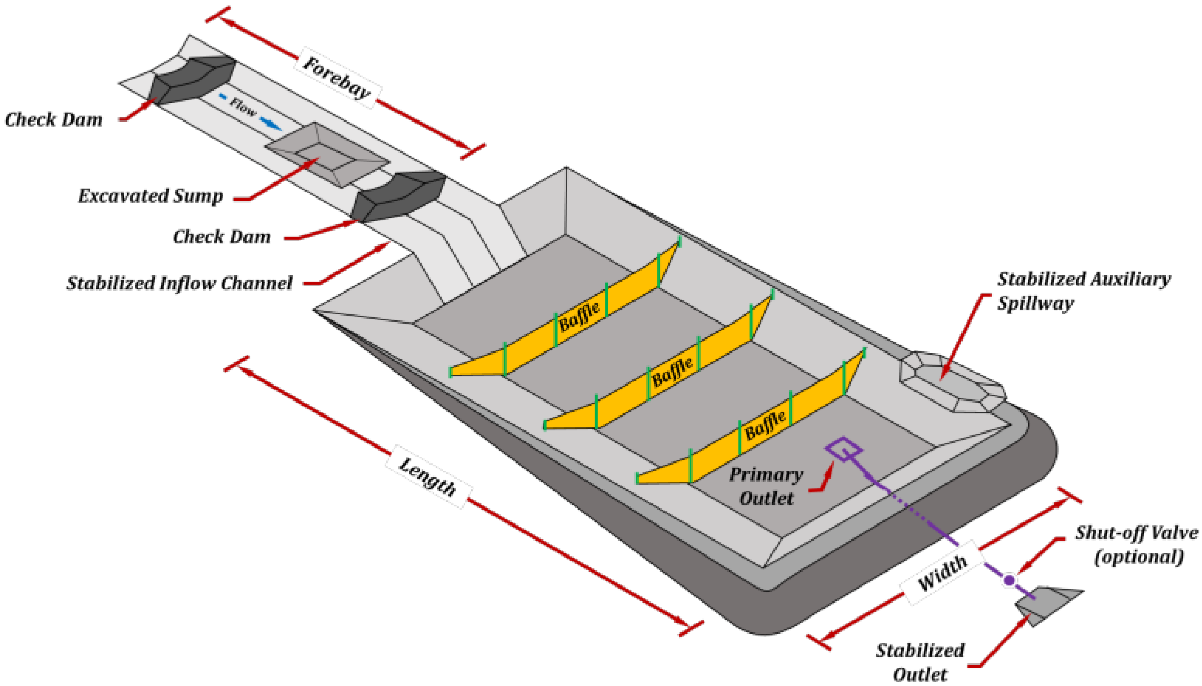

Figure 2.1 Sediment Basin Design Diagram (IECA 2021)

Sediment basin design and performance vary by jurisdiction due to soil properties, along with the frequency and severity of precipitation events. One study indicated that sediment control systems with sediment basins along highway construction sites effectively remove 35% to 60% of incoming sediment (McLaughlin et al. 2009). Another study determined that, overall, sediment basins utilizing sediment control systems are capable of removing up to 98% of suspended sediment after rainfall events (Fang et al. 2015).

2.2.2 Sediment Basin Dewatering

It is imperative that sediment basins be properly designed to provide adequate storage volume for capture after rain events, while also allowing sufficient time for sedimentation; therefore, a dewatering mechanism is essential to discharge treated runoff and avoid prolonged ponding (Thaxton et al. 2004). Sediment basin dewatering is the process of slowly releasing captured stormwater runoff off-site after detention time has been met. Dewatering in a sediment basin has a two-to-five-day requirement to ensure sufficient time for sedimentation to occur while also keep adequate storage volume available (ASWCC 2022). To allow for greater control of dewatering, principal spillways such as riser structures, auxiliary spillways, and floating surface skimmers have been adopted to improve the quality of water discharged from sediment basins (Perez et al. 2016). Recently, floating surface skimmers have emerged as the leading dewatering mechanism adopted by state and federal environmental regulatory agencies for sediment basin dewatering.

Perforated riser structures have historically been used as the principal spillway for regulating sediment basin dewatering (Perez et al. 2016). Perforated riser structures are passive flow systems that dewater throughout the water column. These mechanisms are fabricated from corrugated aluminum pipe or a plywood box with a geotextile wrap and aggregate backfill for filtration (Perez et al. 2015). Holes are drilled into the sides to allow for water to flow through. Studies have shown that perforated riser structures can intercept sediment at rates of 88% or higher when properly designed (Edwards et al. 1999; Fennessey and Jarrett 1997; Millen et al. 1997). Despite the potential for a high rate of sediment capture, perforated riser structures are usually inadequately designed due to a lack of design guidance, and consequently, will dewater sediment basins too quickly (Jarrett 1993). Additionally, hydrostatic head above the holes affects discharge rates depending on water levels; when the sediment basin is closer to capacity, dewatering occurs more rapidly, thus more sediment is present in the effluent than desired (Perez et al. 2015).

2.2.3 Floating Surface Skimmers

Currently, the Construction General Permit issued by the USEPA mandates that outlet structures in sediment basins must drain from the top of the water column (USEPA 2022). One such device utilized for sediment basin dewatering that meets this requirement is a floating surface skimmer. A floating surface skimmer is a device designed to float at the water surface and decant from the top of the water column, dewatering through an inlet (Perez et al. 2015). Floating surface skimmers are the most efficient mechanism for sediment basin dewatering, not only because skimmers allow for increased settling time, but also because they facilitate control over discharge rates (Zech et al. 2014). In addition, skimmers can be reused across multiple construction sites and generally require minimal maintenance, except for cleaning debris from the inlet. Researchers have indicated that with a skimmer installed, most sediment loss in a sediment basin occurred in the first 5-9 hours following the start of a storm event (Millen et al. 1997; Vaughan and Jarrett 2001). Skimmers are manufactured in a variety of shapes and sizes, as seen in Figure 2.2. It has been verified that skimmers with an inlet at the top of the barrel have significantly more sediment retention in a sediment basin than if the orifice were located at the bottom of the apparatus (Vaughan and Jarrett 2001).

(a) Faircloth Skimmer (b) Marlee Skimmer

(c) IAS Skimmer (Innovative Applied Sol. 2014) (d) ESC Skimmer (Perez 2016)

Figure 2.2 Common Skimmer Types

Several studies have been conducted to verify skimmer performance compared to traditional dewatering methods. Skimmers consistently outperform riser structures in terms of reducing sediment present in sediment basin effluent: one study conducted by Millen et al. (1997) found that skimmers have a sediment retention efficiency of 97%, while two additional studies showed a retention efficiency of over 99% (Hoechst 1997; McCaleb and McLaughlin 2008). Furthermore, in a study performed by Jarret (2001), perforated riser spillways had a sediment loss of 1.8 times greater than that of a skimmer. .

2.2.4 Skimmer Selection and Sizing

Though skimmers are effective in controlling dewatering of sediment basins, they must be properly sized to meet detention requirements. The required skimmer size is calculated from the basin discharge volume and detention time to obtain the required outflow rate. This required outflow rate can then be used to select a skimmer size based on the manufacturer's selection charts. It is also increasingly common for skimmers to have a customizable orifice. As a more precise alternative, flow through a specific orifice can be computed using an orifice flow equation, as seen in Equation 2.1 (ASWCC 2022).

$$Q= CA\sqrt{2gH} \qquad \text{Equation 2.1}$$

Where:

Q = required discharge rate (ft^3/s or m^3/s)

C = orifice coefficient

A = cross-sectional area of the orifice (ft^2 or m^2)

g = acceleration due to gravity (32.2 ft/s^2 or 9.81 m/s^2)

H = driving head on the orifice center (ft or m)

C is typically chosen to be 0.6 for sharp orifices. If the desired flow rate is known, the orifice equation can be simplified to determine the orifice diameter using Equation 2.2.

$$D= \sqrt{\frac{Q}{2310\sqrt{H}}} \qquad \text{Equation 2.2}$$

Where:

D = Diameter of the orifice (in. or cm)

Q = Required discharge rate (ft^3/h or m^3/h)

H = Head (ft or m)

This step may not be necessary if calculated outflow rates are equal or near the required outflow rates based on sediment basin parameters. It should be noted that calculated flow rates are theoretical and may not accurately reflect skimmer performance throughout the water column. As mentioned before, skimmer selections should be verified with the manufacturer's selection charts and other supplementary information.

In a study performed by Perez et al. (2016), a tool was constructed for sediment basin design using Microsoft Excel. When considering floating surface skimmer sizing, the tool calculates the discharge rate and the orifice diameter using Equation 2.3. The author specifies that users should verify the orifice size with the manufacturer to confirm the skimmer is properly sized for the designed outflow rate, as outputs are approximations (Perez et al. 2016).

$$O_{skim} = xQ_{skim}^{2/5} \qquad \text{Equation 2.3}$$

Where:

O_{skim} = orifice diameter (in. or cm),

x = 0.2665 or 2.8166 for U.S. customary units or SI units, respectively

Q_{skim} = required discharge rate (ft^3/s or m^3/s).

Skimmer designs differ across manufacturers, which results in varied performance, even with similar orifice sizes (Sharpe et al. 2023). Therefore, there is a need to conduct experimental testing on skimmers as discharge rates are dependent on design. Experimental testing is the optimal approach to obtain accurate flow rates, as theoretically calculated flow rates can lead to errors in determining dewatering times and result in increased sediment concentration in discharge. Furthermore, altering the size and shape of the inlet using an adjustable or customizable inlet also affects hydraulic performance, thus providing additional need for experimental testing to define discharge rates and assess skimmer behavior.

2.2.5 Post-Construction Detention and Retention Basins

Storage basins, such as detention and retention basins, are a common post-construction stormwater management practice that helps mitigate flooding in urbanized areas and downstream pollutant loading in receiving waterways. The primary function of detention and retention basins is to reduce runoff volumes and minimize peak flows (Travis and Mays 2008). Both detention and retention basins treat runoff by allowing pollutants to settle from suspension. Detention basins provide temporary storage and gradually discharge stormwater runoff. Detention basins are designed to accommodate a settling time of 12 hours to 3 days (USEPA 2021a). Since detention basins typically lack permanent standing pools, they are less effective at removing soluble pollutants (USEPA 2021a). Retention basins have permanent standing water pools and facilitate pollutant removal through extended settling times and uptake from vegetation. Several states require that stormwater quality measures remove 80% of TSS in urban runoff. When designed and constructed properly, retention basins are presumed to remove 80% of TSS present in urban runoff, while detention basins are presumed to remove 60% of TSS present in urban runoff (Atlanta Regional Commission 2016). As a result, detention basins may require additional SCMs such as grass-lined channels placed upstream. While detention and retention basins are capable of retaining onsite runoff, they are designed to attenuate runoff; capturing and infiltrating runoff is not their primary purpose (Osouli et al. 2017).

Detention and retention basins are commonly dewatered through an outlet pipe, riser structure, or spillway. Furthermore, there is an opportunity for skimmer applications in detention and retention basins to increase capture of suspended pollutants and provide greater control over available basin storage. Perez et al. (2023) performed large-scale testing to evaluate a 1.5 in. (3.81 cm) Faircloth® skimmer used for post-construction water quality improvement. Results of this testing indicated significant improvement in water quality with the skimmer, with TSS in the effluent decreasing by an average of 92%. Like skimmers designed for sediment basins, post-construction skimmers must be appropriately sized to meet detention requirements; therefore, accurate flow rates must be obtained. A study performed by Sharpe et al. (2023) evaluated a skimmer specifically designed for post-construction detention basins. The skimmer featured an adjustable sluice gate that can be used to meet required detention times. Six sluice gate openings ranging from 6 in. (15.2 cm) to 1 in. (2.54 cm) were tested across two different barrel lengths, 8 ft (2.44 m) and 12 ft (3.66 m), in triplicate for 36 total tests. The post-construction skimmer was determined to be capable of achieving outflow rates as low as 0.5 ft^3/s (0.017 m^3/s) to as high as 2.5 ft^3/s (0.070 m^3/s) for the 1 in. (2.54 cm) and 6 in. (15.2 cm) openings, respectively.

2.3 Means and Methods

This section outlines the testing procedures and methodology, including the testing apparatus, data collection measures, and testing regime. The objective of this testing is to provide an accurate assessment of skimmer discharge rates and evaluate overall performance in a controlled environment. Skimmer testing was performed in two parts: (1) evaluating skimmers manufactured for use in sediment basins on construction sites and (2) assessing skimmers designed for use in post-construction retention basins. Skimmers were primarily assessed using the testing apparatus and methodology described in Sharpe et al. (2023).

2.3.1 Testing Apparatus

Testing was performed at the Auburn University – Stormwater Research Facility (AU-SRF), a 12-acre (4.9 ha) outdoor testing facility dedicated to training, research, and evaluation of stormwater management practices. The skimmer evaluation apparatus, as seen in Figure 2.3, utilized for testing is the same as that used by Sharpe et al. (2022). The apparatus is a refurbished and sealed 40 yd^3 (30.6 m^3) steel roll-off dumpster. The skimmer tank is 21.8 ft (6.6 m) in length, 6.9 ft (2.1 m) in width, and 7.0 ft (2.1 m) in height. Based on these measurements, the tank has a bottom surface area of 150.4 ft^2 (14.0 m^2) and a volume of 1053 ft^3 (29.8 m^3). The tank features 8 in. (20.3 cm) and 4 in. (10.2 cm) flanges on the bottom of the south wall. Each skimmer was connected to the 8 in. (20.3 cm) flange; if necessary, appropriately sized connection reducers were used. The flange connects to an underground outlet pipe 8 in. (20.3 cm) in diameter that discharges to an adjacent retention pond.

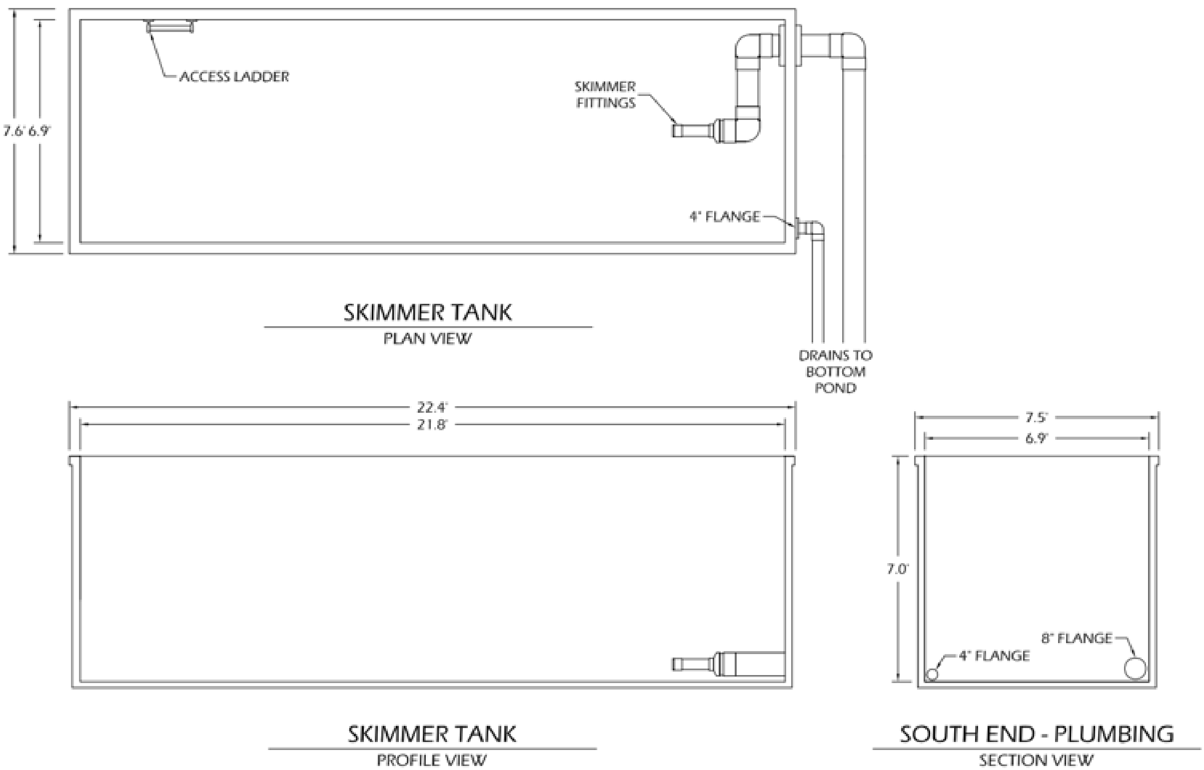

Figure 2.3 Skimmer Evaluation Tank Schematic (Sharpe 2022)

Water was delivered to the evaluation tank using two 4 in. (10.2 cm) polyvinyl chloride (PVC) pipes outfitted in a "T" configuration. The pipes were placed on the wall of the tank for minimal buoyancy effects while the tank was being filled for testing, as seen in Figure 2.4(b). The PVC delivery pipes were connected using 4 in. (10.2 cm) hoses to two Honda GX 270 pumps. The pumps delivered water with an approximate flow rate of 1.0 ft^3/s (0.03 m^3/s) each, resulting in a total flow rate of 2.0 ft^3/s (0.06 m^3/s) when filling the tank for each test. Figure 2.4 illustrates a photo of the outside view of the evaluation tank, along with the water delivery system set up.

(a) skimmer evaluation tank (b) water delivery system

Figure 2.4 Skimmer Evaluation Apparatus Components at AU-SRF

2.3.2 Floating Surface Skimmer Apparatus

A total of thirteen skimmer prototypes were evaluated throughout experimental testing: eight sediment basin skimmers and five post-construction skimmers. The skimmers were provided by J.W. Faircloth & Son, Inc. Each skimmer consists of a head, barrel, and flexible hose. The head floats at the water surface and is where the inlet is located. Some manufacturers include a grate to protect the inlet from debris. The head is attached to a drainage pipe or "barrel," which varies in length and diameter depending on the skimmer size. Barrel length, diameter, and material type are typically specified by the manufacturer. These specifications can alter the flow of the skimmer. For example, if the barrel is made of a heavier material, the skimmer will be weighed down, and the flow will be faster. In addition, the barrel diameter is typically smaller than the inlet diameter to promote laminar flow in the barrel. Finally, the length of the barrel influences the angle the barrel makes with the bottom of the basin. A shorter barrel will lend faster flow rates, and a longer barrel will provide slower flow rates. The barrel is attached to a flexible hose using PVC cement, which allows for proper flotation as the basin is filled, and is connected to the outlet flange in the evaluation tank. Figure 2.5 shows an example of a skimmer installed in the skimmer evaluation tank, along with its components.

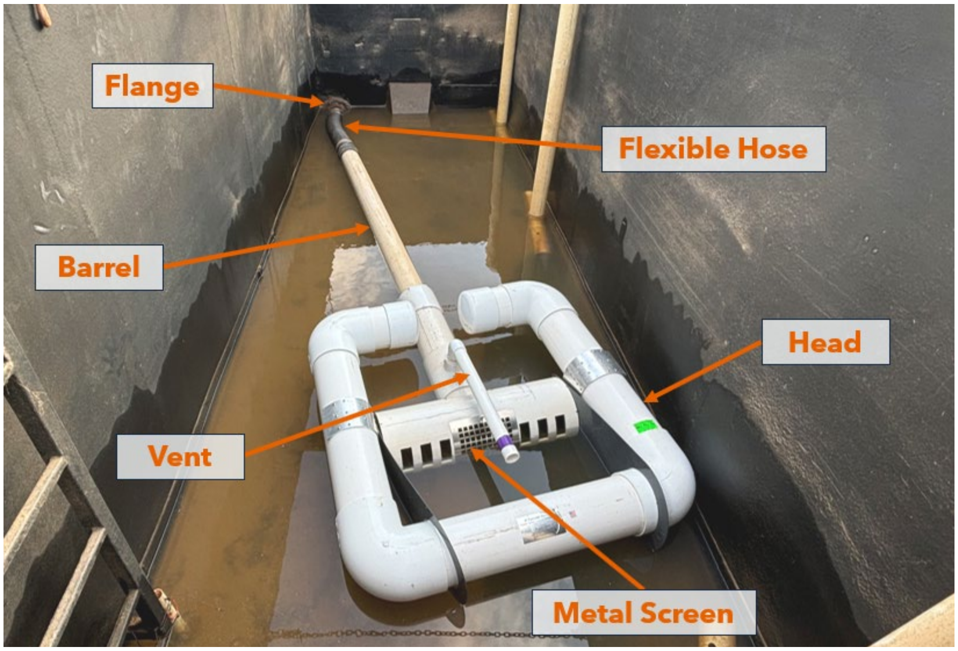

Figure 2.5 Example of Skimmer Components

2.3.2.1 Sediment Basin Skimmer Apparatus

The eight sediment basin skimmer models assessed were designed for temporary use in sediment basins on active construction sites. The following skimmer sizes were evaluated: 1.5 in. (3.8 cm), 2 in. (5.1 cm), 2.5 in. (6.4 cm), 3 in. (7.6 cm), 4 in. (10.2 cm), 5 in. (12.7 cm), 6 in. (15.2 cm), and 8 in. (20.3 cm). Each skimmer is constructed using schedule 40 polyvinyl chloride (PVC) pipe and has a circular orifice. In addition, each skimmer had a schedule 40 PVC barrel with a length and diameter that corresponded to the skimmer size. For all sediment basin skimmers, the manufacturer states that the barrel length should be 1.4 times the maximum depth of the sediment basin, but no less than 6 ft (1.8 m) (J.W Faircloth & Son Inc. and Evans 2024). However, each barrel was chosen based on the standard manufacturer recommendation provided in the instructions included with each skimmer. The barrel specifications used for testing can be found in Table 2.1.

Table 2.1 Sediment Basin Skimmer Barrel Specifications

Skimmer Size, in. (cm)	Barrel Length, ft (m)	Barrel Diameter, in. (cm)
8.0 (20.3)	10.0 (3.0)	6.0 (15.2)
6.0 (15.2)	10.0 (3.0)	6.0 (15.2)
5.0 (12.7)	8.0 (2.4)	4.0 (10.2)
4.0 (10.2)	8.0 (2.4)	3.0 (7.6)
3.0 (7.6)	8.0 (2.4)	2.0 (5.1)
2.5 (6.4)	6.0 (1.8)	1.5 (3.8)
2.0 (5.1)	6.0 (1.8)	1.5 (3.8)
1.5 (3.8)	6.0 (1.8)	1.5 (3.8)

A ventilation pipe was also attached where the head attaches to the barrel to expose the flow to atmospheric pressure, which stabilizes the flow. The flow is controlled by an adjustable slider attached to the inlet. Figure 2.6 shows the 8 in. (20.3 cm) and 1.5 in. (3.8 cm) skimmers installed in the skimmer evaluation tank prior to testing.

(a) 8 in. (20.3 cm) skimmer (b) 1.5 in. skimmer (3.8 cm)

Figure 2.6 8 in. (20.3 cm) and 1.5 in. (3.8 cm) Sediment Basin Skimmer Installed in Skimmer Evaluation Apparatus

Of the five largest skimmers, four orifice openings were assessed using the adjustable slider: 100% open, 75% open, 50% open, and 25% open. The 25% open setting was omitted for the three smallest skimmers, as the orifice limits flow rates to levels below meaningful application. Figure 2.7 exhibits the adjustable slider set to each desired opening on the 6 in. (15.2 cm) skimmer.

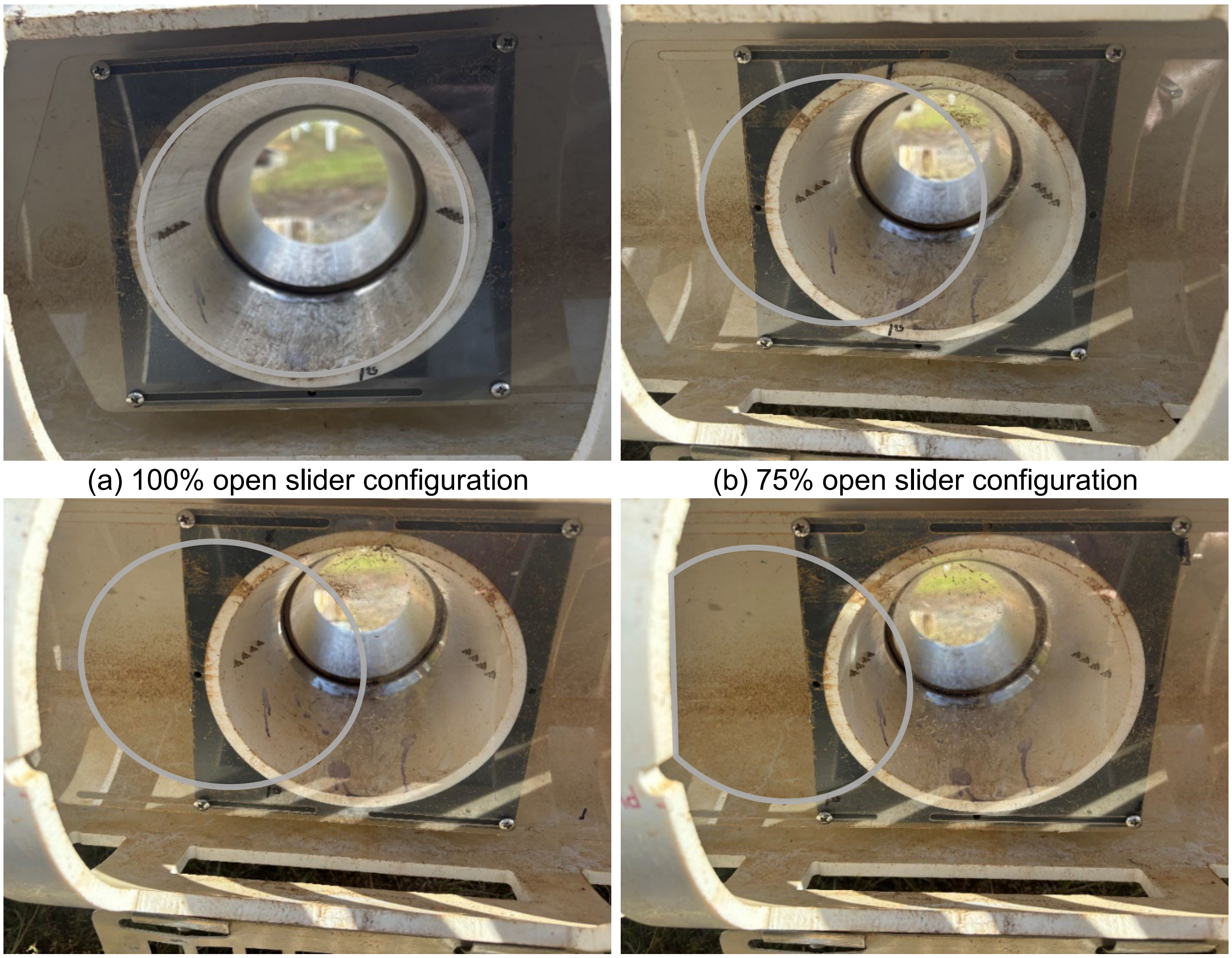

(a) 100% open slider configuration (b) 75% open slider configuration

(c) 50% open slider configuration (d) 25% open slider configuration

Figure 2.7 Adjustable Slider Configuration Photos on 6 in. (15.2 cm) Skimmer

2.3.2.2 Post-Construction Skimmer Apparatuses

The five post-construction skimmers evaluated are designed for long-term use in permanent retention or detention basins. The prototypes were 1.5 in. (3.8 cm), 2 in. (5.1 cm), 3 in. (7.6 cm), 4 in. (10.2 cm), and 8 in. (20.3 cm) in size. The skimmers were built using chlorinated polyvinyl chloride (CPVC) and high-density polyethylene (HDPE) pipe. A schedule 80 PVC barrel was used for each post-construction skimmer. The length and diameter of the barrel corresponded to the size of the skimmer, based on the manufacturer's specification. These specifications can be found in Table 2.2. It should be noted that the manufacturer recommends a 10 ft (3.0 m) barrel length for the 8 in. (20.3 cm) skimmer; however, the barrel was cut to 9.67 ft (2.9 m) to fit the skimmer in the skimmer evaluation apparatus.

Table 2.2 Post-Construction Skimmer Barrel Specifications

Skimmer Size, in. (cm)	Barrel Length, ft (m)	Barrel Diameter, in. (cm)
8.0 (20.3)	9.67 (2.9)	6.0 (15.2)
4.0 (10.2)	8.0 (2.4)	4.0 (10.2)
3.0 (7.6)	8.0 (2.4)	2.0 (5.1)
2.0 (5.1)	6.0 (1.8)	1.5 (3.8)
1.5 (3.8)	6.0 (1.8)	1.5 (3.8)

The 1.5 in. (3.8 cm), 2 in. (5.1 cm), and 3 in. (7.6 cm) skimmers were the same design as the sediment basin skimmers. However, the post-construction prototypes were approximately 5% heavier due to the materials used to construct the skimmer. Figure 2.8 shows a photo of the 3 in. (7.6 cm) post-construction skimmer installed in the skimmer evaluation tank prior to testing. The three smallest post-construction skimmers have a circular orifice, and the flow was controlled using an adjustable slider. Three orifice openings were examined across these skimmers: 100%, 75%, and 50%. Figure 2.9 shows photos of each slider configuration tested on the 3 in. (7.6 cm) post-construction skimmer. In addition, a ventilation pipe was included throughout all testing of these skimmers.

Figure 2.8 3 in. (7.6 cm) Post-Construction Skimmer Installed in the Skimmer Evaluation Tank

(a) 100% open

(b) 75% open

(c) 50% open

Figure 2.9 Adjustable Slider Configurations on the 3 in. (7.6 cm) Skimmer

The 4 in. (10.2 cm) and 8 in. (20.3 cm) skimmers had a different design from those previously described. Instead of a circular orifice, these skimmers have a rectangular inlet. Flow was controlled using removable plates that were pre-cut to the desired size. Five inlet openings were evaluated for the two largest post-construction skimmers. 100%, 75%, 50%, 25%, and 1% openings were tested on the 8 in. (20.3 cm) skimmer; and 100%, 70%, 50%, 30%, and 1% openings were examined on the 4 in. (10.2 cm) skimmer. Figure 2.10 shows photos of the rectangular inlet, as well as the 50% and 1% plates used on the 4 in. (10.2 cm) skimmer. For each inlet opening, these skimmers were assessed with and without a ventilation pipe. This was done to investigate skimmer performance under different flow conditions. Figure 2.11 shows the 4 in. (10.2 cm) and 8 in. (20.3 cm) post-construction skimmers installed in the skimmer tank with and without the ventilation pipe.

(a) 100% open

(b) 50% plate

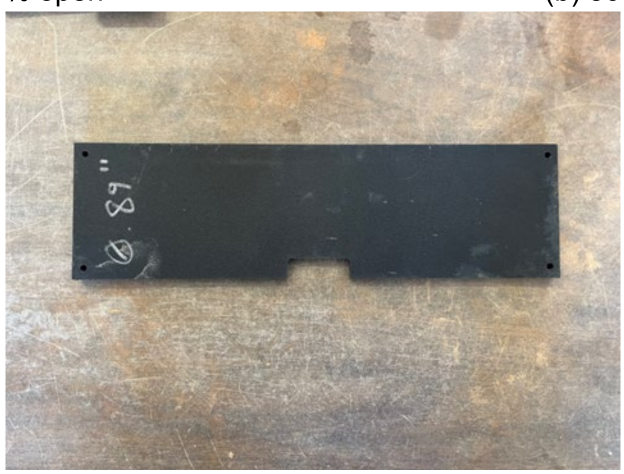

(c) 1% plate

Figure 2.10 Removable Plates and Inlet Openings on the 4 in. (10.2 cm) Skimmer

(a) 4 in. (10.2 cm) skimmer, vented

(b) 4 in. (10.2 cm) skimmer, unvented

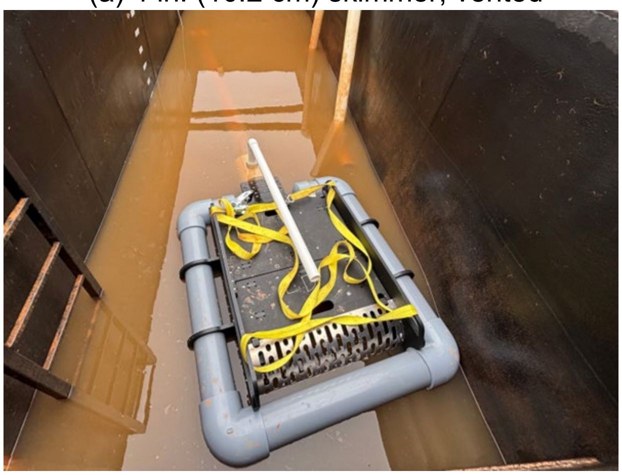

(c) 8 in. (20.3 cm) skimmer, vented

(d) 8 in. (20.3 cm) skimmer, unvented

Figure 2.11 Photos of 4 in. (10.2 cm) and 8 in. (20.3 cm) Skimmers Vented and Unvented

2.3.3 Data Collection

Flow rate data were collected using a Solinst Levelogger® 5 Model 3001 and a Solinst Barologger® 5 Model 3001. A Solinst Levelogger® is a pressure gauge datalogger that measures and records the changes in water levels as the tank is filled and emptied. A Solinst Barologger® is a datalogger that records atmospheric pressure and is used to compensate the water level readings collected from the Levelogger®. According to the manufacturer, the resolution of the Levelogger® ranges from 0.002% full scale to 0.0006% full scale (Solinst Canada Ltd. 2025). The Levelogger® was programmed to record changes in water level every 15 s for all skimmers except the 4 in. (10.2 cm) and 8 in. (20.3 cm) post-construction skimmers, which were programmed for 10 s recording intervals. In addition, an offset was adjusted to 0.0417 ft (0.0127 m) to account for the shape of the bottom of the sensor to the floor of the evaluation tank. Throughout testing, the Levelogger® was placed inside a small PVC pipe attached to the bottom of the access ladder using zip ties. The sensor was secured using a bolt inserted through a small PVC pipe. Visual observations of water level changes throughout testing were made using the tape measure attached to the wall next to the access ladder in the skimmer tank. These data collection components can be seen in Figure 2.12.

(a) PVC pipe holder for Levelogger® (b) access ladder and ruler

Figure 2.12 Data Collection Components in the Skimmer Evaluation Tank

Following each test, data collected from the dataloggers were uploaded to Solinst Levelogger Software (version 4.6.3), where the data were compensated for atmospheric pressure and exported to Microsoft Excel for flow rate calculations.

2.3.4 Testing Regime

Testing methodology followed an enhanced version of the ASTM D8107 "*Standard Practice for Determining Sediment Pond Skimmer Flow Rate*" (ASTM D8107 2018). These enhancements enabled greater apparatus depth and more comprehensive data collection. After the experimental setup was completed, the inlet was positioned to the desired opening. The inlet was blocked, or the skimmer was suspended to prevent discharge as the tank filled. The pumps were turned on, and the tank was filled via the water delivery system. Once the tank reached maximum capacity, the pumps were switched off, and obstructions were removed so the skimmer could begin dewatering the tank. The skimmer was allowed to fully drain the tank until the water level reached approximately 4.25 in. (10.8 cm), the point at which the skimmer was unable to continue discharging water. Once the test was completed, the data were collected from the dataloggers. To address measurement uncertainty and assess repeatability, each skimmer configuration was evaluated in triplicate. 87 tests were completed for both sediment basin skimmers and post-construction skimmers, for a total of 174 across all skimmers.

2.3.5 Data Analysis Methods

Skimmer performance was evaluated using data from the Levelogger® to develop plots of flow rate as a function of depth. To begin constructing these plots, the flow rate was calculated. The volume of the tank was computed by multiplying the tank's surface area by the recorded water depth at a point in time. Flow rates were calculated from changes in volume every 10 s or 15 s. Plots from each triplicate test were combined to observe trends in the data and ultimately create a model to predict the skimmer flow rate at depths below 7 ft (2.1 m). This section describes the outlier removal methods, along with the procedure for developing flow rate-depth models for the sediment basin and post-construction skimmers.

2.3.5.1 Outlier Removal

In each dataset, outliers were observed. This was likely due to sensor inaccuracies caused by noise in the tank throughout a test. The data were cleaned in each individual test dataset using a combination of the z-score method and visual observation. A data point was considered an outlier if Equation 2.4 was true:

$$|x-\bar{x}|>k*s \qquad \text{Equation 2.4}$$

Where:

x = flow rate at given depth (ft^3/s or m^3/s)

$\bar{x}$ = average flow rate (ft^3/s or m^3/s)

k = threshold value

s = standard deviation

The value *k* was typically set to a value between 1 and 3, depending on the individual dataset, as the quantity of outliers removed varied across datasets. Greater threshold values result in less sensitivity, and vice versa.

2.3.5.2 Sediment Basin Skimmer Analysis Methods

Figure 2.13 depicts the flow rate versus depth plot for the 8 in. (20.3 cm) skimmer with a 100% open slider configuration. This graph shows combined data from the three tests performed for this configuration. In addition, this plot shows the dataset after outliers have been removed.

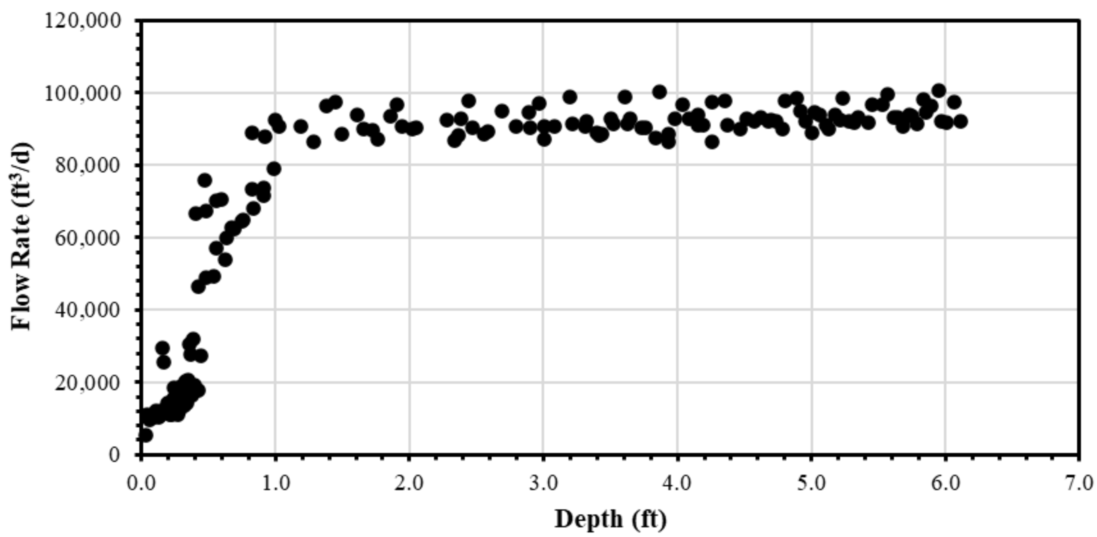

Figure 2.13. Flow Rate vs. Depth: 8 in. (20.3 cm) Skimmer, 100% Open

For all evaluated skimmer configurations, a similar trend was observed: the plots could be divided into two sections (labeled as Zone 1 and Zone 2). Zone 1 reflects the section in which the flow rate decreases to zero, while Zone 2 reflects the section starting at the greatest depth until a turn is observed, where the flow rate begins to decline more rapidly. For example, in the 100% open configuration data set shown in Figure 2.13, Zone 2 ranges from 6.1 ft (1.86 m) to 1.1 ft (0.34 m). The start of Zone 1 occurs at 1.1 ft (0.34 m) and encompasses depths less than 1.1 ft (0.34 m).

The linear equation extracted from the Zone 2 section was used to create a model to predict the flow rate at a given depth in the evaluation tank. Using the linear equation from Zone 2 and the transition depth, a new slope was calculated to model Zone 1 as the flow decreases to zero. Figure 2.14(a) displays the same data set shown in Figure 2.13; however, it depicts Zone 1 and Zone 2 split into two separate linear sections. Figure 2.14(b) exhibits the model created using the linear equations acquired from the plot in Figure 2.14(a). It should be noted that the R^2 value seen in Figure 2.14(a), as well as for the Zone 2 sections for all skimmer configurations, is relatively low due to the low variance in the dataset for that section. Once all slider openings were tested for each skimmer, the datasets were combined to examine the differences in skimmer behavior across all slider configurations. Figure 2.15 shows the models for all four slider configurations assessed for the 8 in. (20.3 cm) skimmer.

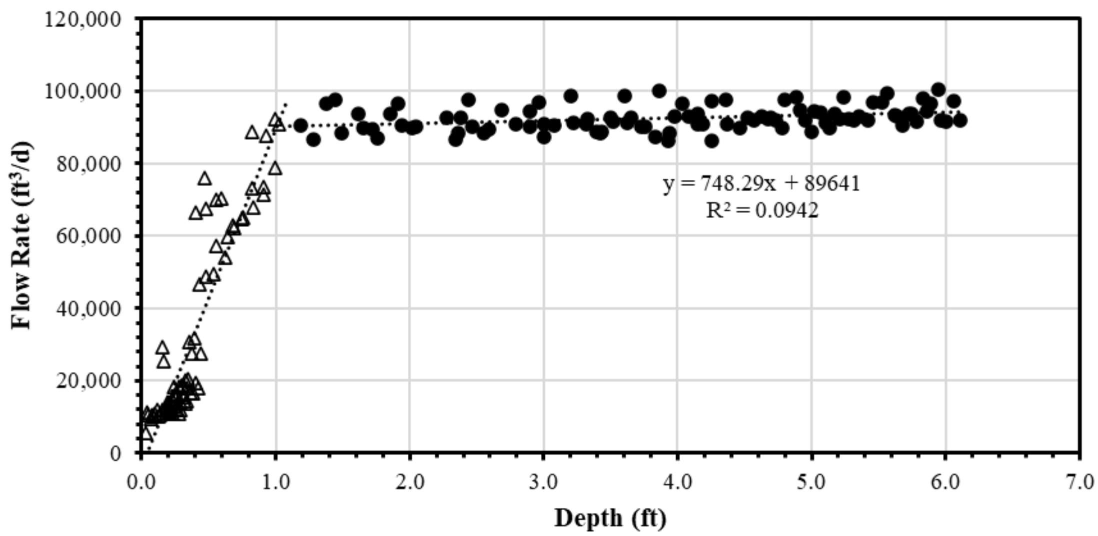

(a) flow rate vs. depth linear trendlines

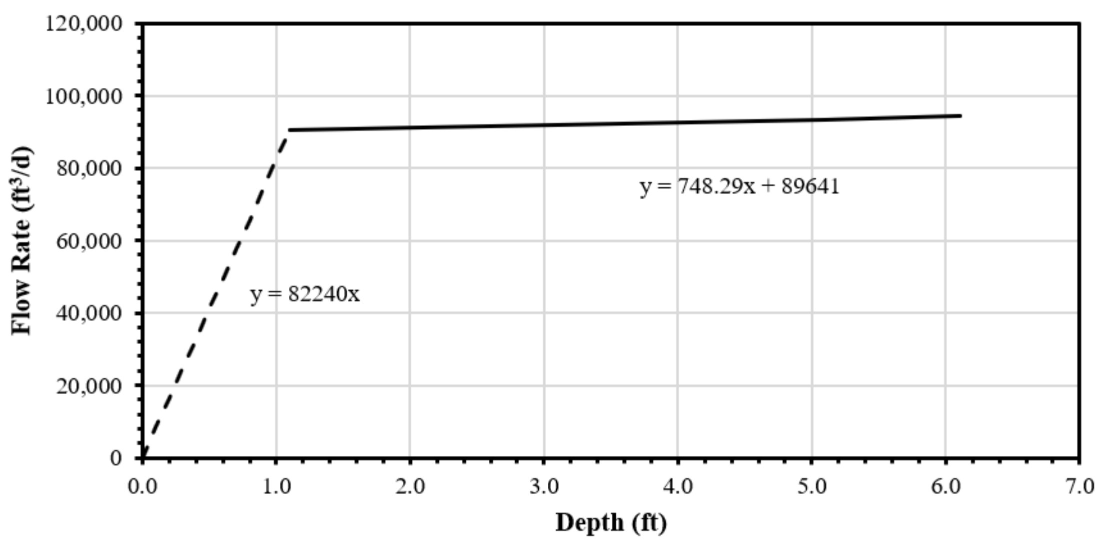

(b) flow rate vs. depth model

Figure 2.14 Flow Rate vs. Depth Linear Trendlines and Model: 8 in. (20.3 cm) Skimmer; 100% Open

Note: (a) triangles represent Zone 1, black dots represent Zone 2, dotted lines represent the best-fit linear trendline; (b) dashed line represents Zone 1, solid line represents Zone 2

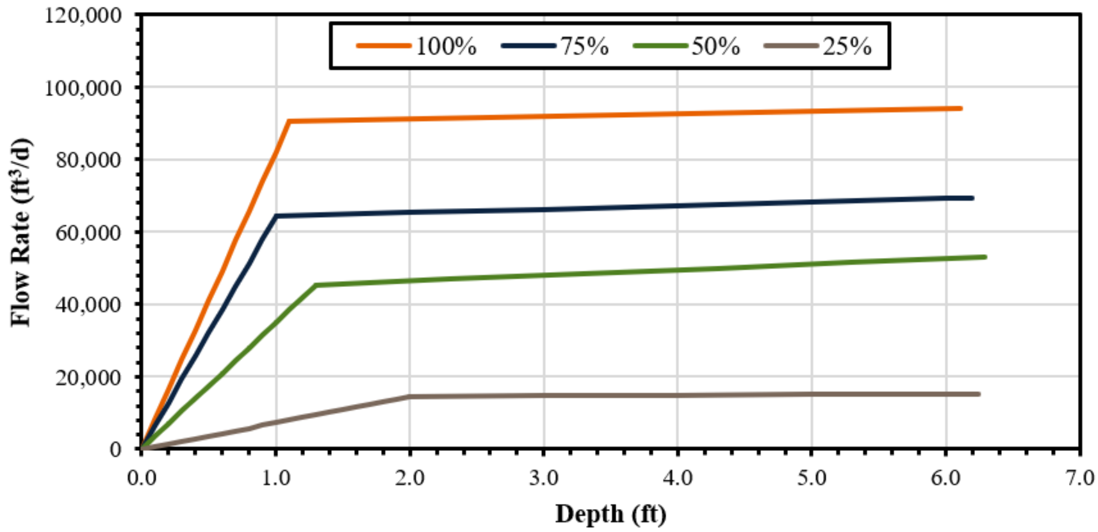

Figure 2.15 Flow Rate vs. Depth Models: All 8 in. (20.3 cm) Skimmer Slider Configurations

2.3.5.3 Post-Construction Skimmer Analysis Methods

Unlike the sediment basin skimmers, post-construction skimmer behavior across all evaluated sizes and configurations did not necessarily follow a distinct two-zone pattern. Moreover, alternative analysis methods were employed to develop flow rate models that fit across the entire dataset. Based on trends observed in the flow rate versus depth plots, one of three models was chosen to fit the data: a two-section segmented regression, a three-section segmented regression, or a Hill-type saturated function. These three models were used as a more robust method for modeling flow rates rather than dividing the experimental data into two or three linear sections. All models were fit to the combined datasets using the Microsoft Excel Solver function.

The two-section segmented regression model was used for plots that could be divided into two approximately linear sections with a breakpoint, as observed in the sediment basin skimmer plots. However, instead of visually determining where the breakpoint is between Zone 1 and Zone 2, the breakpoint was calculated using the regression model. The model was fit to the data using Equation 2.5.

$$Q(H)=\beta_0+\beta_1 H+\beta_2[\max(0,H-H_b)] \qquad \text{Equation 2.5}$$

Where:

$Q(H)$ = flow rate at some depth (ft^3/s or m^3/s)

H = depth (ft or m)

β_0 = intercept

β_1 = slope before breakpoint

β_2 = change in slope after breakpoint

H_b = depth at which breakpoint occurs (ft or m)

Parameters were set so that H_b was greater than or equal to 0 and less than or equal to 7, so that the breakpoint depth would be within the depth range of the skimmer tank. B_2 was set to be less than -0.01 to ensure that the slope of the upper line increases at a slower rate. Figure 2.16 provides an example of a plot that features the dataset from the 4 in. (10.2 cm) skimmer, 100% open, vented configuration. This dataset can be divided into two approximate linear sections, and the subsequent two-section segmented regression model is used to model the dataset. Figure 2.16(a) shows the experimental dataset, which depicts flow rate values at a given depth, represented by the black circles. Figure 2.16(b) shows the final two-section model, represented by the solid black line.

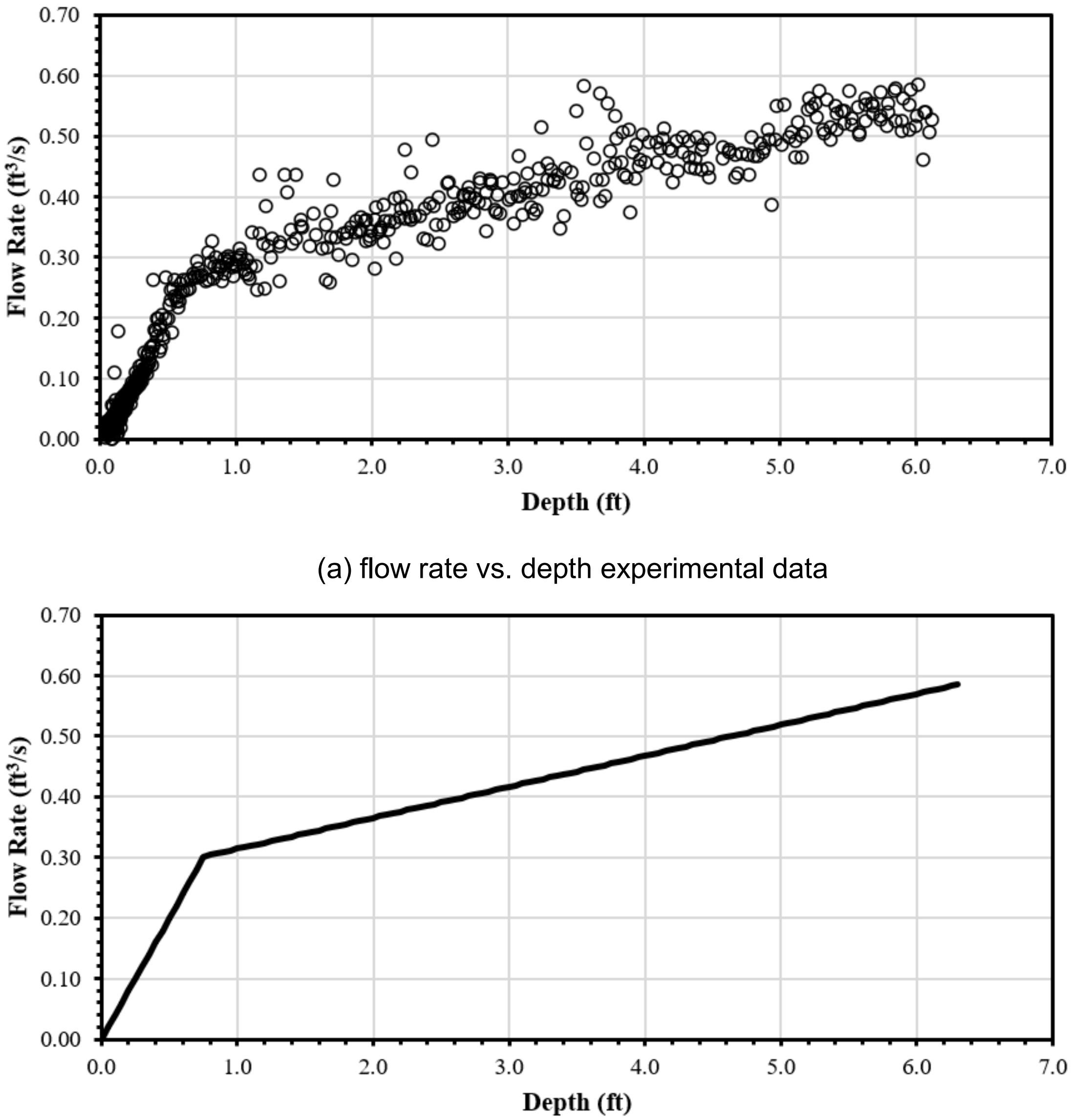

(a) flow rate vs. depth experimental data

(b) flow rate vs. depth two-section model

Figure 2.16 Flow Rate vs. Depth Experimental Data and Two-Section Model: 4 in. (10.2 cm) Skimmer; 100% Open; Vented

If a plot indicated three approximate sections, a three-section segmented regression model was used. Plots exhibiting three-section behavior were a result of the barrel being full of air at the start of each test. Since excess air was present in the barrel, the skimmer would float unevenly at the greatest depths. This caused the third section to be seen at the greatest depths until the skimmer stabilized, and a transition in the flow pattern was observed. The three-section segmented regression model followed a similar process to the two-section segmented regression. The two-section segmented regression model, as shown in Equation 2.5, was used to first model the entire dataset. This was done to determine the breakpoint between the middle section and the section where the flow rate decreases to zero, known as Zone 1 and Zone 2, respectively. Once the first breakpoint was determined, the second breakpoint was found using a two-section segmented regression model applied to Zone 2 and the third section, known as Zone 3. This model was only applied to the Zone 2 and Zone 3 sections, not the entire dataset.

After the second breakpoint was found, the Zone 1 and Zone 2 two-section model was then adjusted so that the model would not exceed the second breakpoint depth. A final adjustment was then made to the Zone 2 and Zone 3 model. Once the Zone 1 and Zone 2 and the Zone 2 and Zone 3 two-section segmented regression models were finalized, they were overlaid to verify that the two models match continuously. The final three-section model was developed using Equation 2.6.

$$Q(H)=\begin{cases} H\geq H_{b,2}, & \beta_{0,2}+\beta_{1,2}H+\beta_{2,2}[\max(0,H-H_{b,2})] \\ H\leq H_{b,2}, & \beta_{0,1}+\beta_{1,1}H+\beta_{2,1}[\max(0,H-H_{b,1})] \end{cases} \qquad \text{Equation 2.6}$$

Where:

$Q(H)$ = flow rate at some depth, H (ft^3/s or m^3/s)

H = depth (ft or m)

$\beta_{0,1}$ = intercept, Zone 1 and Zone 2 model

$\beta_{1,1}$ = slope before breakpoint, Zone 1 and Zone 2 model

$\beta_{2,1}$ = change in slope after breakpoint, Zone 1 and Zone 2 model

$H_{b,1}$ = depth at which breakpoint occurs, Zone 1 and Zone 2 model (ft or m)

$\beta_{0,2}$ = intercept, Zone 2 and Zone 3 model

$\beta_{1,2}$ = slope before breakpoint, Zone 2 and Zone 3 model

$\beta_{2,2}$ = change in slope after breakpoint, Zone 2 and Zone 3 model

$H_{b,2}$ = depth at which breakpoint occurs, Zone 2 and Zone 3 model (ft or m)

Parameters were set so that $H_{b,1}$ was greater than or equal to 0 and less than or equal to $H_{b,2}$. Similarly, $H_{b,2}$ was less than or equal to 7 and greater than or equal to $H_{b,1}$. This was done to ensure that the individual two-section regression models remained separate while remaining within the confines of the skimmer tank. Additionally, $\beta_{2,1}$ and $\beta_{2,2}$ were set to be less than -0.01. Figure 2.17 illustrates the process of creating a three-section segmented regression model using the dataset for the 4 in. (10.2 cm), 30% open, vented configuration. Figure 2.17(a) shows the experimental dataset, which depicts flow rate values at a given depth, represented by the black circles. Figure 2.17(b) depicts the two overlaid two-section segmented regression models. Figure 2.17(c) shows the final three-section model, represented by the solid black line.

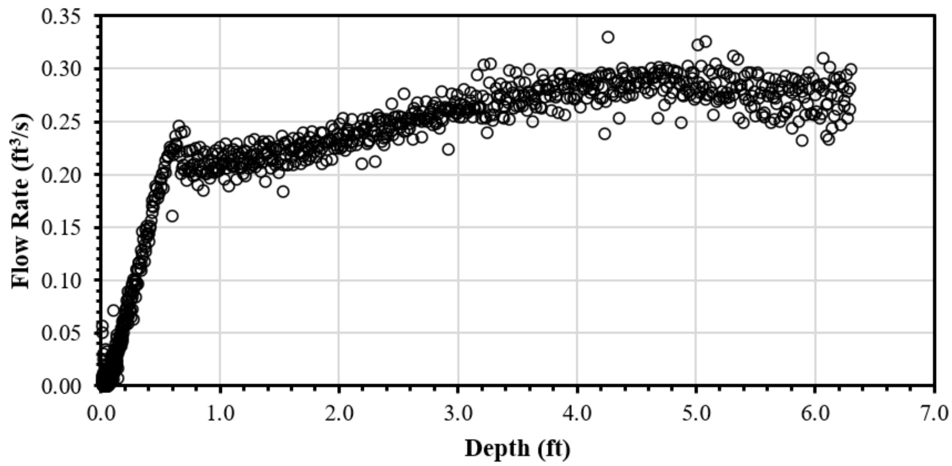

(a) flow rate vs. depth experimental data

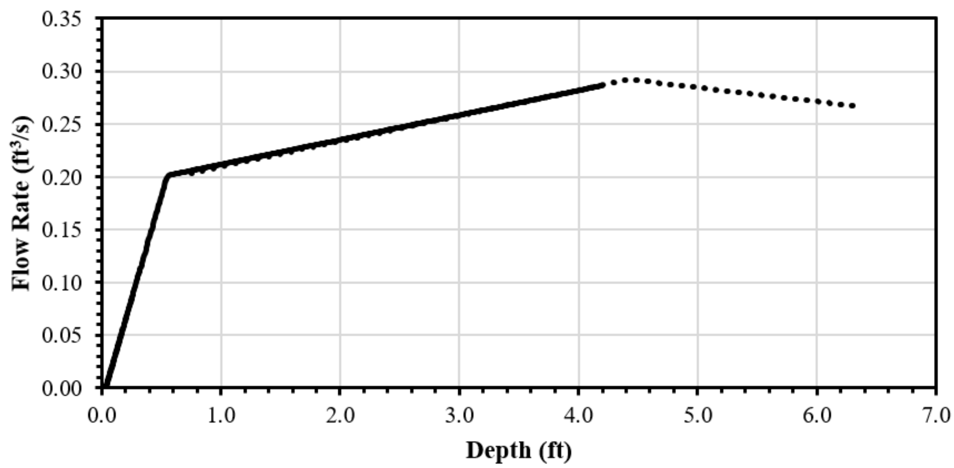

(b) flow rate vs. depth zone 1 and zone 2 with zone 2 and zone 3 two-section model overlays

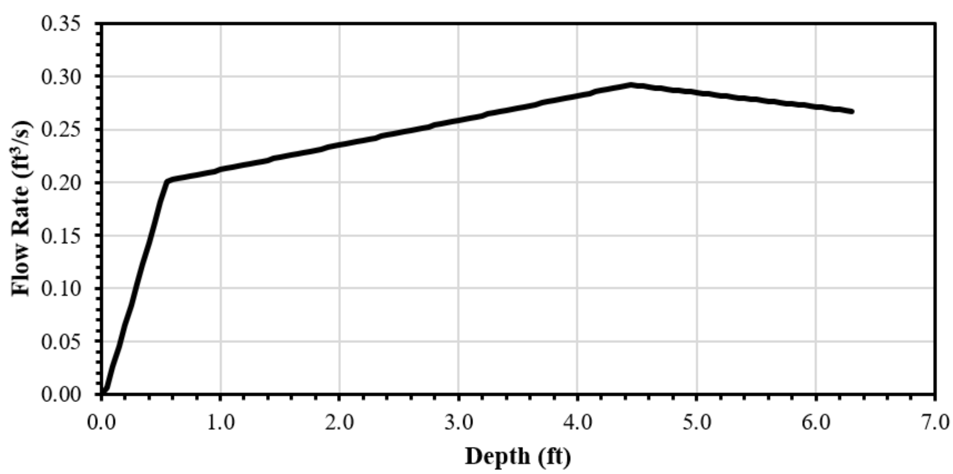

(c) flow rate vs. depth three-section model

Figure 2.17 Flow Rate vs. Depth Experimental Data, Model Overlay and Three-Section Model: 4 in. (10.2 cm) Skimmer; 30% Open; Vented

Note: (b) solid line represents the Zone 1 and Zone 2 model, dotted line represents the Zone 2 and Zone 3 model

A Hill-type saturated model was used to fit the data if flow rates exhibited a plateau at greater depths, and a gradual transition in the flow pattern was observed rather than a distinct breakpoint. This model was also chosen since the data exhibit asymptotic behavior. The Hill-type saturated function is represented by Equation 2.7 (Hill 1910).

$$Q(H)=Q_{max}\frac{H^n}{H^n+H_{50}^n} \qquad \text{Equation 2.7}$$

Where:

$Q(H)$ = flow rate at some depth (ft^3/s or m^3/s)

Q_{max} = maximum flow rate (ft^3/s or m^3/s)

H = depth (ft or m)

n = Hill slope

H_{50} = height at one half of the Q_{max} (ft or m)

Parameters were set so that *n* is greater than or equal to 0. Figure 2.18(a) shows the experimental dataset, which depicts flow rate values at a given depth, represented by the black circles. Figure 2.18(b) shows the final Hill-type saturated model, represented by the solid black line.

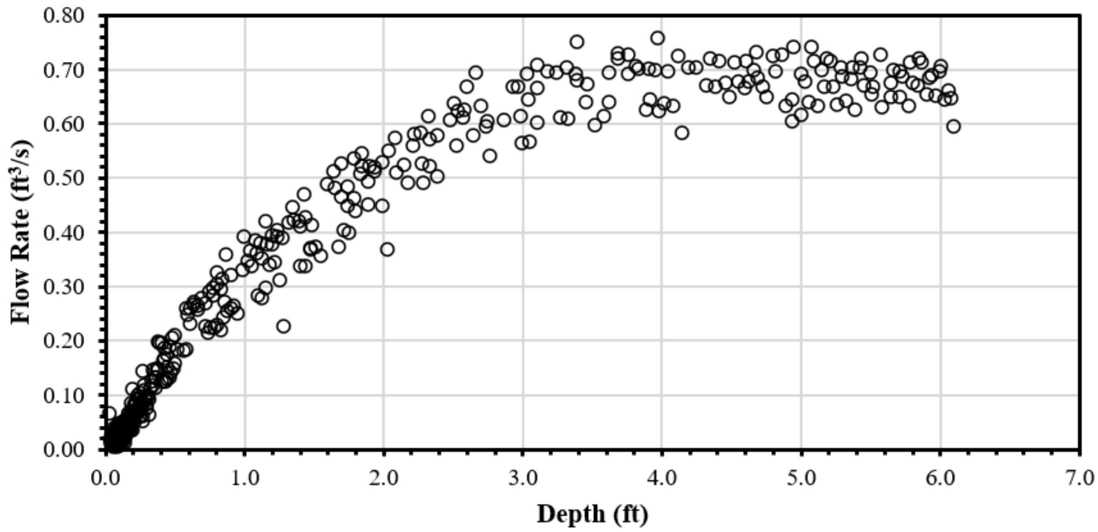

(a) flow rate vs. depth experimental data

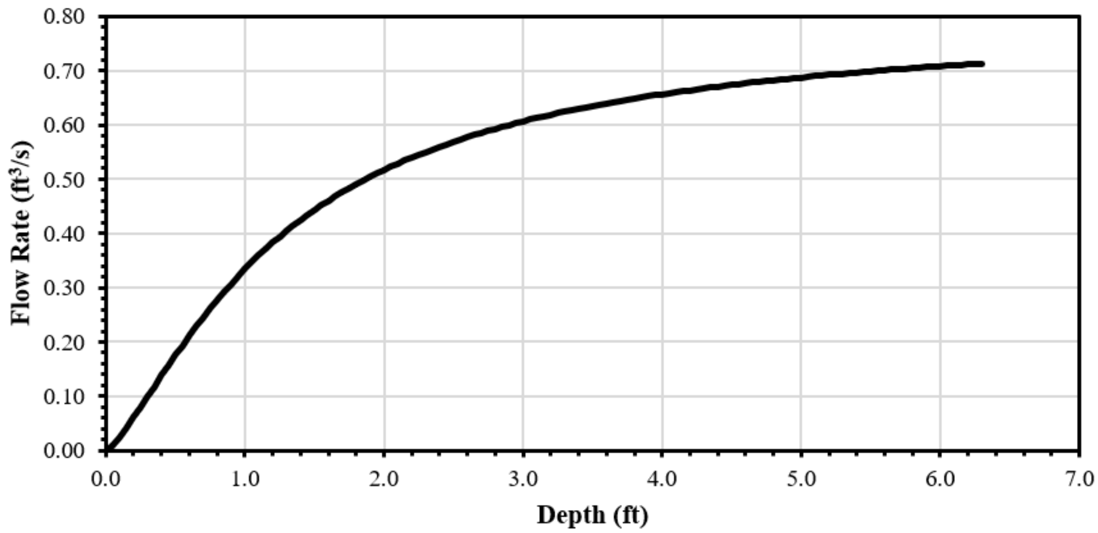

(b) flow rate vs. depth Hill-type saturated model

Figure 2.18 Flow Rate vs. Depth Experimental Data and Hill-Type Saturated Model: 4 in. (10.2 cm) Skimmer; 100% Open; Unvented

Once models were developed for all configurations tested at a given skimmer size, they were combined to examine trends in skimmer behavior across all inlet openings. Models for each inlet opening were combined for a given skimmer size and vent configuration. Figure 2.19 shows the combined flow rate-depth models for the 4 in. (10.2 cm) skimmer, vented configuration.

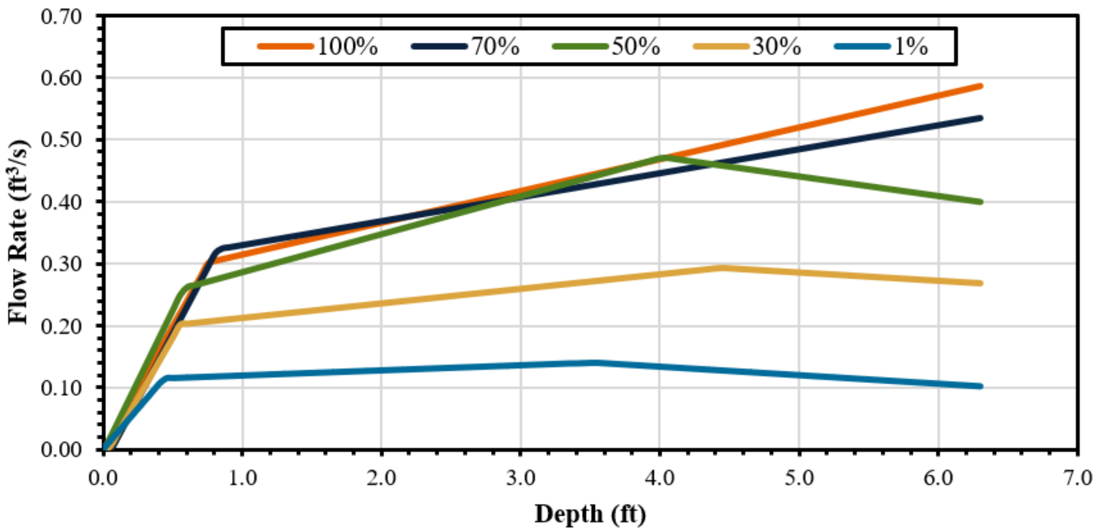

Figure 2.19 Flow Rate vs. Depth Model Comparisons: 4 in. (10.2 cm) Skimmer, Vented

2.4 Results and Discussion

This section summarizes the findings from sediment basin skimmer testing and post-construction skimmer testing. Each configuration was evaluated by observing trends in flow rate as depth decreased, to develop models that predict flow rates at depths less than 7 ft (2.1 m). Additionally, an average flow rate was determined for each sediment basin skimmer configuration, while a maximum flow rate was obtained for each post-construction skimmer configuration.

2.4.1 Sediment Basin Skimmer Results

Eight skimmers intended for use in sediment basins were evaluated to observe differences in overall behavior and flow rates using an adjustable orifice slider. Four orifice openings were assessed on the five largest skimmers, while three were tested on the three smallest skimmers. A total of 29 slider configurations were tested across the eight sediment basin skimmers. Flow rate-depth plots developed for each skimmer configuration were used to create models predicting flow rates at specified depths.

2.4.1.1 Flow Rate Analysis

Once flow rate-depth plots were developed for each skimmer configuration, the datasets were divided into two approximate linear sections, Zone 1 and Zone 2. The plot was divided into two linear sections for modeling purposes and to better portray flow behavior, particularly in Zone 2, which accounts for the majority of dewatering time and is most applicable to real-world performance. Zone 2 behaves approximately linearly due to factors such as entrance and friction losses, barrel angle, and the presence of air in the barrel. With dominating losses, the flow does not simulate ideal simple-orifice conditions; instead, the system responds linearly as depth decreases. The breakpoint where Zone 2 transitions to Zone 1 observed in the plot represents the shift from subcritical to supercritical flow, as confirmed by the dataset and by visual and auditory observations throughout testing. Since the transition describes a gradual shift in flow behavior and varied slightly among individual tests in a triplicate, the transition point was selected visually for consistency and repeatability.

Skimmer performance varied across slider configurations. The depth at which the transition occurred between Zone 1 and Zone 2 differed for each opening. For example, on the 8 in. (20.3 cm) skimmer, when the slider was set to 100% open, the transition occurred at 1.1 ft (0.34 m), 1.0 ft (0.30 m) at 75% open, 1.3 ft (0.40 m) at 50% open, and 2.0 ft (0.61 m) at 25% open. The transition depths likely varied due to changes in the barrel angle, changes in the head acting on the orifice, and airflow affecting the water velocity through the inlet. More specifically, as the skimmer is dewatering, there is less head acting on the orifice. When the skimmer reaches a certain depth, there is increased airflow present in the barrel, and the flow pattern changes. The depth at which this increased airflow is occurring in the barrel changes depending on the size of the orifice using the adjustable slider. Figure 2.20 presents flow rate versus depth models for all skimmer sizes and slider configurations assessed.

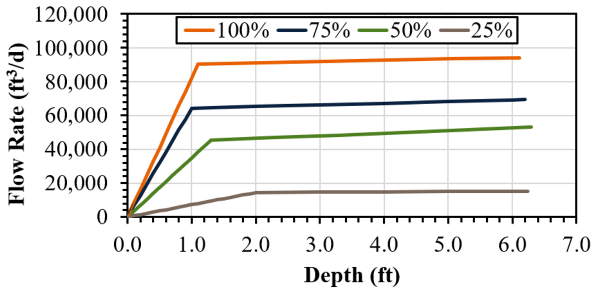

(a) 8 in. (20.3 cm) skimmer flow rate vs. depth model

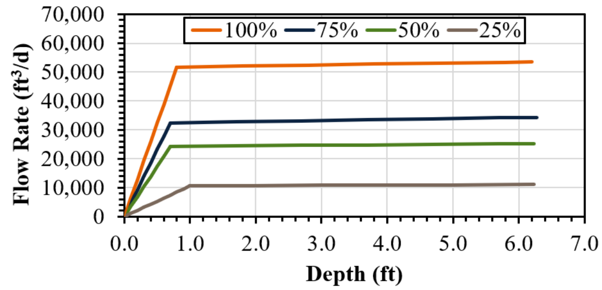

(b) 6 in. (15.2 cm) skimmer flow rate vs. depth model

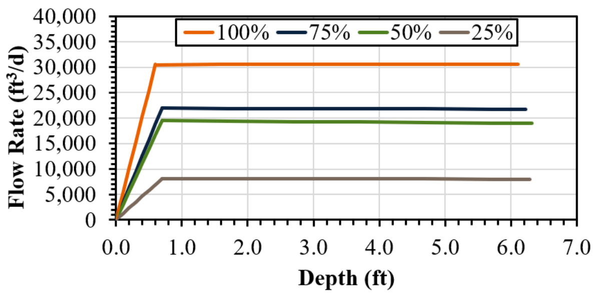

(c) 5 in. (12.7 cm) skimmer flow rate vs. depth model

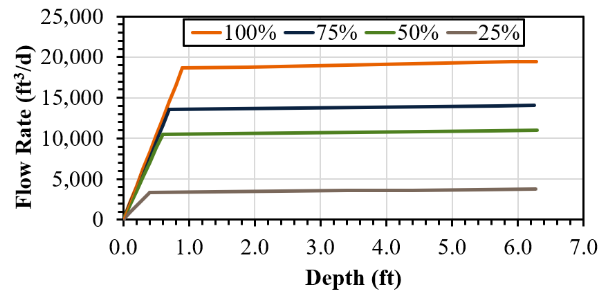

(d) 4 in. skimmer (10.2 cm) flow rate vs. depth model

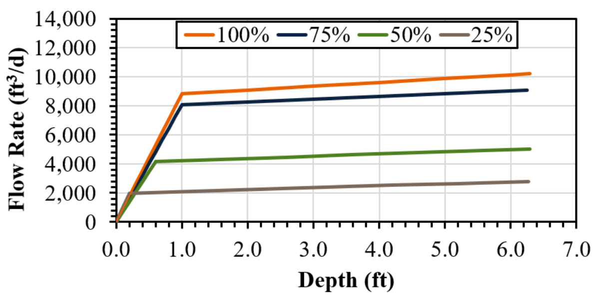

(e) 3 in. (7.6 cm) skimmer flow rate vs. depth model

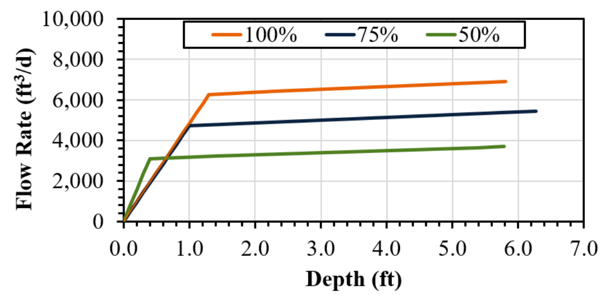

(f) 2.5 in. (6.4 cm) skimmer flow rate vs. depth model

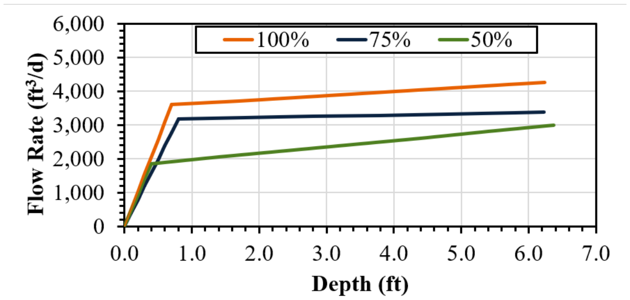

(g) 2 in. (5.1 cm) skimmer flow rate vs. depth model

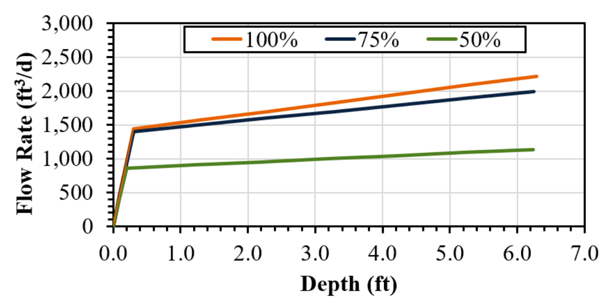

(h) 1.5 in. (3.8 cm) skimmer flow rate vs. depth model

Figure 2.20 Flow Rate vs. Depth Models for All Skimmer Configurations

Figure 2.20 illustrates how each skimmer configuration resulted in a unique relationship between flow and depth. Performance among certain slider configurations was not necessarily evenly distributed. For example, Figure 2.20(c) shows less variation between the 75% and 50% open configurations on the 5 in. (12.7 cm) skimmer than the other opening configurations. However, this is not the case across all skimmer sizes. The model for the 3 in. (7.6 cm) skimmer, as seen in Figure 2.20(e), demonstrates that the 100% and 75% open configurations are much closer in proximity, as well as the 50% and 25% open configurations. Another observation made during testing is how the slider shape alters the orifice. When the slider is set to limit flow, the orifice becomes a weir, which impacts expected skimmer behavior and flow. In addition, the orientation of the slider may impact skimmer performance; since water is no longer being collected through the center of an orifice, air is more likely to enter the inlet on one side. Table 2.3 presents an example of the linear equations and transition depths used to create the models for the 8 in. (20.3 cm) skimmer configuration shown in Figure 2.20.

Table 2.3 Equations used for 8 in. (20.3 cm) Flow vs. Depth Model

	Zone 1		Zone 2	
Slider Configuration	**Linear Equation**	**Parameter, ft (m)**	**Linear Equation**	**Parameter, ft (m)**
100%	y = 82,240.11x	0 ≤ x ≤ 1.1 (0.34)	y = 748.29 + 89,641	x ≥ 1.1 (0.34)
75%	y = 64,323.2x	0 ≤ x ≤ 1.0 (0.30)	y = 977.20x + 63,346	x ≥ 1.0 (0.30)
50%	y = 34,931.26x	0 ≤ x ≤ 1.3 (0.40)	y = 1522.80x + 43,431	x ≥ 1.3 (0.40)
25%	y = 7,249.06x	0 ≤ x ≤ 2.0 (0.61)	y = 190.56x + 14,117	x ≥ 2.0 (0.61)

Once testing was completed and plots were constructed for each skimmer and slider configuration, average flow rates were calculated using data from each triplicate test. Average flow rates were taken using only Zone 2 data. Zone 2 data was used because it most accurately represents skimmer behavior throughout the majority of the test's duration and, likewise, their usage in sediment basins. Table 2.4 displays the Zone 2 average flow rates for each evaluated skimmer configuration.

Table 2.4 Average Flow Rates for Each Skimmer Configuration

Skimmer Size, in. (cm)	Average Flow Rate, ft^3/d (m^3/d)			
	100%	75%	50%	25%
8.0 (20.3)	92,585 (2,622)	67,051 (1,899)	49,052 (1,389)	14,906 (422)
6.0 (15.2)	52,645 (1,491)	32,337 (916)	24,731 (700)	10,875 (308)
5.0 (12.7)	30,526 (864)	21,831 (618)	19,232 (545)	8,059 (228)
4.0 (10.2)	19,063 (540)	13,796 (391)	10,747 (304)	3,562 (101)
3.0 (7.6)	9,517 (269)	8,586 (243)	4,580 (130)	2,347 (66)
2.5 (6.4)	6,605 (187)	5,062 (143)	3,402 (96)	N/A
2.0 (5.1)	3,928 (111)	3,282 (93)	2,363 (67)	N/A
1.5 (3.8)	1,782 (50)	1,655 (47)	981 (28)	N/A

Note: N/A = not applicable

Compared to the manufacturer's previously published flow rates, excluding an adjustable orifice slider or plug, the 6 in. (15.2 cm), 2.5 in. (6.4 cm), 2 in. (5.1 cm), and 1.5 in. (3.8 cm) skimmers had greater experimentally tested flow rates. Conversely, the 8 in. (20.3 cm), 5 in. (12.7 cm), 4 in. (10.2 cm), and 3 in. (7.6 cm) skimmers had lower experimentally tested flow rates. Average flow rates were then used to create a visual representation to distinguish how the flow rates overlap among each skimmer configuration, as seen in Figure 2.21.

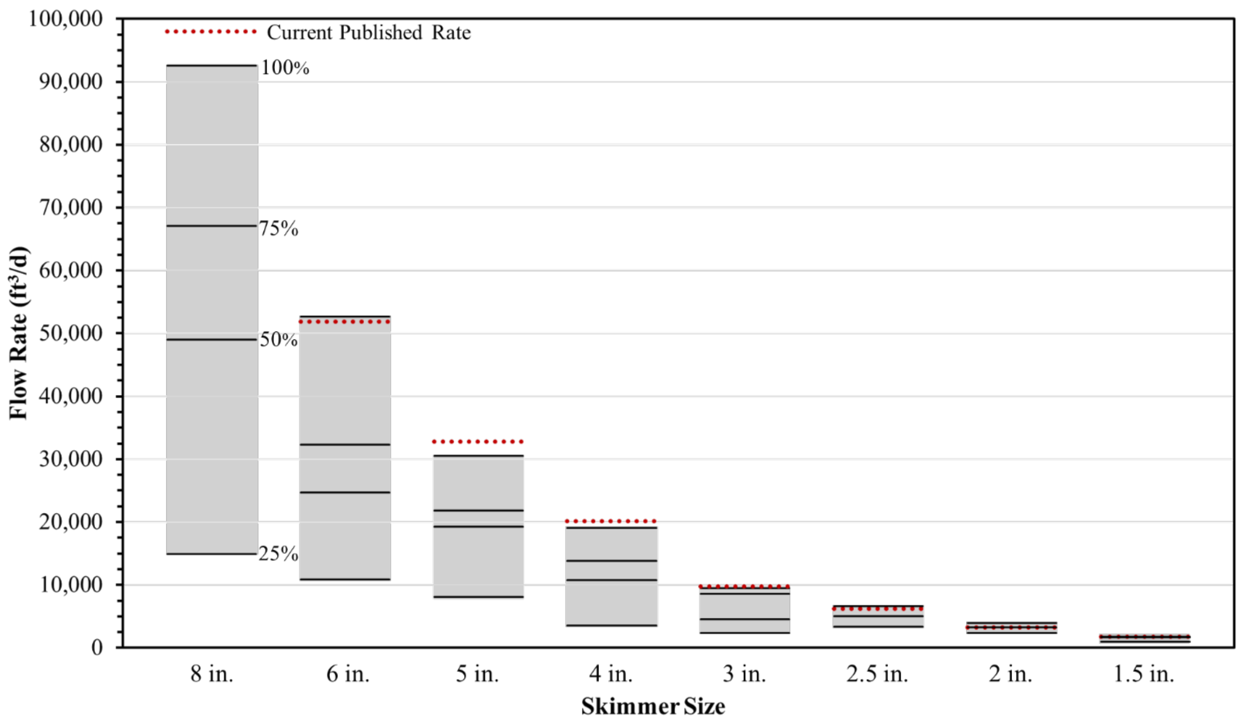

Figure 2.21 Skimmer Flow Rate Overlap Chart

As mentioned previously, skimmer performance varied across each slider configuration. To further investigate these relationships, the average flow rate for each slider opening was plotted as a function of the area of the orifice opening. These plots for each skimmer are shown in Figure 2.22. Overall, the plots indicate that there is not a linear relationship between the average flow and the area of the orifice across each slider opening tested on a given skimmer. This is likely due to factors such as the losses occurring at the inlet from friction, as well as how changes in head affect flow rates as the skimmer is dewatering.

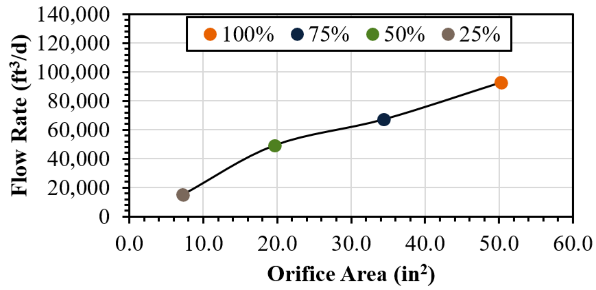

(a) 8 in. (20.3 cm) skimmer flow rate vs. orifice area plot

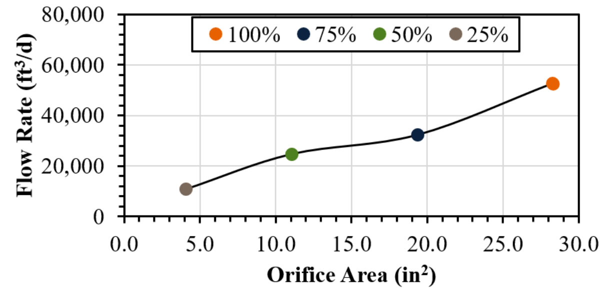

(b) 6 in. (15.2 cm) skimmer flow rate vs. orifice area plot

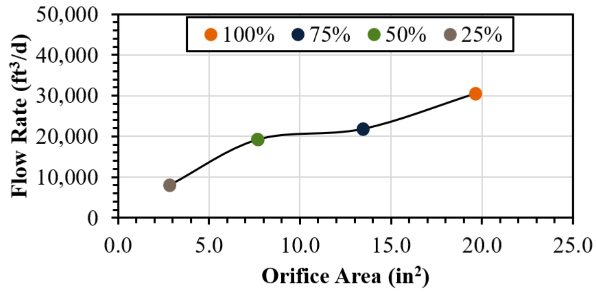

(c) 5 in. (12.7 cm) skimmer flow rate vs. orifice area plot

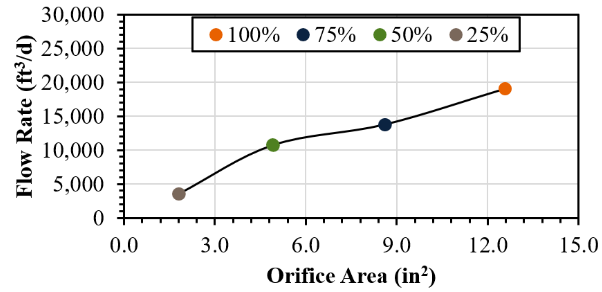

(d) 4 in. skimmer (10.2 cm) flow rate vs. orifice area plot

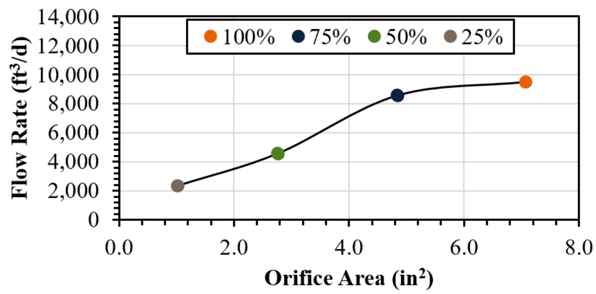

(e) 3 in. (7.6 cm) skimmer flow rate vs. orifice area plot

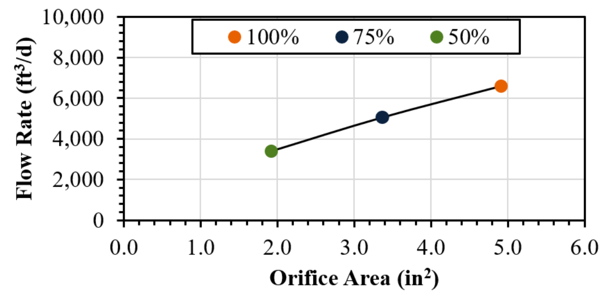

(f) 2.5 in. (6.4 cm) skimmer flow rate vs. orifice area plot

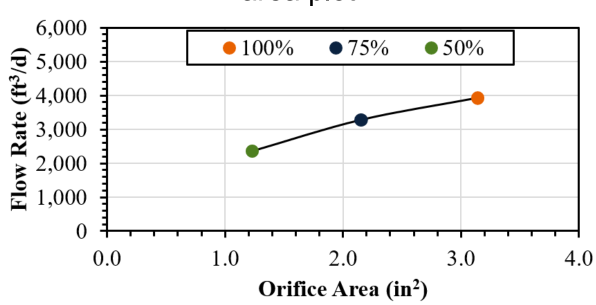

(g) 2 in. (5.1 cm) skimmer flow rate vs. orifice area plot

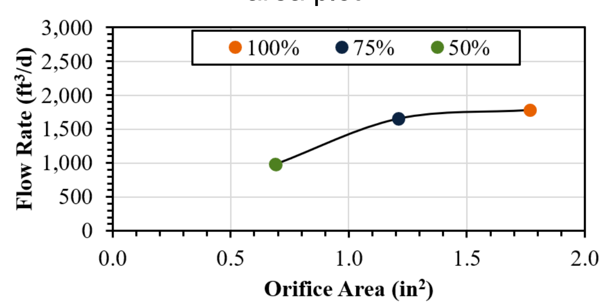

(h) 1.5 in. (3.8 cm) skimmer flow rate vs. orifice area plot

Figure 2.22 Flow Rate vs. Orifice Area Comparisons for All Skimmer Configurations

2.4.1.2 Flow Rate Analysis Using Alternative Methods

An alternative derivative-based method developed for flow rate calculations was considered to reduce outlier values recorded by the Levelogger® and assess the robustness of the trends identified in the previous section. Instead of calculating flow rates using the change in volume every 15 s, depth vs. time plots were constructed using the raw data recorded by the Levelogger®, as seen in Figure 2.23(a). The curve depicted in the depth vs. time plot was divided into two sections: an approximately linear section representing Zone 2 and a section where the line begins to curve and flatten, representing Zone 1. Figure 2.23(b) illustrates the trendlines obtained from Test 1 performed on the 8 in.(20.3 cm) skimmer.

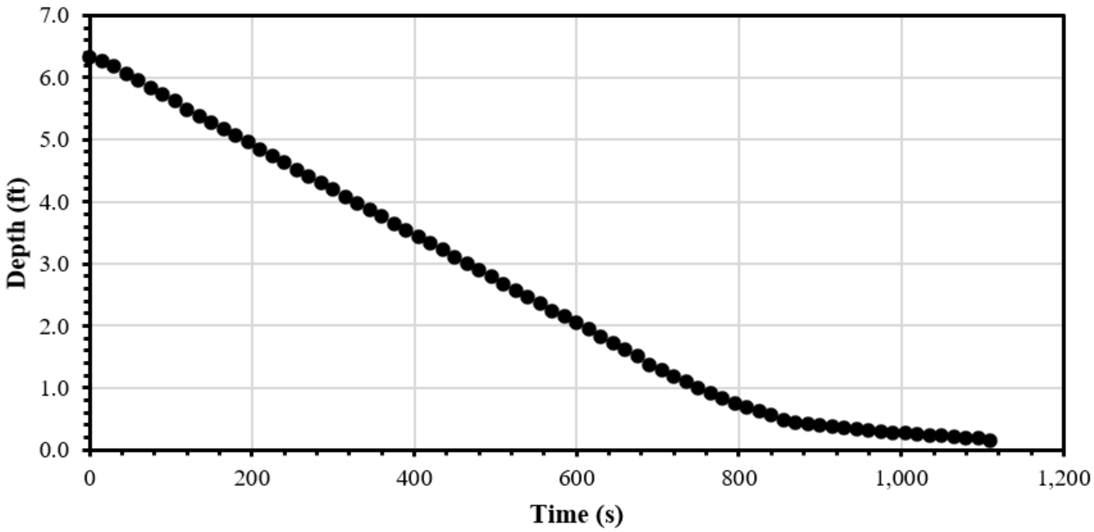

(a) depth vs. time plot

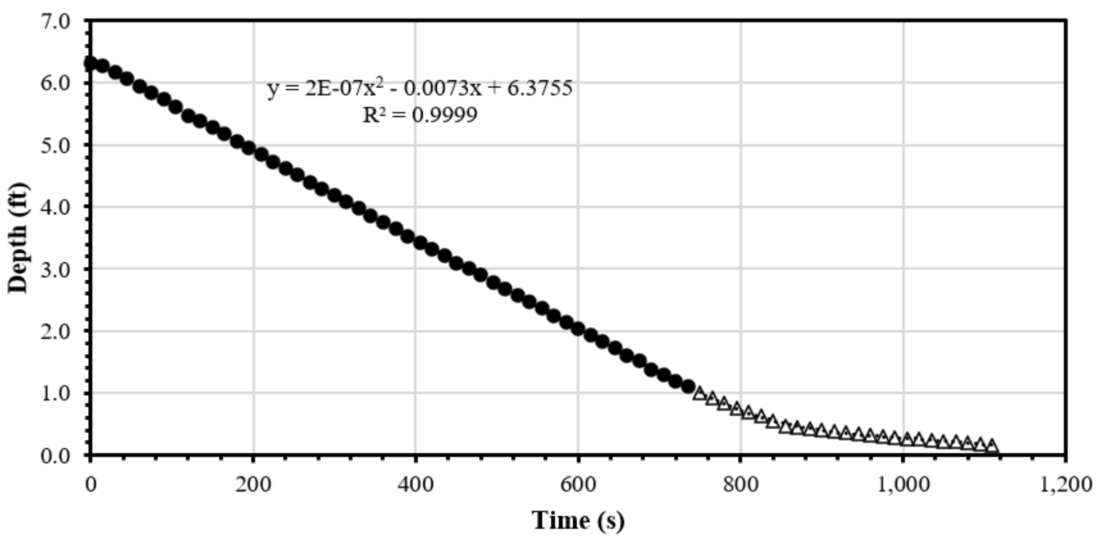

(b) separated depth vs. time plot with linear trendlines

Figure 2.23 Depth vs. Time Charts: 8 in. (20.3 cm) Skimmer, 100% Open

Note: (b) block dots represent Zone 2, triangles represent Zone 1

The trendlines from the Zone 2 section of the depth versus time plot were used to obtain an equation. The derivative of this trendline equation was taken to determine a flow rate at a given depth. Additionally, computed flow rates were used to observe the overall trend that describes skimmer behavior. As mentioned earlier, only the Zone 2 trendline equation was used as Zone 2 most accurately reflects overall skimmer performance. Figure 2.24(a) shows the flow rate versus depth plot created using the newly calculated flow rate values for Test 1 of the 8 in. (20.3 cm) skimmer, 100% open. Flow rate vs. depth plots from each test were then combined to observe differences in each triplicate, as seen in Figure 2.24(b).

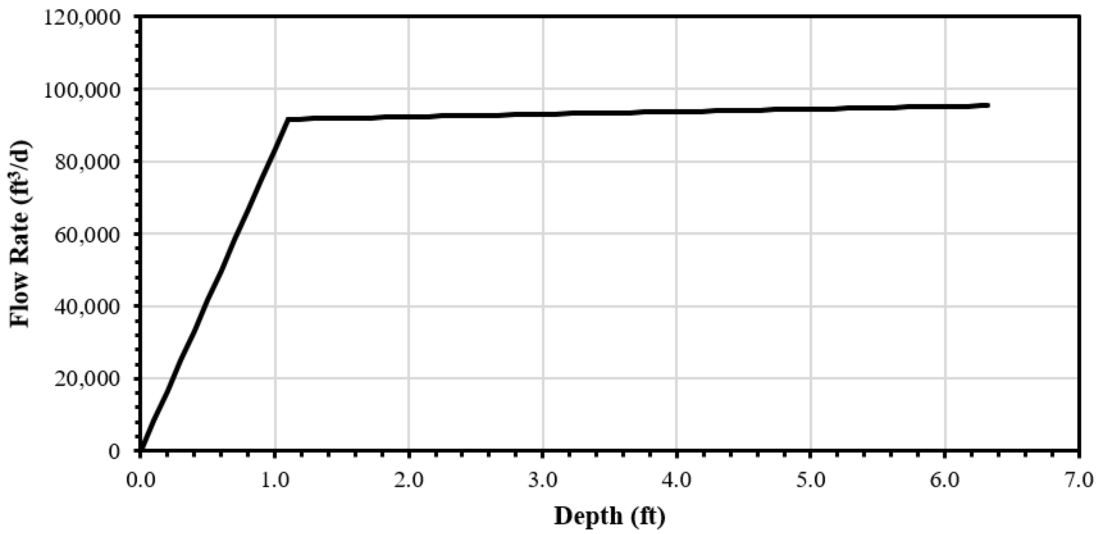

(a) test 1 model

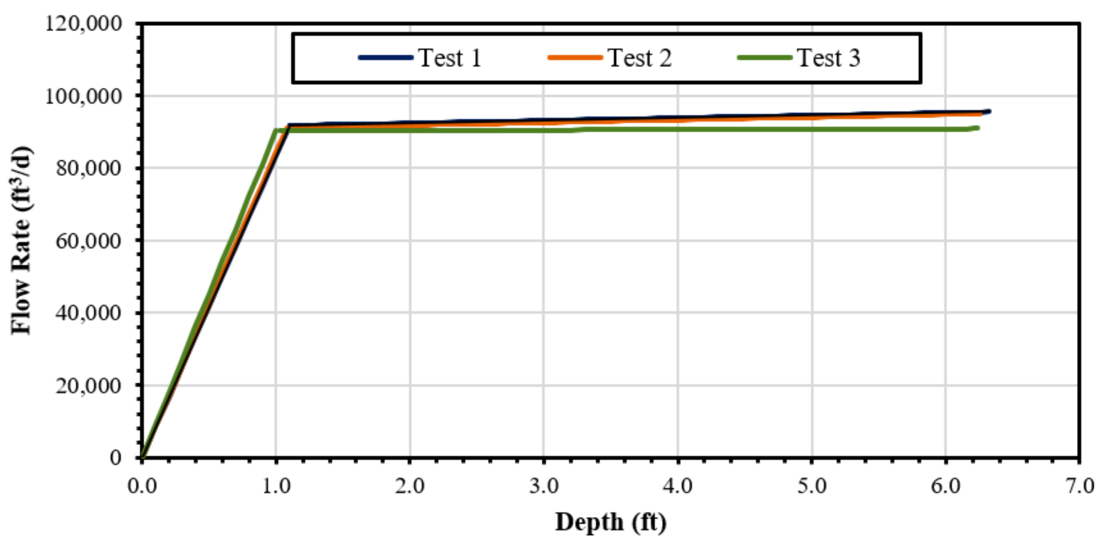

(b) combined triplicate model

Figure 2.24 Flow Rate vs. Depth Models: 8 in. (20.3 cm) Skimmer, 100% Open

Combined flow rate vs. depth plots were then used to obtain a new trendline representing all three tests. This new trendline was used to create a flow rate model similar to that depicted in Figure 2.14(b). This process was repeated for all slider configurations tested on the 8 in. (20.3 cm) skimmer. Flow rate models using this method, referred to as Method 2, were compared with those created using the traditional flow rate calculation method, referred to as Method 1. Figure 2.25 shows a side-by-side comparison of the models created using Method 1 and Method 2.

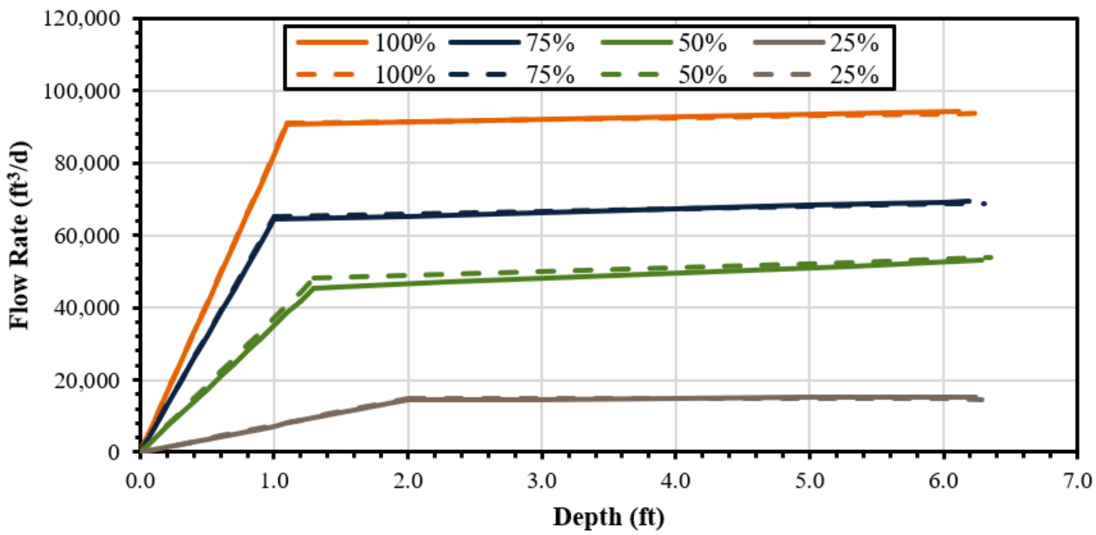

Figure 2.25 Depth vs. Time Charts: 8 in. (20.3 cm) Skimmer, 100% Open

Note: solid lines represent Method 1 flow rate models, dashed lines represent Method 2 flow rate models

Results from each method were found to be similar, as the flow rate model comparison seen in Figure 2.25 shows considerable overlap for each slider configuration. Average flow rates were also computed using Method 2 and were compared to those calculated using Method 1. Table 2.5 displays a comparison of the average flow rates calculated using each method for the 8 in. (20.3 cm) skimmer.

Table 2.5 Average Flow Rates for Each 8 in. (20.3 cm) Skimmer Configuration Using Method 1 and Method 2

Slider Configuration	Average Flow Rate, ft^3/d (m^3/d)	
	Method 1	Method 2
100%	92,585 (2,615)	92,348 (2,622)
75%	67,051 (1,899)	67,004 (1,897)
50%	49,052 (1,389)	50,884 (1,441)
25%	14,906 (422)	14,950 (423)

It should be noted that the process of calculating flow rates using Method 2 is still being optimized. There was difficulty determining where to split the depth vs. time plot to obtain the trendline equation used for derivation. Quantitative methods, such as a second derivative test, were also employed to determine the transition depth. However, these methods yielded transition depths inconsistent with observed skimmer behavior throughout testing. Determining the depth where Zone 2 transitions to Zone 1 is more obvious using Method 1. The main advantage of using Method 2 is eliminating the need to remove outliers, a step that is necessary when calculating flow rates using Method 1. While each method provides relatively similar outflow rates that describe skimmer performance, Method 2 is an approximation with greater ambiguity, while Method 1 provides a more accurate representation of skimmer behavior throughout a given test. It is recommended that Method 2 be further reviewed for future testing.

2.4.2 Post-Construction Skimmer Results

Five post-construction skimmers were assessed to examine their performance and determine their flow rates across various inlet openings and vent configurations. Five inlet sizes were tested on the 8 in (20.3 cm) and 4 in. (10.2 cm) skimmers using removable plates; three inlet sizes were tested on the 3 in. (7.6 cm), 2 in. (5.1 cm), and 1.5 in. (3.8 cm) skimmers. In addition, the 8 in (20.3 cm) and 4 in. (10.2 cm) skimmers were tested with and without a vent across all inlet openings. Furthermore, a total of 29 configurations were tested across the post-construction skimmers. Plots showing flow rate as a function of depth were constructed to examine skimmer behavior throughout testing. Flow rate analysis results of post-construction skimmer testing were divided into two sections: flow rate analysis of the 8 in. (20.3 cm) and 4 in. (10.2 cm) skimmers, and flow rate analysis of the 3 in. (7.6 cm) to 1.5 in. (3.8 cm) skimmers.

2.4.2.1 Large Post-Construction Skimmer Flow Rate Analysis

For the 8 in. (20.3 cm) and 4 in. (10.2 cm) skimmers, models for each inlet opening were compared for vented and unvented configurations. Figure 2.26 illustrates the flow rate model comparisons for the 8 in. (20.3 cm) skimmer, vented and unvented configurations. For the vented comparison, two-section segmented regression models were used for the 100%, 75%, 50%, and 25% inlet openings. Breakpoint depths for the 100%, 75%, 50%, and 25% inlet openings occurred at 0.81 ft (0.25 m), 0.63 ft (0.19 m), 0.88 ft (0.27 m), and 0.70 ft (0.21 m), respectively. A Hill-type saturated model was used for the 1% opening.

Moreover, for the unvented comparison, Hill-type saturated models were used for the 100%, 75%, and 50% openings. Three-section segmented regression models were used for the 25% and 1% openings. For the 25% opening, the first breakpoint occurred at 4.02 ft (1.23 m) and the second breakpoint occurred at 0.66 ft (0.20 m). For the 1% opening, the first breakpoint occurred at 4.91 ft (1.50 m) and the second breakpoint occurred at 0.67 ft (0.20 m). Table 2.6 summarizes the models and their specific equations used to construct the plots in Figure 2.26.

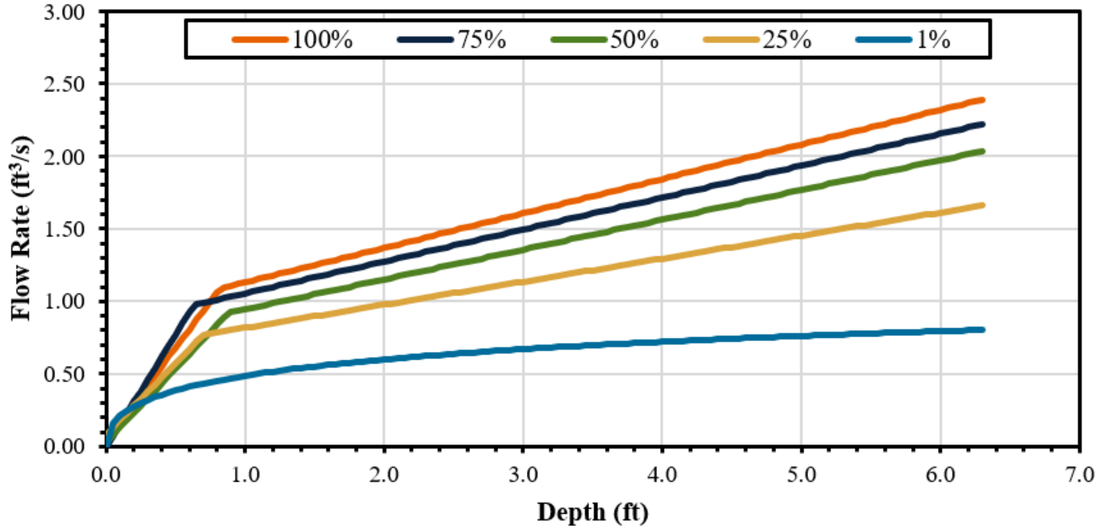

(a) vented model comparison

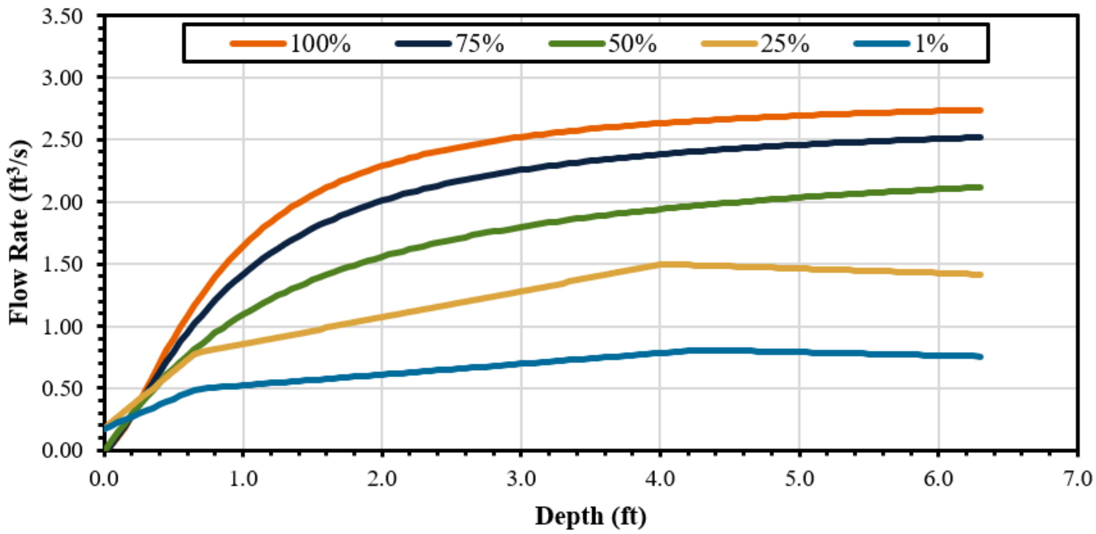

(b) unvented model comparison

Figure 2.26 Flow Rate vs. Depth Model Comparisons: All 8 in. (20.3 cm) Skimmer Configurations

Table 2.6 Flow Rate Model Equations on 8 in. (20.3 cm) Skimmer

Inlet Opening	Vent Config.	Model Type	Equation
100%	Vented	Two-Section	$Q(H) = 0.037 + 1.284H + -1.046[\max(0, H - 0.818)]$
	Unvented	Hill-Type	$Q(H) = 2.850 \frac{H^{1.571}}{H^{1.571} + 0.820^{1.571}}$
75%	Vented	Two-Section	$Q(H) = -0.004 + 1.549H + -1.329[\max(0, H - 0.631)]$
	Unvented	Hill-Type	$Q(H) = 2.686 \frac{H^{1.408}}{H^{1.408} + 0.925^{1.408}}$
50%	Vented	Two-Section	$Q(H) = 0.029 + 1.013x + -0.807[\max(0, H - 0.880)]$
	Unvented	Hill-Type	$Q(H) = 2.456 \frac{H^{1.117}}{H^{1.117} + 1.221^{1.117}}$
25%	Vented	Two-Section	$Q(H) = 0.082 + 0.982H + -0.823[\max(0, H - 0.700)]$
	Unvented	Three-Section	$Q(H) = \begin{cases} H \geq 4.019, 0.645 + 0.212H + -0.249[\max(0, H - 4.019)] \\ H \leq 4.019, 0.175 + 0.927H + -0.714[\max(0, H - 0.658)] \end{cases}$
1%	Vented	Hill-Type	$Q(H) = 1.561 \frac{H^{0.463}}{H^{0.463} + 5.527^{0.463}}$
	Unvented	Three-Section	$Q(H) = \begin{cases} H \geq 4.291, 0.439 + 0.086H + -0.112[\max(0, H - 4.291)] \\ H \leq 4.291, 0.175 + 0.480H + -0.394[\max(0, H - 0.666)] \end{cases}$

Once all models for the 8 in. (20.3 cm) skimmer were completed, they were compared to assess how well they fit the combined datasets and to determine the skimmer's maximum flow rate. This was done by calculating R^2, Root Mean Squared Error (RMSE), and Mean Bias Error (MBE). A summary of the values for each configuration tested on the 8 in. (20.3 cm) skimmer is given in Table 2.7. Overall, results show that the 100% open, unvented configuration had the highest observed maximum flow rate of 2.984 ft^3/s (0.075 m^3/s) and the model maximum flow rate at 2.739 ft^3/s (0.078 m^3/s). Moreover, the 1% open, unvented configuration had the lowest maximum observed flow rate at 0.877 ft^3/s (0.025 m^3/s), while 1% open, vented configuration had the lowest model maximum flow rate at 0.804 ft^3/s (0.023 m^3/s). In addition, statistical parameters across all configurations indicate that the models fit their respective datasets closely, with high R^2 values of at least 0.89, low RMSE values of at most 0.21, and low MBE values of 0 or slightly less than 0. Configurations with negative MBE values have models that slightly underestimate the corresponding datasets.

Table 2.7 Flow Rate and Statistical Comparison for Data and Model on 8 in. (20.3 cm) Skimmer

Inlet Opening	Vent Configuration	Max. Observed Flow Rate, ft^3/s (m^3/s)	Max. Model Flow Rate, ft^3/s (m^3/s)	R^2	RMSE	MBE
100%	Vented	2.637 (0.075)	2.391 (0.068)	0.99	0.17	0.00
	Unvented	2.984 (0.085)	2.739 (0.078)	0.97	0.17	0.00
75%	Vented	2.140 (0.061)	2.222 (0.063)	0.99	0.20	-0.01
	Unvented	2.720 (0.077)	2.517 (0.071)	0.96	0.19	-0.02
50%	Vented	2.025 (0.057)	2.036 (0.058)	0.99	0.21	0.00
	Unvented	2.321 (0.066)	2.117 (0.060)	0.96	0.14	-0.01
25%	Vented	1.626 (0.046)	1.660 (0.047)	1.00	0.10	0.00
	Unvented	1.779 (0.050)	1.498 (0.042)	1.00	0.09	0.00
1%	Vented	0.961 (0.027)	0.804 (0.023)	0.89	0.07	0.00
	Unvented	0.877 (0.025)	0.809 (0.023)	1.00	0.03	0.00

Note: Maximum depth used for models is 6.30 ft (1.92 m)

Similarly, models for vented and unvented configurations were compared for each inlet opening on the 4 in (10.2 cm) skimmer. Figure 2.27 shows the model comparisons for the 4 in (10.2 cm) vented and unvented configurations. Table 2.8 summarizes the model equations used for all configurations tested on the 4 in. (10.2 cm) skimmer. For the vented configuration, two-section segmented regression models were used for the 100% and 70% openings. Breakpoints for the 100% and 70% openings occurred at 0.75 ft (0.23 m) and 0.82 ft (0.25 m), respectively. Three-section segmented regression models were used for the 50%, 30%, and 1% openings. The breakpoints occurred at 4.01 ft (1.22 m) and 0.57 ft (0.17 m) for the 50% opening; 4.42 ft (1.35 m) and 0.55 ft (0.17 m) for the 30% opening; and 3.53 ft (1.08 m) and 0.43 ft (0.13 m) for the 1% opening.

Furthermore, for the unvented configuration, Hill-type saturated models were used for the 100% and 70% openings, while a three-section segmented regression model was used for the 30% and 1% openings. The breakpoints occurred at 4.18 ft (1.22 m) and 0.65 ft (0.17 m) for the 30% opening, and 3.36 ft (1.02 m) and 0.39 ft (0.12 m) for the 1% opening. The 50% opening on the unvented configuration exhibited a unique behavior. For each test performed using this configuration, flow rates above approximately 4.24 ft (1.29 m) were roughly constant, thus showing a horizontal section. The average flow rate value of the entire upper section was used at depths above 4.24 ft (1.29 m) to model this section. At approximately 4.24 ft (1.29 m), a jump occurred, and a two-section segmented regression model was fit to the plot for depths less than 4.24 ft (1.29 m). The reason for this behavior is that the system experienced better airflow and stabilized once the depth reached approximately 4.24 ft (1.29 m).

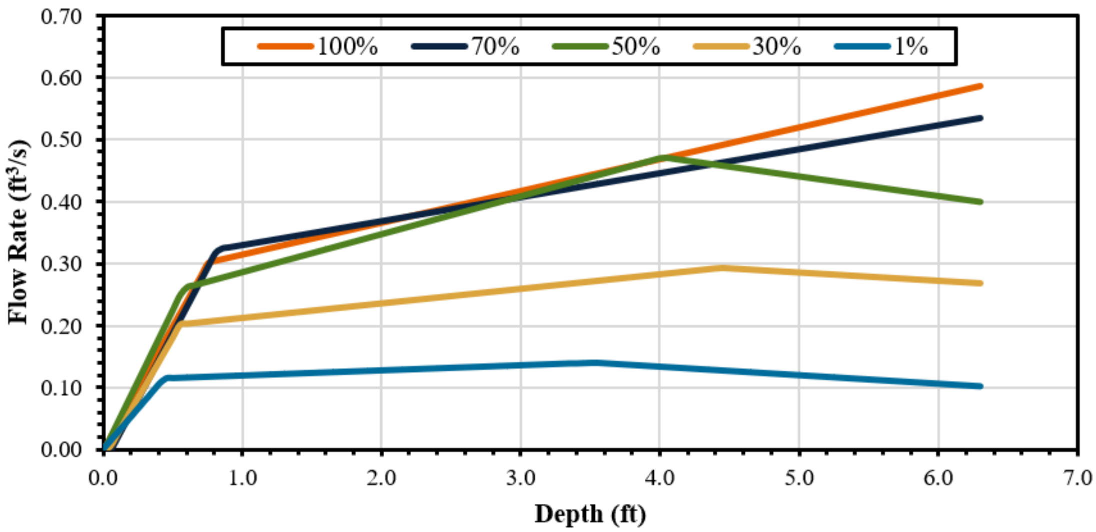

(a) vented model comparison

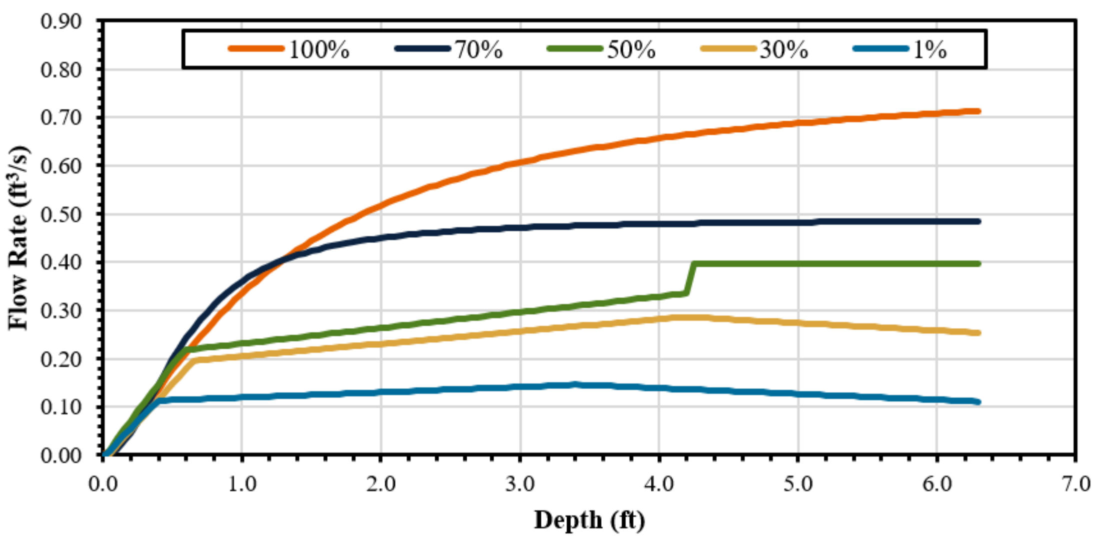

(b) unvented model comparison

Figure 2.27 Flow Rate vs. Depth Model Comparisons: All 4 in. (10.2 cm) Skimmer Configurations

Table 2.8 Flow Rate Model Equations on 4 in. (10.2 cm) Skimmer

Inlet Opening	Vent Config.	Model Type	Equation
100%	Vented	Two-Section	$Q(H) = -0.001 + 0.401H + -0.349[\max(0, H - 0.754)]$
	Unvented	Hill-Type	$Q(H) = 0.793 \frac{H^{1.360}}{H^{1.360} + 1.260^{1.360}}$
70%	Vented	Two-Section	$Q(H) = -0.024 + 0.425H + -0.386[\max(0, H - 0.817)]$
	Unvented	Hill-Type	$Q(H) = 0.489 \frac{H^{2.049}}{H^{2.049} + 0.607^{2.049}}$
50%	Vented	Three-Section	$Q(H) = \begin{cases} H \geq 4.015, & 0.223 + 0.062H + -0.093[\max(0, H - 4.015)] \\ H \leq 4.015, & -0.002 + 0.456H + -0.395[\max(0, H - 0.574)] \end{cases}$
	Unvented	Two-Section & Horizontal	$Q(H) = \begin{cases} H \geq 4.240, & 0.397 \\ H \leq 4.240, & -0.006 + 0.386H + -0.353[\max(0, H - 0.580)] \end{cases}$
30%	Vented	Three-Section	$Q(H) = \begin{cases} H \geq 4.424, & 0.185 + 0.024H + -0.037[\max(0, H - 4.424)] \\ H \leq 4.424, & -0.013 + 0.389H + -0.366[\max(0, H - 0.551)] \end{cases}$
	Unvented	Three-Section	$Q(H) = \begin{cases} H \geq 4.183, & 0.180 + 0.026H + -0.041[\max(0, H - 4.183)] \\ H \leq 4.183, & -0.012 + 0.319H + -0.293[\max(0, H - 0.652)] \end{cases}$
1%	Vented	Three-Section	$Q(H) = \begin{cases} H \geq 3.534, & 0.109 + 0.009H + -0.022[\max(0, H - 3.534)] \\ H \leq 3.534, & 0.001 + 0.261H + -0.252[\max(0, H - 0.433)] \end{cases}$
	Unvented	Three-Section	$Q(H) = \begin{cases} H \geq 3.357, & 0.103 + 0.013H + -0.025[\max(0, H - 3.357)] \\ H \leq 3.357, & -0.005 + 0.301H + -0.290[\max(0, H - 0.393)] \end{cases}$

All models developed for the 4 in. (10.2 cm) skimmer were also compared to assess how well they fit the combined datasets and to determine the skimmer's maximum flow rate using the same parameters used for the 8 in. (20.3 cm) skimmer. A summary of the values for each configuration tested on the 4 in. (10.2 cm) skimmer is given in Table 2.9. The maximum observed and model flow rates achieved on this skimmer were 0.758 ft^3/s (0.021 m^3/s) and 0.713 ft^3/s (0.020 m^3/s), respectively, in the 100% unvented configuration. The 1% vented configuration had the lowest maximum observed and model flow rates at 0.162 ft^3/s (0.005 m^3/s) and 0.139 ft^3/s (0.004 m^3/s), respectively. Statistical parameters across all configurations indicate that the models fit their respective datasets closely, with high R^2 values of at least 0.93, low RMSE values of at most 0.08, and MBE values of 0.

Table 2.9 Flow Rate and Statistical Comparison for Data and Model on 4 in. (10.2 cm) Skimmer

Inlet Opening	Vent Configuration	Max. Observed Flow Rate, ft^3/s (m^3/s)	Max. Model Flow Rate, ft^3/s (m^3/s)	R^2	RMSE	MBE
100%	Vented	0.586 (0.017)	0.585 (0.017)	1.00	0.08	0.00
	Unvented	0.758 (0.021)	0.713 (0.020)	0.98	0.04	0.00
70%	Vented	0.562 (0.016)	0.535 (0.015)	1.00	0.05	0.00
	Unvented	0.686 (0.019)	0.485 (0.014)	0.93	0.05	0.00
50%	Vented	0.489 (0.014)	0.469 (0.013)	1.00	0.03	0.00
	Unvented	0.427 (0.012)	0.397 (0.011)	1.00	0.04	0.00
30%	Vented	0.330 (0.009)	0.292 (0.008)	1.00	0.01	0.00
	Unvented	0.326 (0.009)	0.286 (0.008)	1.00	0.02	0.00
1%	Vented	0.162 (0.005)	0.139 (0.004)	1.00	0.04	0.00
	Unvented	0.186 (0.005)	0.146 (0.004)	1.00	0.03	0.00

Note: Maximum depth used for models is 6.30 ft (1.92 m)

Results indicate that unvented configurations generally had higher maximum observed and model flow rates than vented configurations, with some exceptions, particularly for smaller inlet openings. However, vented configurations tended to exhibit more predictable, stable flow patterns than unvented configurations. This phenomenon likely results from a siphoning effect in unvented configurations. The vent allows air to enter the barrel, simulating open-channel flow conditions and preventing the barrel from completely filling with water. An unvented configuration prevents air from entering the barrel; thus, the flow rate will increase.

It was also observed throughout testing that there were gaps and spaces in both the 8 in. (20.3 cm) and 4 in. (10.2 cm) skimmers, allowing water to enter the skimmers through submerged bottom and side surfaces. Therefore, flow is not confined to the inlet for these skimmers and is controlled by the angle of the barrel. Furthermore, because water does not enter the skimmer exclusively through the inlet, it drains faster. Another observation made during testing is that several configurations experienced weir flow rather than orifice flow through the inlet because the skimmer head sat too high on the water surface. This occurred in all 8 in. (20.3 cm) skimmer configurations, except for the 1% opening, which was fully submerged due to the size and location of this inlet. All inlet configurations on the 4 in. (10.2 cm) skimmer were submerged except for the 100%, unvented configurations. This was likely due to the head sitting higher on the water surface so that air could enter the barrel.

2.4.2.2 Small Post-Construction Skimmer Flow Rate Analysis

As mentioned previously, all three of the smallest post-construction skimmers were tested with a vent, so only the orifice sizes using an adjustable slider were compared. Three inlet sizes were evaluated on each of the three smallest skimmers: 100%, 75%, and 50%. Figure 2.28 displays the model comparison for the 3 in. (7.6 cm) skimmer. The model types used for each configuration include a three-section segmented regression model for the 100% open and a two-section segmented regression model for the 75% open and 50% open. Table 2.10 provides the equations used to model each configuration. On the 100% open model, the first breakpoint depth occurred at 2.70 ft (0.82 m) and the second occurred at 0.83 ft (0.25 m). The breakpoint depths on the 75% and 50% models occurred at 0.75 ft (0.23 m) and 0.51 ft (0.16 m), respectively.

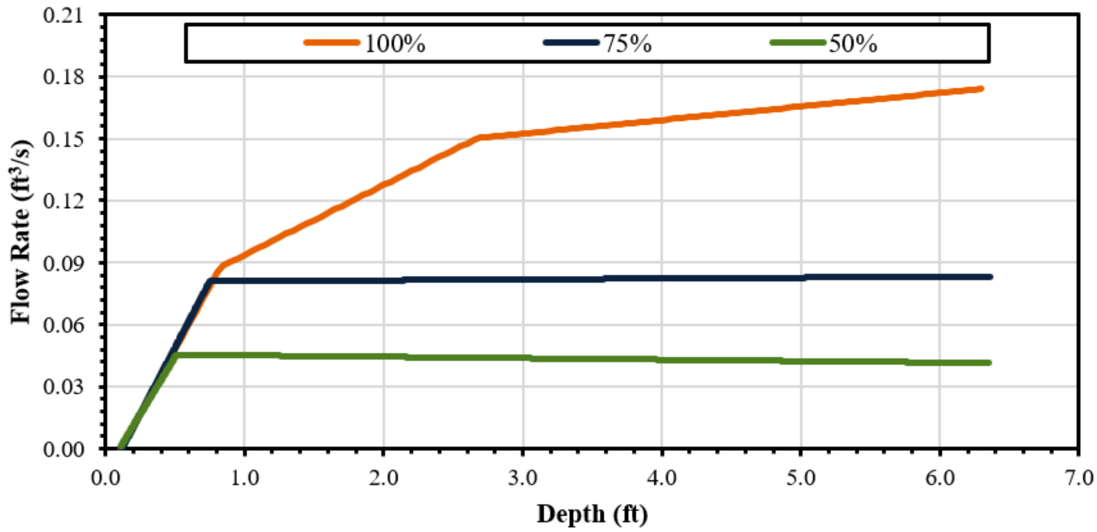

Figure 2.28 Flow Rate vs. Depth Model Comparisons: All 3 in. (7.6 cm) Skimmer Configurations

Table 2.10 Flow Rate Model Equations on 3 in. (7.6 cm) Skimmer

Inlet Opening	Model Type	Equation
100%	Three-Section	$Q(H)=\begin{cases} H \geq 2.698, 0.061 + 0.033H + -0.027[\max(0, H - 2.698)] \\ H \leq 2.698, -0.014 + 0.123H + -0.089[\max(0, H - 0.825)] \end{cases}$
75%	Two-Section	$Q(H)= -0.015 + 0.128H + -0.128[\max(0, H - 0.749)]$
50%	Two-Section	$Q(H)= -0.011 + 0.111H + -0.111[\max(0, H - 0.511)]$

Table 2.11 shows the flow rate results and statistical parameters calculated to distinguish how closely the flow rate models fit their respective datasets. The maximum observed flow rate was 0.229 ft^3/s (0.006 m^3/s) at 100% open. Likewise, the maximum model flow rate was 0.174 ft^3/s (0.005 m^3/s). The lowest observed and model flow rates occurred at 50% open and were 0.078 ft^3/s (0.002 m^3/s) and 0.046 ft^3/s (0.001 m^3/s), respectively. Statistical parameters indicated that models closely fit the respective datasets with R^2 values of approximately 1.0, RMSE values of at most 0.04, and MBE values of 0.

Table 2.11 Flow Rate and Statistical Comparison for Data and Model on 3 in. (7.6 cm) Skimmer

Inlet Opening	Max. Observed Flow Rate, ft^3/s (m^3/s)	Max. Model Flow Rate, ft^3/s (m^3/s)	R^2	RMSE	MBE
100%	0.229 (0.006)	0.174 (0.005)	1.00	0.04	0.00
75%	0.122 (0.003)	0.083 (0.002)	1.00	0.02	0.00
50%	0.078 (0.002)	0.046 (0.001)	1.00	0.02	0.00

Note: Maximum depth used for models is 6.30 ft (1.92 m)

Two-section segmented regression models were used for all three slider openings tested on the 2 in. (5.1 cm) skimmer. Figure 2.29 shows the flow rate model comparisons for the 2 in. (5.1 cm) skimmer, while the equations used to develop the flow rate models are summarized in Table 2.12. The breakpoints for the 100%, 75%, and 50% openings occurred at 1.0 ft (0.30 m), 0.72 ft (0.22 m), and 0.48 ft (0.15 m), respectively.

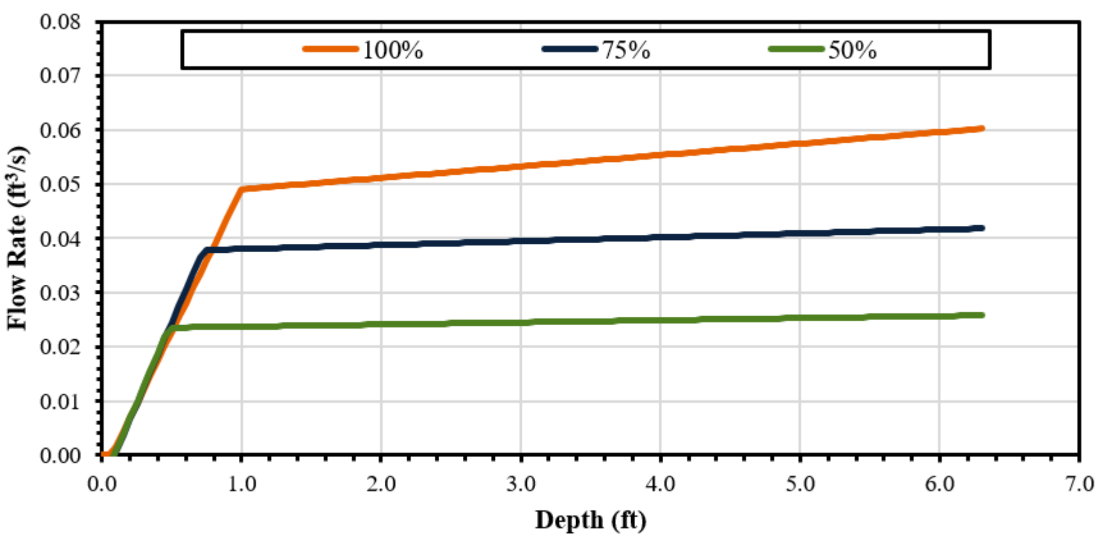

Figure 2.29 Flow Rate vs. Depth Model Comparisons: All 2 in. (5.1 cm) Skimmer Configurations

Table 2.12 Flow Rate Model Equations on 2 in. (5.1 cm) Skimmer

Inlet Opening	Model Type	Equation
100%	Two-Section	$Q(H) = -0.004 + 0.053H + -0.051[\max(0, H - 0.998)]$
75%	Two-Section	$Q(H) = -0.005 + 0.060H + -0.059[\max(0, H - 0.723)]$
50%	Two-Section	$Q(H) = -0.005 + 0.059H + -0.059[\max(0, H - 0.481)]$

Table 2.13 shows the maximum flow rate values and statistical parameters used to determine how close the flow rate models are to the datasets for the 2 in. (5.1 cm) skimmer. The maximum observed and model flow rate was 0.124 ft^3/s (0.004 m^3/s) and 0.060 ft^3/s (0.002 m^3/s), respectively, at 100% open. Moreover, the lowest observed and model flow rates occurred at 50% open and were 0.088 ft^3/s (0.002 m^3/s) and 0.026 ft^3/s (0.001 m^3/s), respectively. Statistical parameters indicated that models closely fit the respective datasets with R^2 values of approximately 1.0, RMSE values of at most 0.04, and MBE values of 0.

Table 2.13 Flow Rate and Statistical Comparison for Data and Model on 2 in. (5.1 cm) Skimmer

Inlet Opening	Max. Observed Flow Rate, ft^3/s (m^3/s)	Max. Model Flow Rate, ft^3/s (m^3/s)	R^2	RMSE	MBE
100%	0.124 (0.004)	0.060 (0.002)	1.00	0.04	0.00
75%	0.089 (0.003)	0.042 (0.002)	1.00	0.02	0.00
50%	0.088 (0.002)	0.026 (0.001)	1.00	0.03	0.00

Note: Maximum depth used for models is 6.30 ft (1.92 m)

Figure 2.30 shows the comparison plot of all orifice openings testing on the 1.5 in. (3.8 cm) skimmer. Likewise, Table 2.14 summarizes the equations used to create the flow rate models for each orifice opening. Two-section segmented regression models were used for the 100% and 75% openings on the 1.5 in. (3.8 cm) skimmer. The breakpoint depths for the 100% and 75% openings occurred at 0.63 ft (0.19 m) and 0.51 ft (0.16 m), respectively. The 50% opening model showed a trend similar to the 4 in. (10.2 cm) skimmer, 50% open, unvented configuration. The flow rates at depths greater than 2.80 ft (0.85 m) were approximately constant; therefore, an average flow rate of this section, 0.021 ft^3/s (0.006 m^3/s), was used to model this approximately horizontal portion of the plot. Furthermore, a two-section segmented regression model was used to model the remainder of the plot at depths less than 2.80 ft (0.85 m). The breakpoint of this model occurred at 0.57 ft (0.17 m).

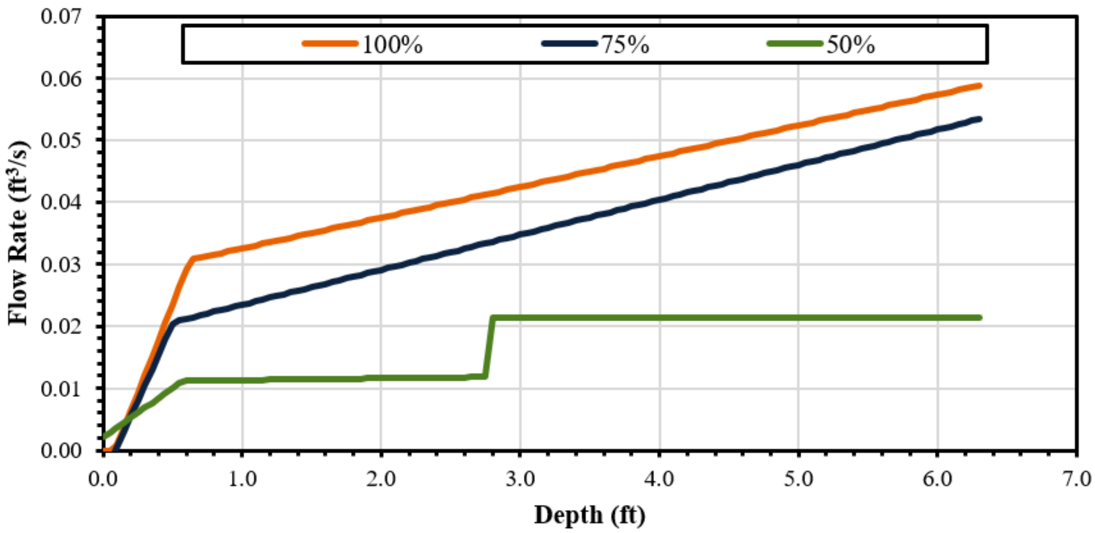

Figure 2.30 Flow Rate vs. Depth Model Comparisons: All 1.5 in. (3.8 cm) Skimmer Configurations

Table 2.14 Flow Rate Model Equations on 1.5 in. (3.8 cm) Skimmer

Inlet Opening	Model Type	Equation
100%	Two-Section	$Q(H) = -0.005 + 0.057H + -0.052[\max(0, H - 0.627)]$
75%	Two-Section	$Q(H) = -0.005 + 0.050H + -0.044[\max(0, H - 0.506)]$
50%	Two-Section & Horizontal	$Q(H) = \begin{cases} H \geq 2.800, 0.021 \\ H \leq 2.800, 0.002 + 0.016H + -0.016[\max(0, H - 0.574)] \end{cases}$

Table 2.15 shows the maximum flow rate values and statistical parameters used to determine how close the flow rate models are to the datasets for the 1.5 in. (3.8 cm) skimmer. The maximum observed and model flow rate was 0.087 ft^3/s (0.002 m^3/s) and 0.059 ft^3/s (0.002 m^3/s), respectively, at 100% open. Moreover, the lowest observed and model flow rates occurred at 50% open and were 0.045 ft^3/s (0.001 m^3/s) and 0.021 ft^3/s

(0.001 m^3/s), respectively. Statistical parameters indicated that models closely fit the respective datasets with R^2 values of approximately 1.0, RMSE values of at most 0.02, and MBE values of 0.

Table 2.15 Flow Rate and Statistical Comparison for Data and Model on 1.5 in. (3.8 cm) Skimmer

Inlet Opening	Max. Observed Flow Rate, ft^3/s (m^3/s)	Max. Model Flow Rate, ft^3/s (m^3/s)	R^2	RMSE	MBE
100%	0.087 (0.002)	0.059 (0.002)	1.00	0.02	0.00
75%	0.074 (0.002)	0.053 (0.002)	1.00	0.02	0.00
50%	0.045 (0.001)	0.021 (0.001)	1.00	0.01	0.00

Note: Maximum depth used for models is 6.30 ft (1.92 m)

Unlike the 8 in. (20.3 cm) and 4 in. (10.2 cm) skimmers, flow was confined to the orifice on the three smallest post-construction skimmers since there are no other gaps that allowed water to enter the head. However, as observed throughout sediment basin skimmer testing, the slider adhered to the orifice alters its shape, which can cause the orifice to become a weir. This impacts expected skimmer behavior and flow. In addition, the orientation of the slider may impact skimmer performance, as water is no longer being collected through the center of an orifice.

2.5 Skimmer Sizing Tools

Once testing and analysis were completed across all skimmer configurations, flow rate models were used to develop interactive skimmer sizing tools for engineers and designers. The aim of developing these skimmer sizing tools was to apply experimentally tested flow rate data and to simplify the selection of an appropriate skimmer size, inlet opening, and vent configuration based on basin parameters. Two sizing tools were ultimately made for the sediment basin and post-construction skimmers: one for engineers and the other for estimators. Each tool was constructed using Microsoft Excel and was designed to be simple and intuitive. The engineer's calculator for both skimmer types was modeled after the skimmer sizing tool developed by Sharpe et al. (2023). However, modifications were made to create a more simplistic sizing tool.

2.5.1 Sediment Basin Skimmer Sizing Tool

Flow rate models developed during data analysis were used to predict the flow rates provided by the sizing tools. Equations obtained from flow rate models, along with the depth at which the transition from Zone 2 to Zone 1 takes place, were the basis of constructing both sediment basin skimmer sizing tools. The adjustable slider openings range from 50% open to 100% open in 5% increments. Furthermore, 25% open data was not programmed into the sizing tools, as flow rates typically fell within the range of the next smallest skimmer. Linear interpolation was used to estimate flow rates in 5% increments falling between experimentally obtained data at 50%, 75%, and 100% openings.

The engineer’s calculator describes the stage-storage relationship that occurs as a skimmer is dewatering a sediment basin. The tool provides the average flow rate, available storage, and design drawdown times. These parameters are necessary for proper sizing and are calculated based on user inputs in the tool. Figure 2.31 illustrates the engineer’s calculator interface after all necessary information is entered. Cells requiring user input are highlighted in blue, while values provided by the tools are highlighted in gray.

Faircloth Skimmer Sizing Tool: Engineer's Calculator

Project Name:		**Designer:**	
Location:		**Date:**	

Skimmer Selection	**User Input**				**Calculator Output**
Faircloth Skimmer Size	8 in.	Max. Target Dewatering Time (hr)	72.0	Avg. Flow Rate (ft^3/d)	92,585
Slider Opening (%)	100%	Min. Target Dewatering Time (hr)	24.0	Orifice Opening (in.)	8.00
Skimmer Start Elevation (ft)	0.0	Calculated Dewatering Time (hr)	50.8		

Sediment Basin Elev. (ft)	Sediment Basin Surface Area (ft^2)	Incremental Storage Vol. (ft^3)	Available Storage Vol. (ft^3)	Dewatering Flow Rate (ft^3/d)	Incremental Dewatering Time (hr)	Cumulative Dewatering Time (hr)
10.0	40,000	19,500	200,000	97,124	4.82	0.00
9.5	38,000	18,500	180,500	96,750	4.59	4.82
9.0	36,000	17,500	162,000	96,376	4.36	9.41
8.5	34,000	16,500	144,500	96,001	4.12	13.77
8.0	32,000	15,500	128,000	95,627	3.89	17.89
7.5	30,000	14,500	112,500	95,253	3.65	21.78
7.0	28,000	13,500	98,000	94,879	3.41	25.43
6.5	26,000	12,500	84,500	94,505	3.17	28.85
6.0	24,000	11,500	72,000	94,131	2.93	32.02
5.5	22,000	10,500	60,500	93,757	2.69	34.96
5.0	20,000	9,500	50,000	93,382	2.44	37.64
4.5	18,000	8,500	40,500	93,008	2.19	40.08
4.0	16,000	7,500	32,000	92,634	1.94	42.28
3.5	14,000	6,500	24,500	92,260	1.69	44.22
3.0	12,000	5,500	18,000	91,886	1.44	45.91
2.5	10,000	4,500	12,500	91,512	1.18	47.35
2.0	8,000	3,500	8,000	91,138	0.92	48.53
1.5	6,000	2,500	4,500	90,763	0.66	49.45
1.0	4,000	1,500	2,000	82,240	0.44	50.11
0.5	2,000	500	500	41,120	0.29	50.55
0.0	0	0	0			50.84

Figure 2.31 Sediment Basin Engineer’s Calculator Sizing Tool

To begin, the user must enter their sediment basin parameters, including elevation and corresponding surface area at each stage. Once this information is input, incremental storage volume and available storage volume are calculated in their respective columns. Incremental storage volume is calculated using the average end area method, as seen in Equation 2.8. This method was used to account for irregular sediment basin shapes, so that the designer can use information from the contours of their specific site (Kilgore et al. 2024). Available storage volume is computed by summing the incremental volume at each cross-section at the greatest elevation, and subsequently subtracting the available storage volume and incremental storage volume of the upper cross-section.

$$V=\frac{A_1+A_2}{2}\times h \qquad \text{Equation 2.8}$$

Where:

V = incremental volume (ft^3 or m^3)

A_1 = area of upper cross section (ft^2 or m^2)

A_2 = area of lower cross section (ft^2 or m^2)

h = elevation difference among cross sections (ft or m)

Next, the user selects their desired skimmer size and slider opening from their respective dropdown lists. The user can choose one of eight sediment basin skimmer sizes, along with an adjustable slider opening ranging from 50% to 100%. The skimmer size and slider opening selections are programmed in Excel so that their corresponding flow rates are used. The tool supplies the average flow rate and orifice opening in inches based on the selected skimmer size and slider opening. Additionally, the dewatering flow rate column will be populated based on the selected skimmer configuration and the basin elevation. These flow rates are determined using the flow rate models developed from the experimental data for the given skimmer configuration. Once the skimmer configuration is selected, the user can specify a skimmer start elevation, which determines the depth at which the skimmer begins dewatering in the sediment basin. The user may then enter anticipated maximum and minimum dewatering times. Based on previously entered parameters, the tool will indicate whether the calculated dewatering time falls within the maximum and minimum target dewatering times; the cell will turn red if the value falls outside the desired range or green if the value falls within the range. The calculated dewatering time is determined by the incremental and cumulative dewatering time columns. Incremental dewatering time is calculated by dividing the incremental storage volume by the dewatering flow rate. Cumulative dewatering time is the sum of the incremental dewatering time and the accumulated dewatering time at the upper cross-section. The final design drawdown time is the cumulative dewatering time at the basin's minimum elevation, as input by the user.

The tool also provides a graph that illustrates stage-storage discharge over time, providing the user with a visual summary of the results. The graph automatically updates as the user changes the highlighted blue cells; therefore, the user can adjust the design parameters if necessary. Figure 2.32 shows the resulting stage-storage versus time graph based on the parameters input in the tool, as seen in Figure 2.31. Furthermore, a logical flowchart was created to simplify the process of sizing an appropriate skimmer using the engineer's calculator, as seen in Figure 2.33.

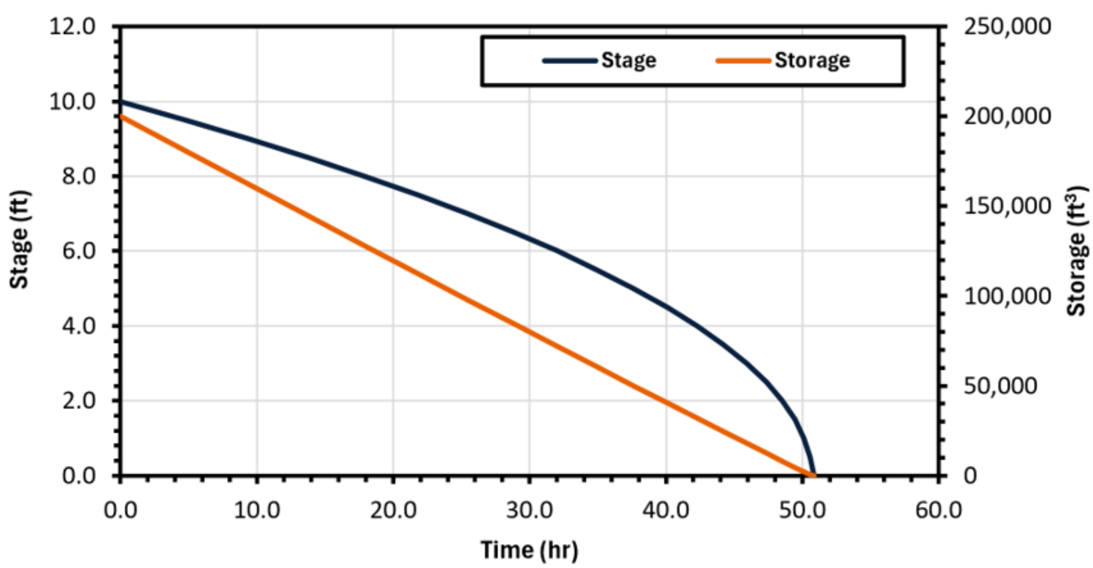

Figure 2.32 Stage-Storage Graph Based on Calculator Output

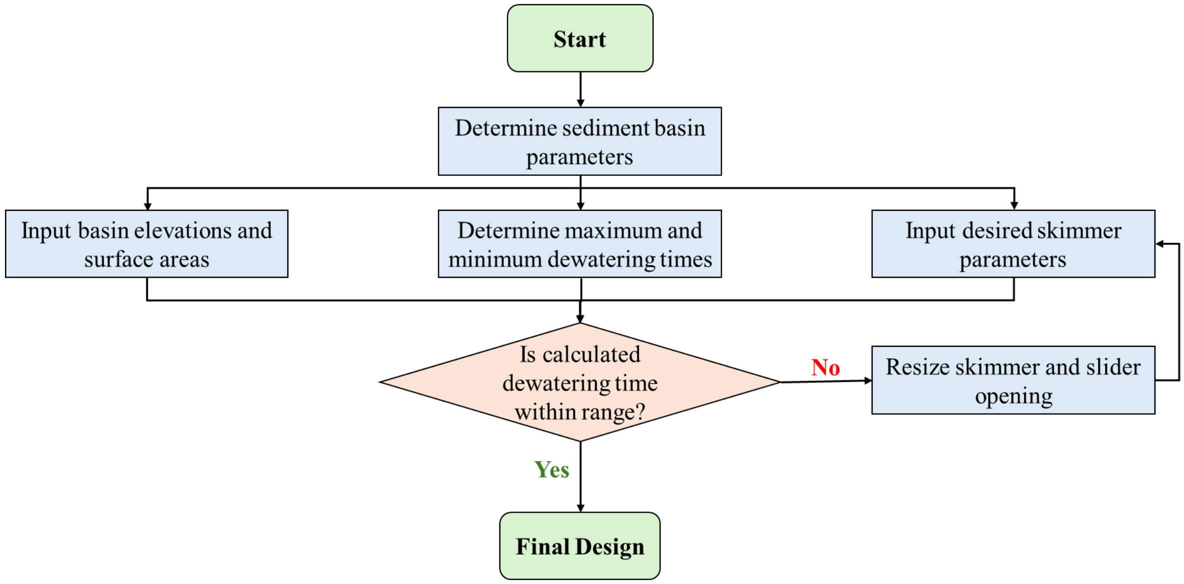

Figure 2.33 Engineer's Calculator Logic Flow Chart

The estimator's calculator is simpler than the engineer's calculator. This tool was intended to provide designers with a skimmer size and an adjustable slider opening based on sediment basin volume and time to dewater. This tool allows users to enter a known basin volume or calculate the sediment basin volume based on geometry parameters. Like the engineer's calculator, user input boxes are highlighted in blue while values yielded by the sizing tool are highlighted in gray. Figure 2.34 shows the estimator's calculator interface when the basin volume is known, as well as when the basin volume must be computed.

Skimmer Sizing Tool: Estimator's Calculator

Project Name:	Designer:
Location:	Date:

Basin Parameters	**User Input**	Basin Parameters (Manual)			**Calculator Output**
Is Required Basin Volume Known?	Yes				
Known Basin Volume (ft^3)	40,000				
Time to drain (days)	2.0				
Final Basin Volume (ft^3)	40,000				

Recommended Skimmer and Orifice Opening					
Skimmer Size	5 in.	Previously Published Equivalent Skimmer Size	4 in.	Avg. Flow Rate (ft^3/d)	19,752
Slider Opening (%)	55%	Previously Published Equivalent Orifice Size (in.)	2.0	Previously Published Equivalent Orifice Size (%)	50%

(a) known required basin volume example

Skimmer Sizing Tool: Estimator's Calculator

Project Name:	Designer:
Location:	Date:

Basin Parameters	**User Input**	Basin Parameters (Manual)			**Calculator Output**
Is Required Basin Volume Known?	No	Bottom Width (ft)	50.0	Side Slopes (H:V)	3.0
Known Basin Volume (ft^3)		Bottom Length (ft)	70.0	Depth (ft)	7.0
Time to drain (days)	2.0	Calculated Basin Volume (ft^3)	46,256		
Final Basin Volume (ft^3)	46,256				

Recommended Skimmer and Orifice Opening					
Skimmer Size	5 in.	Previously Published Equivalent Skimmer Size	5 in.	Avg. Flow Rate (ft^3/d)	21,831
Slider Opening (%)	75%	Previously Published Equivalent Orifice Size (in.)	2.1	Previously Published Equivalent Orifice Size (%)	42%

(b) unknown required basin volume example

Figure 2.34 Sediment Basin Estimator's Calculator Sizing Tool

The user must start by selecting whether the sediment basin's volume is known or unknown. If the basin volume is known, the volume must be entered in the respective cell. If the volume of the sediment basin is unknown, the user will input additional geometry parameters used in Equation 2.9 to determine an approximate volume.

$$V= LWD+(L+W)ZD^2+\frac{4}{3}Z^2D^3 \qquad \text{Equation 2.9}$$

Where:

V = volume at a specific depth (ft^3 or m^3)

L = bottom length (ft or m)

W = bottom width (ft or m)

D = depth (ft or m)

Z = horizontal- to- vertical ratio of the side slopes

This equation assumes a trapezoidal basin geometry with a rectangular bottom (Connecticut Department of Transportation 2000). It should be noted that this tool provides the total volume, not the required volume of the sediment basin, and professional judgment should be applied when selecting skimmer size. Once the basin volume has been determined, the user will input the desired dewatering time.

After all basin parameters have been entered, the tool provides the recommended skimmer size and orifice opening. The tool has been programmed to select the skimmer and orifice sizes based on the flow rate calculated from the basin volume and time to dewater. The tool will select the skimmer with the next lowest average flow rate. This was done as a conservative measure so that the minimum dewatering time requirements are met. In addition, the tool will supply an equivalent skimmer size and orifice opening using previously published data and orifice opening calculations. This information is based on a previously used orifice design in which a customizable hole could be drilled into an orifice plug. The average flow rate of the chosen skimmer and orifice opening is also provided. Figure 2.35 shows a logical flowchart depicting the steps needed to use the estimator's calculator.

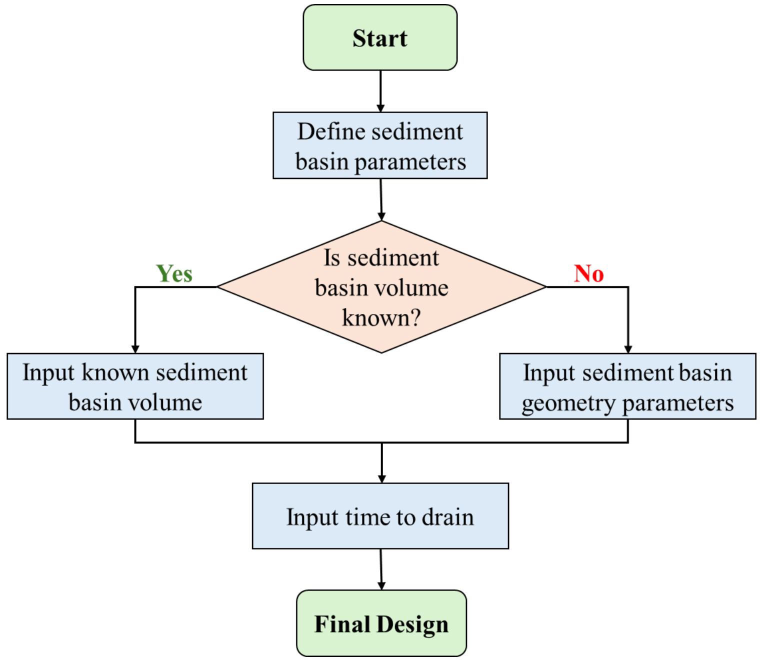

Figure 2.35 Logical Flowchart for Sediment Basin Skimmer Sizing Tool Use

2.5.2 Post-Construction Skimmer Sizing Tool

Like the sediment basin skimmer sizing tools, all flow rate models developed through data analysis were used to predict the flow rates provided by the sizing tools. Flow rate model equations served as the foundation for developing the post-construction skimmer sizing tools. The skimmer sizes incorporated in each tool include all skimmer sizes evaluated; however, the 8 in. (20.3 cm) and 4 in. (10.2 cm) skimmers were programmed so that vented and unvented configurations are separate options. The inlet openings programmed into both tools were dependent on the skimmer size. For the 8 in. (20.3 cm) and 4 in. (10.2 cm) skimmers, the inlet sizes ranged from 25% or 30% to 100%, respectively; however, the inlet sizes ranged from 50% to 100% for the 3 in. (7.6 cm), 2 in. (5.1 cm), and 1.5 in. (3.8 cm) skimmers. The 1% inlet opening was omitted from the 8 in. (20.3 cm) and 4 in. (10.2 cm) skimmer inlet ranges since these sizes will not be made available by the manufacturer. Linear interpolation was used to estimate flow rates in 5% increments falling between experimentally obtained data at evaluated inlet openings.

The engineer's calculator for the post-construction skimmers was based on the sediment basin skimmer engineer's calculator, with a few modifications to improve usability. The tool describes the stage-storage relationship as the skimmer dewaters a detention basin. This tool provides maximum skimmer flow rate, average flow rate, available storage, and design drawdown times. One minor difference made from the sediment basin skimmer calculator is that all flow rates are shown in cubic feet per second instead of cubic feet per day. In addition, the maximum target dewatering time, minimum dewatering time, and calculated dewatering times are entered and presented in days rather than hours. Figure 2.36 shows the post-construction engineer's calculator interface. Cells requiring user input are highlighted in blue, while values provided by the tools are highlighted in gray.

Faircloth Skimmer Sizing Tool: Engineer's Calculator

Project Name:	**Designer:**
Location:	**Date:**

Basin Elev. & Skimmer Selection	**User Input**				**Calculator Output**	
Top Basin Elevation (ft)	10.0	Max. Target Dewatering Time (day)	5.0	Max. Flow Rate (ft^3/s)	2.84	
Faircloth Skimmer Size	8 in. Vented	Min. Target Dewatering Time (day)	1.0	Avg. Flow Rate (ft^3/s)	1.75	
Inlet Opening (%)	55%	Calculated Dewatering Time (day)	1.12			

Detention Basin Elev. (ft)	Detention Basin Surface Area (ft^2)	Incremental Storage Vol. (ft^3)	Available Storage Vol. (ft^3)	Dewatering Flow Rate (ft^3/s)	Incremental Dewatering Time (hr)	Cumulative Dewatering Time (hr)
10.0	40,000	19,500	200,000	2.84	1.90	0.00
9.5	38,000	18,500	180,500	2.74	1.88	1.90
9.0	36,000	17,500	162,000	2.64	1.84	3.78
8.5	34,000	16,500	144,500	2.53	1.81	5.62
8.0	32,000	15,500	128,000	2.43	1.77	7.43
7.5	30,000	14,500	112,500	2.32	1.73	9.21
7.0	28,000	13,500	98,000	2.22	1.69	10.94
6.5	26,000	12,500	84,500	2.11	1.64	12.63
6.0	24,000	11,500	72,000	2.01	1.59	14.27
5.5	22,000	10,500	60,500	1.91	1.53	15.86
5.0	20,000	9,500	50,000	1.80	1.46	17.39
4.5	18,000	8,500	40,500	1.70	1.39	18.86
4.0	16,000	7,500	32,000	1.59	1.31	20.25
3.5	14,000	6,500	24,500	1.49	1.21	21.56
3.0	12,000	5,500	18,000	1.38	1.10	22.77
2.5	10,000	4,500	12,500	1.28	0.98	23.87
2.0	8,000	3,500	8,000	1.18	0.83	24.85
1.5	6,000	2,500	4,500	1.07	0.65	25.68
1.0	4,000	1,500	2,000	0.97	0.43	26.32
0.5	2,000	500	500	0.58	0.24	26.75
0.0	0	0	0	0.02	0.00	26.99

Figure 2.36 Post-Construction Engineer's Calculator Sizing Tool

The procedure for designing a skimmer using this tool is also similar to that described for the sediment basin engineer's calculator. One key modification made to the post-construction version of the engineer's calculator is that the user must first select a top elevation of the basin. Once the top elevation has been entered, the tool will automatically fill in values in the detention basin elevation column. In addition, the option skimmer start elevation was removed because it was deemed unnecessary and could cause confusion.

Moreover, the post-construction engineer's calculator features a graph depicting the stage-storage relationship over time as the detention basin dewaters, providing a comprehensive summary of the results. This graph also updates in real time as the user changes basin and skimmer parameters. Figure 2.37 shows the stage-storage graph based on the information input in the engineer's calculator interface, as seen in Figure 2.36.

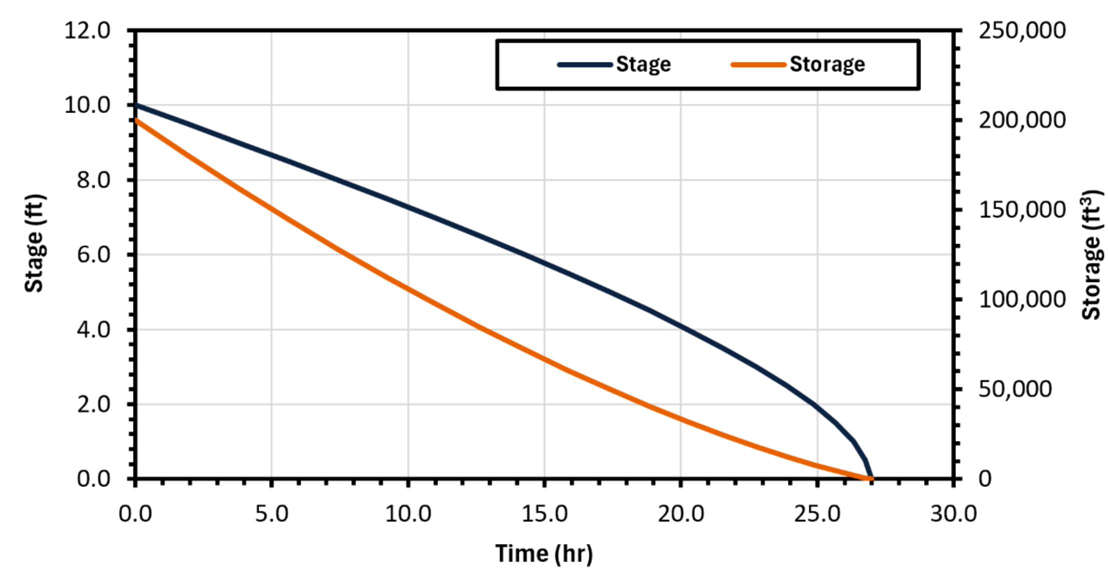

Figure 2.37 Stage-Storage Graph Based on Calculator Output

The post-construction estimator's calculator is also similar to that designed for the sediment basin skimmers. This tool was designed to provide designers with a skimmer size and an inlet opening based on detention basin depth, volume, and time to dewater. Like the sediment basin equivalent tool, this tool allows users to enter a known basin volume or calculate the sediment basin volume based on geometry parameters. Figure 2.38 shows the estimator's calculator interface when the basin volume is known, as well as when the basin volume must be computed. User input boxes are highlighted in blue, while values yielded by the sizing tool are highlighted in gray.

Post-Construction Skimmer Sizing Tool: Estimator's Calculator			
Project Name:		Designer:	
Location:		Date:	

Basin Parameters	**User Input**	Basin Parameters (Manual)			**Calculator Output**
Is Required Detention Volume Known?	Yes				
Basin Depth (ft)	10.0				
Known Detention Volume (ft^3)	40,000				
Desired Time to Drain (days)	2.0				
Final Detention Volume (ft^3)	40,000				

Recommended Skimmer and Inlet Opening					
Skimmer Size	4 in. Unvented	Max. Flow Rate (ft^3/s)	0.28	Actual Time to Drain (days)	1.89
Inlet Opening (%)	30%	Overall Avg. Flow Rate (ft^3/s)	0.22		
Average Flow Rate for Each Day (ft^3/s)					
Day 1	Day 2				
0.24	0.21				

(a) known required basin volume example

Post-Construction Skimmer Sizing Tool: Estimator's Calculator			
Project Name:		Designer:	
Location:		Date:	

Basin Parameters	**User Input**	Basin Parameters (Manual)			**Calculator Output**
Is Required Detention Volume Known?	No	Bottom Width (ft)	40.0	Side Slopes (H:V)	3.0
Basin Depth (ft)		Bottom Length (ft)	50.0	Depth (ft)	10.0
Known Detention Volume (ft^3)		Calculated Detention Volume (ft^3)	59,000		
Desired Time to Drain (days)	2.0				
Final Detention Volume (ft^3)	59,000				

Recommended Skimmer and Inlet Opening					
Skimmer Size	4 in. Unvented	Max. Flow Rate (ft^3/s)	0.40	Actual Time to Drain (days)	1.74
Inlet Opening (%)	50%	Overall Avg. Flow Rate (ft^3/s)	0.33		
Average Flow Rate for Each Day (ft^3/s)					
Day 1	Day 2				
0.40	0.28				

(b) unknown required basin volume example

Figure 2.38 Post-Construction Estimator's Calculator Sizing Tool

The procedure for the post-construction basin estimator's calculator is the same as the sediment basin equivalent. One additional step that the user must take is inputting the depth of the detention basin if the basin volume is known. Basin depth, regardless of whether basin volume was known or unknown, was used to determine the actual number of days it will take the skimmer to dewater. After all basin parameters have been entered, the tool provides the recommended skimmer size and inlet opening. The tool has been programmed to select the skimmer and inlet sizes based on the flow rate calculated from the basin volume and time to dewater. The tool will select the skimmer with the next lowest average flow rate. In addition, the tool will supply the maximum flow rate, average flow rate, and actual time to drain the basin based on the selected skimmer. Finally, the average flow rate for each day is provided to give the user an idea of how the skimmer performs across the total time to drain the basin.

2.6 Floating Surface Skimmer Testing Summary

This chapter outlined the methodology and results of the evaluation of floating surface skimmers designed for sediment basins and post-construction detention basins. A total of 58 skimmer configurations were assessed, resulting in 174 tests across all testing. Flow rate models for each skimmer configuration were developed using different modeling methods to best fit the corresponding datasets. These models were used to predict flow rates at depths under 7 ft (2.13 m).

For all sediment basin skimmers, the plots depicting flow rate as a function of depth were divided into two approximate linear sections: Zone 1 and Zone 2. Linear trendlines from the Zone 2 section were used as the basis of the flow rate models. Average flow rates were also calculated using the Zone 2 linear section. The sediment basin skimmers were found to have average flow rates ranging as high as 92,585 ft^3/d (2,622 m^3/d) on the 8 in. (20.3 cm) skimmer set to 100% open to as low as 981 ft^3/d (28 m^3/d) on the 1.5 in. (3.8 cm) skimmer set to 50% open.

Flow rate-depth trends for the post-construction skimmers did not consistently exhibit two approximately linear sections across all tested configurations. While some configurations featured the two linear section trend, others showed three linear section trends or a plateau at greater depths, with a gradual transition in flow behavior as depth decreases. To create a model for different flow behaviors and to determine a more robust method for predicting flow behavior, three model types were used to fit the datasets based on their trends: a two-section segmented regression model, a three-section segmented regression model, and a Hill-type saturated function model. One of the primary objectives of post-construction skimmer testing was to determine the maximum flow rate of each prototype configuration. Furthermore, the maximum observed flow rates ranged as high as 2.984 ft^3/s (0.085 m^3/s) on the 8 in. (20.3 cm) skimmer, 100% open, unvented configuration, to as low as 0.045 ft^3/s (0.001 m^3/s) on the 1.5 in. (3.8 cm) skimmer, 50% open.

Two design tools, an engineer's calculator and an estimator's calculator, were developed for the sediment basin skimmers and the post-construction skimmers using the flow rate models developed using the experimental datasets. The engineer's calculator is designed to show the stage-storage relationship as the skimmer dewaters a sediment basin or post-construction detention basin. The estimator's calculator provides skimmer information such as size, inlet opening, and corresponding flow rate information, based on basin geometry and time.

Overall, experimental testing provides manufacturers and designers with pragmatic results on skimmer performance and flow rates. The methodology used throughout testing is repeatable for other skimmer prototypes to determine flow rates. Additionally, there is opportunity for the sizing tools to be expanded with future testing of other skimmer prototypes.

Chapter 3 Roadside Channel Stabilization Measures

3.1 Introduction

There are a wide variety of stabilization measures available to protect roadside conveyance systems from erosive forces. Selecting an appropriate channel stabilization practice depends on factors such as channel geometry and local hydrologic conditions, as well as permissible velocity, permissible shear stress, and right-of-way constraints (Kilgore and Cotton 2005). This chapter outlines past research on roadside channel design and effective stabilization measures that can be implemented in roadside channels throughout rural areas, and the development of a design tool that provides recommendations for channel stabilization measures based on hydrologic parameters and channel characteristics.

3.2 Design of Roadside Channels

When considering the design of roadside conveyance systems, there must be a conventional standard that provides a framework for universally applicable design practices. Hydraulic Engineering Circular No. 15, entitled "*Design of Roadside Channels with Flexible Linings"* (HEC-15), is the leading source of roadside channel design and protection. Design guidance in this manual serves as the basis for several state Department of Transportation (DOT) standards, including those of the Alabama Department of Transportation (ALDOT). The channel design concepts discussed in HEC-15 are based on the maximum permissible tractive force method for flexible channel linings (Kilgore and Cotton 2005). This method considers open-channel flow concepts, along with the shear stress acting on the channel lining to evaluate how effective a given channel lining is at withstanding erosion. This method can be divided into two parts: determining the flow conditions of a given design and determining the required level of erosion protection.

3.2.1 Flow Conditions and Design Parameters

Open-channel flow conditions are functions of channel geometry, flow characteristics, design discharge, channel roughness, channel slope, and channel alignment. The flow of the channel should be assumed to be steady and uniform. Uniform and steady flow indicates that the depth and discharge within the channel remain constant along the length of the channel (Kilgore and Cotton 2005). The channel roughness is dependent on the type of lining chosen. In Alabama, roadside channels should be designed for a 10-year, 24-hour storm event for roads that are not considered interstate systems or arterials with full access control (Alabama Department of Transportation 2022). In addition, ALDOT standards require that roadside conveyance systems have trapezoidal or triangular cross-sectional geometries. Roadside channels must align parallel to the roadway and be situated within the right-of-way limits of the roadway. The minimum grade of all channels must be maintained at 0.5%, except for concrete-lined channels, where it may decrease to 0.3% (Alabama Department of Transportation 2022). Soil type must also be taken into consideration, as different soils have varying degrees of erodibility. Soil characteristics as they relate to channel stabilization design selection will be discussed later in this chapter.

3.2.2 Determining Degree of Erosion Protection

Tractive force is the applied hydrodynamic force of the flow of water within a channel (Schall et al. 2008). When designing a stable channel with uniform flow, the critical shear stress of the lining must exceed the tractive force exerted by the flow. Shear stress acting in a channel can be determined in two ways: mean boundary shear stress and maximum shear stress (Kilgore and Cotton 2005). The mean boundary shear stress is the average shear stress acting on the wetted perimeter of the channel, while the maximum shear stress is the shear stress at the maximum hydraulic depth in a straight channel with uniform flow. The maximum shear stress calculation method is a more conservative approach than the mean boundary shear stress method, but it is commonly used for design purposes. Maximum shear stress can be computed using Equation 3.1:

$$\tau_d = \gamma d S_o \qquad \text{Equation 3.1}$$

Where:

τ_d = shear stress at the maximum depth in the channel (lb/ft^2 or N/m^2)

γ = unit weight of water (62.4 lb/ft^3 or 9,810 N/m^3)

d = depth of flow in the channel (ft or m)

S_o = bottom slope of the channel (ft/ft or m/m)

Permissible tractive force is the maximum tractive force a channel may resist without experiencing erosion (Chow 1959). The purpose of a channel lining is to reduce the amount of permissible tractive force acting on subjacent soils, improve hydraulic efficiency, and provide structural stability to underlying soils (Kilgore and Cotton 2005). A channel lining is considered stable if the permissible shear stress for a channel lining is greater than or equal to the shear stress of the channel. Permissible shear stress for a channel liner can be calculated using Equation 3.2:

$$\tau_p \geq SF\tau_d \qquad \text{Equation 3.2}$$

Where:

τ_p = permissible shear stress for channel lining (lb/ft^2 or N/m^2)

SF = safety factor

τ_d = shear stress at the maximum depth in the channel (lb/ft^2 or N/m^2)

The SF must be greater than or equal to 1.0; 1.0 is typically considered the default SF, but the value is ultimately at the designer's discretion (Kilgore and Cotton 2005). Furthermore, the characteristics of soil within a channel are critical to determining its erodibility and, therefore, choosing an optimal channel lining. The shear strength of a soil is influenced by particle size, density, and cohesive strength (Kilgore and Cotton 2005).

3.3 Channel Linings

Channel linings are mechanisms employed to safeguard against erosion. Channel linings tend to fall under two distinct categories: rigid and flexible. Rigid channel linings are permanent and non-erodible; however, movement or displacement of the lining can lead to failure. Flexible channel linings can be temporary or long-term protective measures that adjust to the shape of the channel. Flexible linings are intended to serve as protective mechanisms during transitional periods while vegetation is being established by limiting the shear stress acting on the underlying soil. Selecting an appropriate channel lining is based on site-specific conditions. Rigid linings are particularly beneficial in zones with non-uniform flow conditions or high shear stress. Conversely, flexible linings perform optimally in channels with uniform flow conditions and moderate shear stress (Kilgore and Cotton 2005). In addition, rigid channel linings tend to be more expensive than flexible linings; thus, implementing flexible linings in roadside channels in rural areas may be a more feasible, cost-effective option. There are a wide variety of channel linings, both rigid and flexible, available for implementation, including vegetation, rolled erosion control products (RECPs), geosynthetics, rip rap, and concrete lining.

3.3.1 Bare Channels

Bare slopes can be considered a temporary or transitional lining while vegetation is being established. Leaving soil bare in a channel may be appropriate depending on the climate and certain channel characteristics; the channel must have a mild grade, the soil must be resistant to high shear stress, and flow within the channel must be shallow (Kilgore and Cotton 2005). In addition, the channel must be relatively wide to avoid erosion. Furthermore, channel liners are typically recommended to provide further stabilization and safeguard against erosive forces (Pitt et al. 2020).

3.3.2 Vegetation

Vegetation is an extensively used stabilization measure to protect against flow-induced erosion in channels. Vegetative linings can provide short- or long-term protection, depending on the type of lining used. Using vegetative linings is particularly advantageous as they are typically considered low maintenance, easy to construct, and widely applicable in different areas. Long-term vegetative stabilization typically consists of perennial grass established through permanent seeding and sodding.

3.3.2.1 Grass Lining

Grass-lined channels established through permanent and temporary seeding are among the most commonly employed traditional stabilization practices across the country. Grass linings offer protection against erosion in two ways: grass stems help dissipate the shear force acting at the surface of the lining before reaching the underlying soil, and the grass plant as a whole stabilizes the soil against flow-induced tractive forces (Kilgore and Cotton 2005). Several important parameters regarding plant selection and soil characteristics must be considered when designing grass-lined channels. Furthermore, given that there are several uncertainties and methods of failure when designing grass-lined channels, conservative design criteria and approaches are recommended (Temple et al. 1987). Effective shear stress must be taken into account when designing grass-lined channels; it is the residual stress present at the underlying soil surface that was not dissipated by the channel lining (Kilgore and Cotton 2005; Temple et al. 1987). When determining design parameters for grass-lined channels, three key factors must be considered to ensure stability: geometry, vegetation parameters, and soil parameters (Pitt et al. 2020).

Plant selection depends on several site-specific considerations, such as soil texture, climate, depth of the underlying material, slope, management requirements, and anticipated flow rates (Pitt et al. 2020; Temple et al. 1987). Vegetation parameters for design include the retardance potential and the cover factor of the vegetation. Retardance potential determines the limiting stress of the vegetation and must be calculated. The vegetation cover factor is used to express the degree to which a given vegetative cover can inhibit high velocities and stresses at the soil-water interface, and can be selected from available data (Pitt et al. 2020).

Soil parameters include soil roughness and the allowable effective shear stress. If the shear strength of the soil is less than the effective shear stress acting on the soil, it will erode (Fay et al. 2012). As mentioned earlier, permissible soil shear stress depends on particle size, density, and cohesive strength. Noncohesive soils are considered to have a plasticity index (PI) of less than 10. Noncohesive soils can be coarse- or fine-grained depending on the particle size at which 75% of the material is finer (D_{75}) is greater than or less than 0.05 in. (1.3 mm), respectively. Fine-grained, noncohesive soils have an approximately constant permissible shear stress at 0.02 lb/ft^2 (1.0 N/m^2), while coarse-grained, noncohesive soil permissible shear stress is a function of particle size, and must be calculated or determined from empirical data (Kilgore and Cotton 2005; United States Department of Agriculture 2021). Cohesive soils are considered exclusively fine-grained. Permissible effective shear stress of cohesive soils is a function of the soil's PI and void ratio and can be calculated or determined from empirical data.

While grass-lined channels can be an effective and feasible option for channel stabilization, there are limitations to consider. There is a transitional period between seeding and vegetation establishment, necessitating additional erosion control measures such as erosion control blankets or turf reinforcement mats (TRMs) (Wisconsin Department of Transportation 2012). In addition, grass-lined channels must be properly maintained to ensure adequate protection from erosion. Mowing may be required, and excess sediment may need to be removed. Finally, grass-lined channels cannot withstand high-velocity flows or remain submerged for extended periods, or the vegetation may fail (Iowa Statewide Urban Design & Specifications 2013).

3.3.2.2 Mulching

Mulching is the process of applying plant residue or other loose materials to the soil surface to provide temporary protection while permanent vegetation is established. General design considerations for all mulching applications include the type of cover, channel characteristics, labor and equipment, cost, and whether the mulch will be used alone or with seed (Minnesota Pollution Control Agency 2025). Dry mulch, such as straw, compost, or wood fiber, should be immediately applied after seeding and used on slopes with a horizontal to vertical (H:V) ratio of no greater than 3H:1V (Elzarka et al. 2017). Straw is typically the least expensive option for any type of mulch cover; however, there is a high rate of failure in controlling erosion due to factors such as inadequate cover, slopes that are too steep or long, and insufficient application (Babcock and McLaughlin 2019).

Hydromulch is a hydraulically applied slurry of water, mulch, seed, and fertilizer that is sprayed over slopes. This particular mulching application is useful for channels with steep slopes where it is less feasible to use rolled erosion control products. Additionally, hydromulch requires less seedbed preparation and provides favorable conditions for seed germination, given that there is extra moisture (Oregon Department of Transportation 2023). Hydromulch can be an effective, less labor-intensive option than dry seeding; however, it can be more expensive than dry seeding or mulching. There are a variety of hydromulch products available. When selecting a hydromulch product, functional longevity, slope, curing time, and cost should be considered (Elzarka et al. 2017). Product specifications should be verified with the manufacturer's recommendations before use. It is important to note that hydromulch will fail in concentrated flow conditions, and additional erosion control measures may be necessary for protection. Furthermore, proper application according to manufacturer guidelines is critical to ensuring adequate stabilization.

There are several ways to improve the longevity and effectiveness of mulching to further combat erosive forces, such as the use of crimped straw or using flocculant. One study found that using a crimped straw mulch is comparable to or more effective in protecting soil on 3:1 slopes than a rolled erosion control product (RECP) (Li 2014).

This finding is significant in that straw mulch tends to be much cheaper than RECPs. Another study found that using hydromulch dosed with polyacrylamide (PAM) consistently had the lowest total sediment loss compared to straw mulch and hydromulches without the use of PAM (Babcock and McLaughlin 2013). For a more cost-effective option, however, the study also found that dosing PAM on straw mulch was more effective at reducing sediment loss than dosing hydromulch.

In an intermediate-scale study by Ricks et al. (2020), six treatments consisting of a dry mulch or hydraulically applied mulch were evaluated on 3:1 sloped test boxes. These treatments included crimped conventional straw, tackified conventional straw, wood fiber hydromulch, straw and cotton hydromulch, cotton fiber reinforced matrix hydromulch, and bonded wheat fiber matrix hydromulch. Results indicated that all treatments saw soil loss reduction percentages of 94% or greater compared to the bare soil control. The most effective practice was the bonded wheat fiber matrix (Ricks et al. 2020).

3.3.3 Rolled Erosion Control Products

Rolled erosion control products (RECPs) are fabricated blankets that are rolled onto hillsides or channels to provide temporary or long-term protection against erosive forces and aid in permanent vegetation establishment (Burns et al. 2013). There are three main categories of manufactured RECPs that will be discussed throughout this section: open-weave textiles (OWTs), erosion control blankets (ECBs), and turf reinforcement mats (TRMs). OWTs are temporary, degradable RECPs that are made up of natural or polymer yarns, such as jute or coir. ECBs are also degradable and are typically used for temporary stabilization. ECBs can be made of natural or synthetic materials, such as jute, coir, nylon, or wood fibers. The primary difference between

ECBs and OWTs is that ECBs have a thick, dense matrix compared to OWTs, which have more open area (Erosion Control Technology Council 2020). TRMs are non-degradable and offer long-term or permanent slope protection where there will be limited vegetation establishment. TRMs are typically made up of synthetic materials such as plastic or nylon. RECPs are an effective measure against erosive forces as they provide additional structural stabilization while vegetation establishes (Erosion Control Technology Council 2020). In addition, they offer immediate protection against erosive forces. It is critical that RECPs are installed according to manufacturer guidelines to ensure performance. Installing RECPs typically consists of stapling the liner to the ground and lapping adjacent fabric layers so that water may not run underneath the product (Kilgore and Cotton 2005).

Characteristics of RECPs that influence erosion control performance include density, stiffness, and thickness (Kilgore and Cotton 2005). These factors, along with roughness coefficients and cover factors, should be verified with the manufacturer. In addition, the permissible shear stress of the lining must be considered in the design. Permissible shear stress is found using the subjacent soil properties, as well as RECP properties. ECBs can be used in channels with low flow velocities while vegetation is establishing; TRMs are more useful in channels with high-velocity flows and shear stresses, as well as when vegetation establishment alone offers insufficient protection (Minnesota Pollution Control Agency 2025).

Several studies have been conducted to verify the effectiveness of RECPs. Smith and Bhatia (2009) tested thirteen different types of RECPs using intermediate-scale rainfall simulators to assess effectiveness in reducing soil loss for vegetated and non-vegetated RECPs. Nine ECBs, two OWTs, and two TRMs. Each RECP was tested on a test table with 3:1 slopes. Results indicated that compared to the bare soil control, vegetated RECPs reduced soil loss by an average of 95% or greater. In addition, vegetation improved RECP performance by up 95% of average soil loss reduction. The best performing RECPs were the wood/synthetic ECBs, as they showed the least amount of soil loss (Smith and Bhatia 2009).

Donaldson and Rossetti (2026) evaluated four types of RECPs across four Virginia Department of Transportation project sites. The RECPs were installed on 2:1 slopes with different soil types. Evaluated RECPs include two straw- or coconut-based soil-stabilization blankets, known as EC-2 mats, and two non-degradable plastic mats, known as EC-3 mats. Results indicated that the two EC-2 mats more reliably supported vegetation and thus met the 75% final stabilization requirement faster due to the materials used and soil temperatures.

In a study conducted by the Colorado State University Hydraulics Laboratory, four North American Green TRMs were evaluated to measure the erosion control and vegetative reinforcement capabilities (Nelsen 2005). A large-scale flume was used to assess each TRM at three stages of vegetative establishment in channel linings: unvegetated, 50% vegetated, and fully established. Results from the unvegetated condition and 50% vegetated condition testing indicated that the TRMs could withstand shear stresses with no observed soil loss up to 3.99 lb/ft^2 (191 N/m^2) and 11.99 lb/ft^2 (574 N/m^2), respectively. Fully established vegetative conditions were subjected to short and long-duration flows. Short-duration flows lasted for one hour, while long-duration testing lasted for 10 hours. Results show that TRMs could withstand up to 14.04 lb/ft^2

(672 N/m^2) and 12.03 lb/ft^2 (576 N/m^2) for the short and long duration flows, respectively (Nelsen 2005).

3.3.4 Geosynthetics

Geosynthetics are manufactured synthetic products that are embedded into the ground to provide reinforcement and separation of soils to ultimately minimize erosion (Markiewicz et al. 2024). The term “geosynthetic” encompasses a wide variety of products available, but geotextiles and geogrids are the two that will be discussed in this section. Geotextiles are permeable textile materials, typically made of polymers, and are classified as woven or nonwoven (Chamberlin 1992). Whether a geotextile is woven or nonwoven is dependent on the configuration of the strands that make up the fabric. Geotextiles are known to be effective in reducing erosion by acting as a physical barrier between soil and splash erosion (Bhattacharyya et al. 2010). Geotextiles also provide supplementary protection when used with other erosion and sediment control measures, such as rip rap lining and rock check dams. A geogrid is another type of geosynthetic that is made of flexible material with a grid configuration. Geogrids offer a high tensile strength, which helps stabilize soil on slopes (Chamberlin 1992).

Álvarez-Mozos et al. (2014) performed a large-scale experiment evaluating the effectiveness of different types of geotextiles on steep slopes. The results indicated that geogrids installed on the soil’s surface had the least amount of soil loss compared to other natural and synthetic geotextiles and buried geogrids. Overall, geosynthetics are an effective erosion control practice for channels; however, additional reinforcement may be necessary, and performance is optimal when vegetation is also used.

Song et al. (2021) that conducted small-scale testing on buried geocells. A total of twelve physical models were used to evaluate how rainfall intensity, slope steepness, geocell size, and slope stability influence erosion. Test models with either 1.5:1 or 2:1 slopes were evaluated. Results indicated that found that small geocells are more effective at limiting soil erosion and stabilizing slopes than large geocells. This study also found that geocells placed on gentle slopes performed better than those on steep slopes. Overall, additional reinforcement is needed if geocells are used for erosion control measures (Song et al. 2021).

3.3.5 Riprap

Riprap consists of large, angular stone to stabilize areas experiencing concentrated flows where vegetation may not be suitable (Minnesota Pollution Control Agency 2025; Pitt et al. 2020). Riprap lining is considered a permanent flexible lining where rocks are positioned on a geotextile to form a well-graded mass with minimal voids (Kilgore and Cotton 2005). Rocks used for riprap linings should be hard, durable, angular-shaped, resistant to deterioration from physical or chemical weathering, and free of overburden, shale, and organic material (Wisconsin Department of Transportation 2012). Riprap channels should be designed to accommodate runoff volumes from a 10-year, 24-hour storm event and should not be used in channels where flow velocities exceed 10 ft/s (3.0 m/s) (ASWCC 2022).

There are several different design methods available for designing and sizing rip rap for channel protection; however, ALDOT recommends following design guidance from HEC-23 Volume II, Section 4.2.2 (Alabama Department of Transportation 2022). The primary design parameters for riprap linings, as described in HEC-23, are velocity and depth (Lagasse et al. 2009). The first step in the design process is to calculate the design riprap size for the channel. The equation used to determine the design size is Equation 4.1 in HEC-23, and utilizes various coefficients to consider the safety factor, specific gravity of the stone, bank slope, and bend way character (Lagasse et al. 2009). The authors note that when using Equation 4.1, the longitudinal slope of the channel should be no steeper than 2%. When placing riprap, the stones should have a relatively even thickness layer with minimal protrusion. The layer thickness should not be less than the spherical diameter of the D_{100} stone or 1.5 times the diameter of the D_{50} stone (Lagasse et al. 2009). In addition, the layer thickness should not be less than 1 ft (0.3 m). Once the design size has been determined, a standard size class can be chosen.

3.3.6 Gabion Baskets

Gabion baskets are a modular lining type that consists of riprap enclosed in wire containers, typically made of steel (Kilgore and Cotton 2005). These baskets are connected together and secured to the channel slopes. They can be configured into relatively thin mattresses or boxes. Gabion baskets may be used with an underlying geotextile or granular filtration blanket for filtration. The stability of these systems is reliant on the integrity of the wire, which may fail under conditions with high concentrations of sediment or rocks (Kilgore and Cotton 2005). Drawbacks of using gabion baskets are that they can be expensive and are laborious to construct.

3.3.7 Concrete

Rigid linings are desirable in areas with high shear stress or non-uniform flow conditions. Rigid linings are non-erodible; therefore, any channel shape can be used to convey flow (Kilgore and Cotton 2005). Concrete lining is a rigid lining that can be made of cast-in-place, shotcrete, or precast (Schall et al. 2001). This lining protects against erosive forces by providing a physical barrier between soils and erosive forces. Concrete linings are typically used in channels where flow velocities are greater than 10 ft/s (3.0 m/s) (ASWCC 2022). However, due to the nature of the material, flow velocities within the channel will increase, which can lead to more damage downstream. In addition, insufficient erosion protection measures may cause undermining, causing damage to the foundation and integrity of the channel lining. Concrete lining is also costly in terms of materials used and equipment required for installation. Ultimately, this method of channel stabilization would not be a sustainable practice considering the materials used, the high cost, and the labor needed for installation.

3.3.8 Articulating Concrete Block Mats

Articulating concrete block mats are a type of rigid lining that consists of precast concrete blocks that are tied together using cables or rope. This type of lining should be used in channels experiencing high flow velocities and non-uniform flow conditions (Kilgore and Cotton 2005). Articulating concrete block mats are also used with a geotextile underlay for filtration (Harris County Flood Control District 2001). The benefits of using articulating concrete block mats are that they can be less expensive and more aesthetically pleasing than other types of linings, such as riprap or concrete. Drawbacks of using this type of channel lining are the potential for undermining and subsequent failure if it is not installed properly.

3.3.9 Check Dams

Check dams are temporary structures installed within conveyance channels to minimize the effects of erosion by limiting flow velocities. They are used in channels where vegetation has not yet been established or where lining is not feasible. Check dams can be constructed from a variety of materials such as wattles, silt fence, and rock. General design considerations include height, flow depth, spacing, slopes, and the use of a geotextile underlay (ASWCC 2022). Check dams tend to be less than 3 ft (0.9 m) in height; should have flow depths of less than 1 ft (0.3 m); should be spaced so that the crest of the bottom downstream check dam is at the same elevation as the toe of the upstream check dam; and should be used on no steeper than 2:1 slopes (ASWCC 2022; USEPA 2021b). Check dams are a helpful erosion control measure that should be used in conjunction with other stabilization practices as supplementary protection, but should not be used alone. They require regular maintenance as they are considered a temporary control measure. In addition, vegetation may struggle to establish or perish due to ponded water above check dams (USEPA 2021b).

3.3.9.1 Wattles

Wattles are tubular barriers used for impounding or diverting runoff. Wattles have a wide range of fill materials such as straw, wood chips, excelsior, coir, etc. Wattle performance is influenced by several factors, such as installation, fill material, and encasement material. In a field monitoring study conducted by Schussler et al. (2021), wattles with an excelsior underlay that were secured to the channel using sod staples and nondestructive teepee staking captured 1,158% more sediment than a standard Iowa Department of Transportation installation. In addition to installation practices, the type of fill and the encasement of a wattle impact its effectiveness. Coconut coir and wood chips have been verified to perform favorably across various slopes and flow rates, though synthetic fiber and miscanthus-filled wattles create the most optimal hydraulic conditions (Whitman et al. 2021). A study performed by Clampitt et al. (2023) compared various wattle encasements to observe how different encasements impact impoundment and found that a cotton fabric encasement was found to increase impoundment depths by 30%. Wattles can be a sustainable option when choosing a check dam as they tend to be low in cost, are relatively easy to install, and can be filled with materials that are biodegradable.

3.3.9.2 Silt Fence

Silt fences are impoundment structures that limit flow velocity from sheet flow and trap suspended sediment in runoff. When installed correctly, silt fence ditch checks impound a greater volume of runoff than other commonly used practices due to their height (Donald et al. 2016). In a study conducted by Donald et al. (2016), the most feasible and effective (MFE-I) silt fence ditch check captured over 90% of introduced sediment after longevity testing. Silt fences may also mitigate sediment transport in roadside channels through a tieback or “J-hook” installation; a well-designed, properly installed tieback configuration has been found to reduce up to 90% of solids in discharge (Zech et al. 2008). Silt fences are an effective check dam when installed properly; however, impounded water may interfere with vegetation establishment or negatively impact existing vegetation present in the channel. Additionally, silt fences are commonly made of materials that may not be considered sustainable, such as plastics. Silt fence can also be expensive and more laborious to install than other check dam practices.

3.3.9.3 Rock Check Dams

Rock check dams are another type of impoundment structure that minimizes flow velocity and impounds sediment from runoff using rip rap. Roche et al. (2025) conducted a study that evaluated different design considerations for rock check dams on highway construction sites in Iowa to determine the most efficient and cost-effective design. Out of seven evaluated configurations, the most feasible and effective installation consisted of a rock check dam with a geotextile overlay with dewatering holes that had a reduced width; 63% of sediment upstream of the installation was captured using this modification compared to the standard Iowa DOT installation (Roche et al. 2025). This method is more cost-effective than the current Iowa DOT standard. Like silt fences, rock check dams can be expensive and require more labor than other aforementioned practices.

3.4 Beta Channel Stabilization Design Tool

Using available design guidance, it was determined that a tool would be constructed to provide recommendations for various channel linings based on channel characteristics. There are two primary parts to this design tool: (1) determining peak flow rates and (2) designing an appropriate channel stabilization practice. It should be noted that this design tool is considered a preliminary draft and will be developed further to include additional components such as cost considerations and other stabilization measures.

The first phase of design is to determine the design peak discharge in the channel. The peak discharge page was adopted from Liu (2020) and utilizes the Technical Release 55 (TR-55) method (United States Department of Agriculture 1986). To begin, the user must select their desired system of units, SCS rainfall distribution type, a design storm event, and the rainfall depth. The user will then input the general site considerations. This includes the land cover type, description, hydraulic soil group (HSG), and area. Up to three rows of general site considerations may be used. These considerations, except area, are selected from a dropdown box. Once these parameters have been input, the tool will automatically calculate peak discharge. Figure 3.1 shows the peak discharge design interface with all necessary parameters input.

Drainage Area		*Units:* ***U.S.***
Project Information	**Rainfall Parameters**	
Project:	**SCS Distribution Type:**	Type III
State:	**Design Storm Event:**	2-yr, 24-hr
County:	**Rainfall Depth :**	4.00 in.
Designer:		

Site Characteristics					
Land Cover Type	**Description**	**HSG**	**CN**	**Area**	**Unit**
Open_Space	Fair (grass cover 50% to 75%)	D	84	0.50	*ac*
Woods	Good	C	70	0.60	*ac*
Impervious	-	A	98	1.20	*ac*

Hydrologic Calculations		
Parameter		**Unit**
Total Area	2.30	*ac*
Weighted CN	88	-
Pot. Max. Retention after Runoff, S	1.4	*in.*
Initial Abstraction, I_a	0.3	*in.*
Rainfall Depth, P	4.0	*in.*
Runoff, Q	2.7	*in.*
I_a/P	0.1	-
Rainfall Distribution	Type III	-
Est. Unit Peak Discharge, q_u	645	*$ft^3/s/mi^2/in.$*
Runoff Vol.	**22,514**	***ft^3***
Peak Discharge, Q_P	**6.25**	***ft^3/s***

Figure 3.1 Peak Discharge Design Interface

The second phase of using this design tool is designing the channel armoring. The channel armoring tool, known as "SHEARspread", was adopted from Dr. Michael Perez. This tool utilizes permissible shear stress concepts to indicate if a channel design input by the user is sufficient for implementation. To start, the user must input several values in the "Channel Parameters" section, starting with selecting a system of units. The user has the option to choose U.S. Customary units or SI units; the tool will automatically update to match the unit selection. Next, the desired channel armoring must be chosen from a dropdown list. The current channel armoring options to choose from include none, vegetated, unvegetated TRM, and vegetated TRM. The user will then input the channel slope, bottom width, and left and right side slopes in the

“Channel Parameters” section. A Manning’s roughness coefficient is provided once a channel armoring has been established. In addition, the design flow used is based on the calculated peak discharge that was determined earlier.

Once a channel armoring has been chosen, additional parameters specific to the selection will appear on the right. Regardless of armoring selection, the user must input parameters in the “Unvegetated Channel – No Armoring” section. This was done to ensure that the user selects a soil type and Manning’s roughness for the soil, thereby establishing the allowable shear stress. For any given channel armoring, if the safety factor is greater than 1.0, the design will be considered sufficient and will be denoted by a green check mark. If the safety factor is less than 1.0, a red “X” will appear, and the user should make necessary adjustments. Figure 3.2 shows the channel armoring tool interface if “none” was selected as the channel armoring, with all necessary parameters input. If a vegetative channel armoring is chosen, the user must select a growth form, growth condition, and retardance class. The tool will provide the cover factor, vegetation roughness coefficient, and vegetated Manning’s roughness. Figure 3.3 shows the tool interface for the vegetated channel armoring selection. The vegetated TRM armoring option requires the user to input the vegetation parameters previously mentioned, as well as the TRM allowable shear stress. The tool will yield the vegetated TRM effective shear stress and the vegetated safety factor. Figure 3.4 shows the tool interface with the vegetated TRM selection. Unvegetated TRM armoring requires the user to input the TRM allowable shear stress and Manning’s roughness. The tool will provide the unvegetated TRM effective shear stress and safety factor. Figure 3.5 shows the tool interface with the unvegetated TRM option selected.

Once all parameters have been input by the user, the tool is ready to be run. This is indicated when the border of the button turns from green to red. The tool calculates the properties of the channel: the top width, cross-sectional area, wetted perimeter, hydraulic radius, hydraulic depth, Froude's number, and the flow condition. Additionally, the channel flow parameters are provided by the tool: normal depth, critical depth, velocity, and shear stress. The tool also provides a visual representation of the channel flow characteristics that updates when the tool is run.

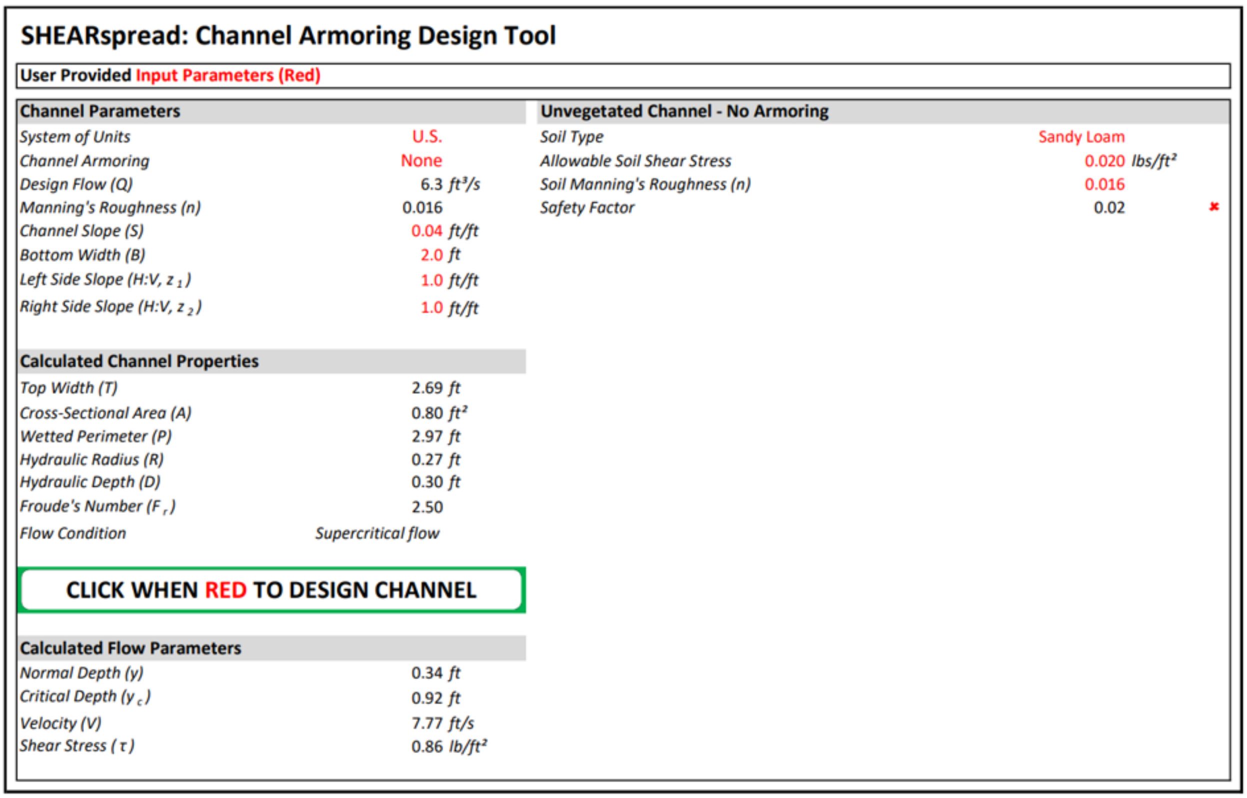

Figure 3.2 Channel Armoring Design: No Armoring

SHEARspread: Channel Armoring Design Tool

User Provided Input Parameters (Red)

Channel Parameters		
System of Units	U.S.	
Channel Armoring	Vegetative	
Design Flow (Q)	6.3	*ft³/s*
Manning's Roughness (n)	0.029	
Channel Slope (S)	0.04	*ft/ft*
Bottom Width (B)	2.0	*ft*
Left Side Slope (H:V, z_1)	1.0	*ft/ft*
Right Side Slope (H:V, z_2)	1.0	*ft/ft*

Calculated Channel Properties		
Top Width (T)	2.97	*ft*
Cross-Sectional Area (A)	1.21	*ft²*
Wetted Perimeter (P)	3.37	*ft*
Hydraulic Radius (R)	0.36	*ft*
Hydraulic Depth (D)	0.41	*ft*
Froude's Number (F_r)	1.43	
Flow Condition	*Supercritical flow*	

CLICK WHEN RED TO DESIGN CHANNEL

Calculated Flow Parameters		
Normal Depth (y)	0.49	*ft*
Critical Depth (y_c)	0.73	*ft*
Velocity (V)	5.17	*ft/s*
Shear Stress (τ)	1.21	*lb/ft²*

Unvegetated Channel - No Armoring		
Soil Type	Sandy Loam	
Allowable Soil Shear Stress	0.020	*lbs/ft²*
Soil Manning's Roughness (n)	0.016	

Vegetative Channel Armoring		
Growth Form	Bunch	
Growth Condition	Poor	
Cover Factor (C_f)	0.41	
Veg. Retardance Class	D	
Veg. Roughness Coefficient (C_n)	0.147	
Veg. Mannings Roughness (n)	0.029	
Effective Shear Stress	0.11	
Safety Factor	0.09	✖

Figure 3.3 Channel Armoring Design: Vegetation Armoring

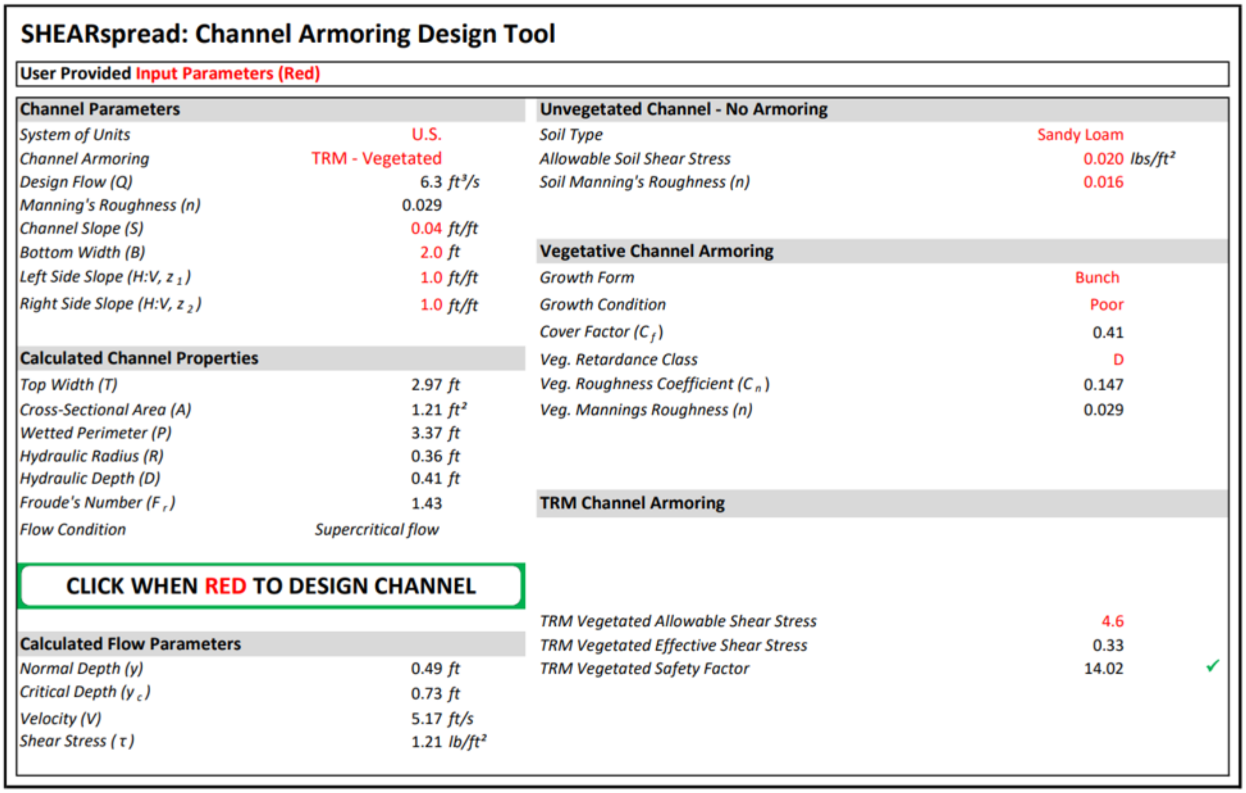

SHEARspread: Channel Armoring Design Tool

User Provided Input Parameters (Red)

Channel Parameters		
System of Units	U.S.	
Channel Armoring	TRM - Vegetated	
Design Flow (Q)	6.3	*ft³/s*
Manning's Roughness (n)	0.029	
Channel Slope (S)	0.04	*ft/ft*
Bottom Width (B)	2.0	*ft*
Left Side Slope (H:V, z_1)	1.0	*ft/ft*
Right Side Slope (H:V, z_2)	1.0	*ft/ft*

Calculated Channel Properties		
Top Width (T)	2.97	*ft*
Cross-Sectional Area (A)	1.21	*ft²*
Wetted Perimeter (P)	3.37	*ft*
Hydraulic Radius (R)	0.36	*ft*
Hydraulic Depth (D)	0.41	*ft*
Froude's Number (F_r)	1.43	
Flow Condition	*Supercritical flow*	

CLICK WHEN RED TO DESIGN CHANNEL

Calculated Flow Parameters		
Normal Depth (y)	0.49	*ft*
Critical Depth (y_c)	0.73	*ft*
Velocity (V)	5.17	*ft/s*
Shear Stress (τ)	1.21	*lb/ft²*

Unvegetated Channel - No Armoring		
Soil Type	Sandy Loam	
Allowable Soil Shear Stress	0.020	*lbs/ft²*
Soil Manning's Roughness (n)	0.016	

Vegetative Channel Armoring	
Growth Form	Bunch
Growth Condition	Poor
Cover Factor (C_f)	0.41
Veg. Retardance Class	D
Veg. Roughness Coefficient (C_n)	0.147
Veg. Mannings Roughness (n)	0.029

TRM Channel Armoring		
TRM Vegetated Allowable Shear Stress	4.6	
TRM Vegetated Effective Shear Stress	0.33	
TRM Vegetated Safety Factor	14.02	✓

Figure 3.4 Channel Armoring Design: TRM-Vegetated Armoring

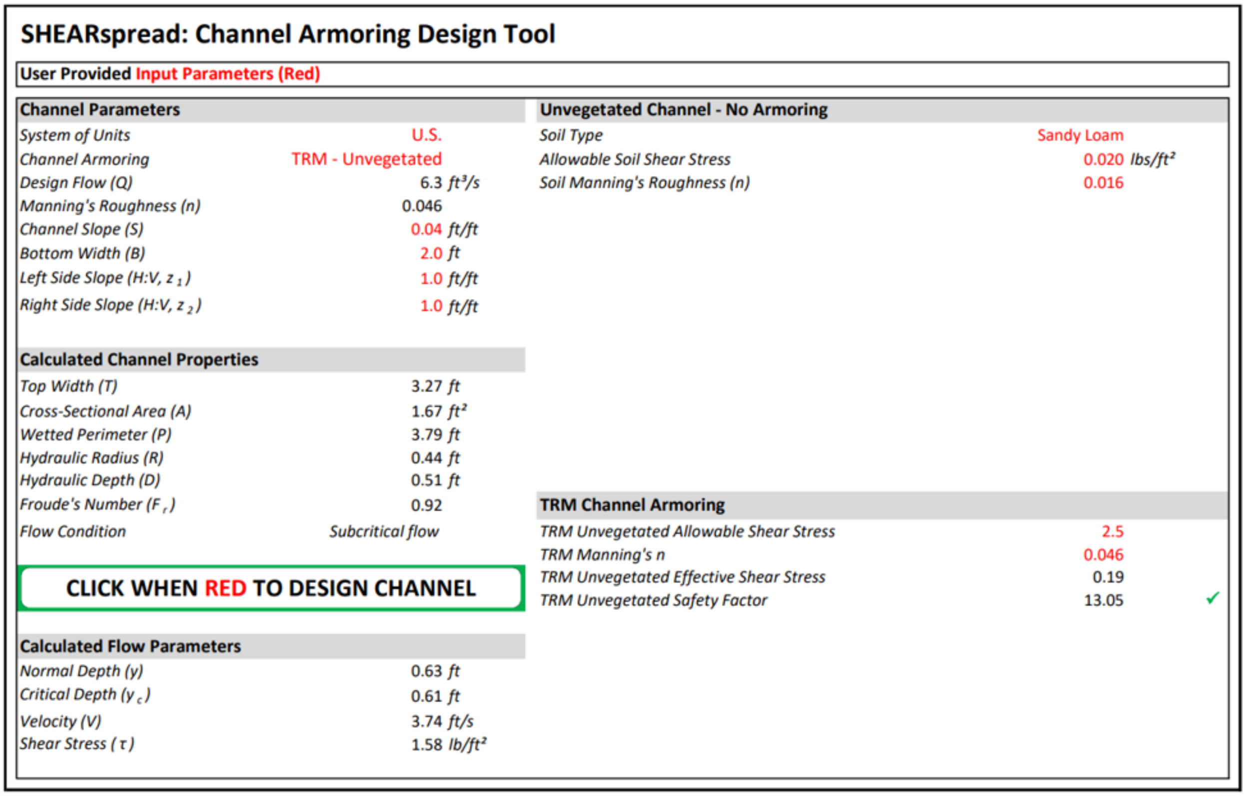

Figure 3.5 Channel Armoring Design: TRM – Unvegetated Armoring

3.5 Summary

This chapter outlines design methods for roadside conveyance channels, as well as various stabilization practices used to protect vulnerable channels from erosion. A comprehensive literature review was conducted to examine various channel stabilization techniques for use on low-volume roads in rural areas in Alabama. Several channel stabilization measures were discussed: bare channels, grass linings, mulch and hydromulch, geosynthetics, rip rap, concrete, and check dams. For each stabilization practice, examples, design considerations, and previous findings were examined.

Using the design concepts investigated throughout the literature review, a preliminary draft of a design tool was developed. The aim of developing this tool was to provide guidance and recommendations to users looking to design stable conveyance channels. The user can determine peak flow following the TR-55 method. Once peak flow has been calculated, the user can determine an appropriate channel armoring measure based on channel geometry, soil type, and available channel stabilization options. The current channel armoring options include bare soil, vegetation, vegetated TRM, and unvegetated TRM. This preliminary version of the tool lays the framework for additional stabilization practices to be added in the future.

The concepts presented in this study will serve as the basis for a field monitoring study aimed at determining the most feasible and effective channel stabilization practices for implementation in rural areas. In addition, a comprehensive cost analysis will be conducted as part of the field monitoring study. Information collected from field monitoring may also be incorporated into the design tool to improve design recommendations. Overall, this chapter lends guidance on design concepts to improve the understanding of different channel stabilization techniques that can be used in areas outside of Alabama.

Chapter 4 Conclusions and Recommendations

4.1 Introduction

Under the USEPA's NPDES program, there must be safeguards in place to protect vulnerable waterbodies from pollutant-laden stormwater runoff. These safeguards include construction ESC practices and post-construction SCMs. With growing urbanization, it is extremely important to effectively implement these stormwater protection measures. The research completed was divided into two sections: evaluating the performance of floating surface skimmers and reviewing roadside channel erosion control practices for implementation in rural areas:

(1) Investigate the performance of floating surface skimmers for use in sediment basins or post-construction detention basins using various configurations.

(2) Outline different erosion control measures for potential implementation in roadside channels in rural areas throughout Alabama.

To accomplish these two objectives, the research plan was divided into the following six tasks:

(1) The completion of a literature review of past research on skimmers as a dewatering mechanism in active and post-construction settings, properly sizing skimmers, and the results of past skimmer performance testing.

(2) Perform controlled testing of sediment basin and post-construction floating surface skimmers across various configurations at AU-SRF.

(3) Create models to predict the flow rate at given depths using experimentally obtained flow rates.

(4) Develop skimmer sizing tools to provide guidance and simplify selecting an appropriate skimmer size for engineers and designers.

(5) Complete a comprehensive literature review on various erosion control measures, as well as their design, that are typically used to protect roadside channels to provide informed decisions for future testing efforts.

(6) Develop a preliminary selection tool that provides guidance on selecting an appropriate stabilization practice for a given channel.

By fulfilling the research objectives through the accomplishment of these six tasks, this study provides valuable insight into the performance capabilities of floating surface skimmers across various configurations, as well as into channel stabilization practices for implementation in rural areas. The results of this study lend guidance to designers, engineers, and manufacturers of floating surface skimmers through repeatable methodologies of analyzing flow rates. In addition, the results of the literature review for roadside channel stabilization provide a foundation for future testing efforts.

4.2 Evaluation of Floating Surface Skimmer Flow Rates

The first objective of this research was to examine the performance of floating surface skimmers designed for active construction and post-construction applications across several configurations. To fulfill this objective, a literature review was conducted on past testing of skimmers in construction and post-construction settings to assess skimmer performance, determine dewatering rates, and evaluate their effectiveness as dewatering mechanisms relative to traditional dewatering practices. This review indicated that, compared to traditional dewatering mechanisms such as perforated riser structures, skimmers are the most effective dewatering mechanism in sediment basins.

In addition, there are several ways to properly size skimmers, which is critical for the required basin retention times. Furthermore, different skimmer designs and inlet configurations exhibit varying hydraulic performance, necessitating experimental testing.

To evaluate the performance of the sediment basin and post-construction skimmers, the skimmer evaluation tank and methodology outlined in Sharpe et al. were used (Sharpe et al. 2023). A total of thirteen skimmers were evaluated, eight sediment basin skimmers and five post-construction skimmers. Three or four orifice openings, using an adjustable slider, were assessed for each sediment basin skimmer, resulting in a total of 29 configurations evaluated across 87 tests. For the post-construction skimmers, a removable plate was used to adjust the inlet size. Additionally, the two largest post-construction skimmers were tested with and without a ventilation pipe to evaluate different flow conditions. A total of 29 configurations were assessed across 87 tests for the post-construction skimmers.

Skimmer performance was examined by plotting experimental flow rates as a function of depth to create models that predict the flow rate at a given depth. Different procedures were followed to model flow rates for the sediment basin skimmers and the post-construction skimmers. All sediment basin skimmers indicated approximately two linear sections and were divided as such to obtain the Zone 2 linear trendline. Conversely, the post-construction skimmer trends fell into three categories. Flow rate models were constructed using a two-section segmented regression model, a three-section segmented regression model, or a Hill-type saturated model to more robustly examine skimmer performance.

For all sediment basin skimmers, average flow rates were also calculated using the Zone 2 linear section. The sediment basin skimmers were found to have average flow rates ranging as high as 92,585 ft^3/d (2,622 m^3/d) on the 8 in. (20.3 cm) skimmer set to 100% open to as low as 981 ft^3/d (28 m^3/d) on the 1.5 in. (3.8 cm) skimmer set to 50% open. One of the primary objectives of post-construction skimmer testing was to determine the maximum flow rate of each prototype configuration. The maximum observed flow rates ranged as high as 2.984 ft^3/s (0.085 m^3/s) on the 8 in. (20.3 cm) skimmer, 100% open, unvented configuration, to as low as 0.045 ft^3/s (0.001 m^3/s) on the 1.5 in. (3.8 cm) skimmer, 50% open.

Following testing, an engineer's calculator and an estimator's calculator were developed for the sediment basin skimmers and the post-construction skimmers using the flow rate models. The engineer's calculator provides the stage-storage relationship as the skimmer dewaters a sediment basin or post-construction detention basin. The estimator's calculator provides skimmer information such as size, inlet opening, and corresponding flow rate information, based on basin geometry and time.

All skimmer configurations were evaluated throughout this study with the aim of assessing performance and determining flow rates. The assessed skimmers were tested in a controlled experimental setting, which may not adequately simulate conditions in a basin, as skimmers also drain while the basin fills with water. An additional limitation is that the location of the adjustable orifice slider used on the sediment basin skimmer and the three smallest post-construction skimmers is no longer located at the center of the inlet when configured. Similarly, it was observed that there were spaces throughout the float of the two largest post-construction skimmers that allowed water to enter the barrel behind the inlet. Thus, the flow of these skimmers was not confined to the inlets. This study also did not evaluate pollutant capture efficacy or evaluate the hydraulic activity at the inlet. One other limitation in this study is the barrel lengths and materials used. If a different barrel configuration is used other than the manufacturer's suggested specifications, the flow rates and corresponding models may be different.

The same testing apparatus and methodology used throughout this research can also be used to assess skimmers designed by other manufacturers. In addition, other inlet configurations can be tested across the evaluated skimmers to gain a better understanding of skimmer performance and to provide further customization to the end user with experimentally validated results.

4.3 Roadside Channel Stabilization Practices

The second objective of this research was to examine different types of erosion controls for use in roadside channels in rural areas in Alabama. In order to accomplish this objective, a comprehensive literature review was completed, outlining the importance of roadside channel stabilization, various stabilization measures used in roadside channels, and key design parameters. In addition, a preliminary design tool was developed to provide recommendations for designers in selecting an appropriate channel stabilization measure based on their individual requirements.

Erosion in roadside channels can degrade road infrastructure, pollute nearby waterways, and increase maintenance costs. Therefore, stabilization is necessary to mitigate its effects. Rural roadways often lack stabilization measures in their adjacent conveyance channels, resulting in severe erosion. This presents a need to examine effective and feasible erosion control measures to implement in these vulnerable channels. When designing erosion control measures for channel stabilization, existing guidance recommends using the permissible tractive force method. This method consists of determining the flow conditions of a given design and determining the required level of erosion protection.

Channel linings fall into two categories: rigid and flexible. Based on the literature, flexible linings are typically preferred over rigid linings as they are easier to install and are more cost-effective. Several different types of channel stabilization measures were outlined: bare channels, grass linings, RECPs, geosynthetics, rip rap, concrete linings, and check dams. Each measure has its own unique design concepts that must be taken into consideration. In addition, previous research was examined for the performance of several practices.

Using the design concepts investigated throughout the literature review, a preliminary draft of a design tool was developed. The goal of this tool was to provide design guidance to users designing stable channels. There are two primary steps of using this tool: determining peak flow and designing a type of channel armoring. Peak flow is computed using the TR-55 method. An appropriate channel armoring measure can then be determined using channel geometry parameters, soil type, and available channel stabilization options. The current channel armoring options include bare soil, vegetation, vegetated TRM, and unvegetated TRM. This preliminary version of the tool lays the framework for additional stabilization practices to be added in the future.

The concepts presented in this study will be used as the basis of a field monitoring study to determine the most feasible and effective channel stabilization practices for implementation in rural areas. In addition, a comprehensive cost analysis will be conducted as part of the field monitoring study. Information collected from field monitoring may also be incorporated into the design tool to improve design recommendations. One primary limitation of this research is the limited number of past studies regarding channelized flow using these stabilization measures. In addition, there are several variations of designing several of the stabilization measures presented throughout this study.

4.4 Expected Benefits and Implementation

The results of floating surface skimmer performance testing provided a deeper understanding of how skimmers and their various configurations behaved across different depths using a repeatable methodology. In addition, the development of the engineer's calculator and the estimator's calculator further simplifies the process of selecting an appropriate skimmer size based on experimental findings. Understanding how skimmers behave and their expected flow rates ultimately improves selection guidance and enhances overall basin functionality. Evaluating the performance of floating surface skimmers provides valuable information to manufacturers, regulatory agencies, contractors, and engineers.

Likewise, the review of past studies and design guidance for roadside channel stabilization provides a foundation for future studies that will ultimately improve the functionality of roadside conveyance channels. The design tool developed for design guidance also simplifies the process of designing a stable channel while allowing for the expansion of different stabilization practices that can be used. This review of roadside channel stabilization practices provides valuable knowledge for future research to further explore effective and feasible options for rural channels, as well as for ALDOT and other regulatory agencies.

4.5 Future Research

All configurations evaluated throughout floating surface skimmer testing aimed to assess various flow rates and hydraulic performance across depths below 7 ft (2.1 m). The methodology used throughout controlled testing conditions can be repeated in the skimmer evaluation tank using other skimmer types and sizes designed by other manufacturers. Testing other types of skimmers will enable further comparisons of performance and flow rates. These comparisons can also be updated in the estimator's calculators and the engineer's calculator to facilitate more accurate skimmer selection. This research did not evaluate skimmer performance with sediment or other pollutant introductions. Future studies may evaluate pollutant removal efficiency using the skimmer evaluation tank at AU-SRF. In addition, full-scale testing may be conducted to determine skimmer flow rates, as well as the pollutant removal of runoff entering a sediment basin or a post-construction detention basin. Another potential future study would be assessing skimmer flow rates across various water temperatures to determine if there is a significant impact on performance due to changes in water viscosity. One other potential future study includes taking a measurement of the depth of the remaining water level after a test to ensure that flow rates decrease to zero, which will reflect in the flow rate-depth models.

The information presented in Chapter 3 will be used in a field monitoring study to evaluate the performance of different channel stabilization measures. A comprehensive cost analysis of each potential practice will also be conducted to determine the feasibility of employing each practice in low-volume roadside conveyance channels in Alabama. Additional stabilization techniques that were not presented in Chapter 3, such as soil biotic amendments, articulated concrete block mats, gabion baskets, or other novel channel stabilization measures, may also be examined using past research and assessed throughout the field monitoring study. The results of the field monitoring study will be used to update the preliminary version of the channel stabilization design tool presented in this study, thereby providing designers with an expanded selection of channel armoring techniques.

4.6 Conclusions

The aim of this research was to contribute to the body of knowledge of floating surface skimmer performance on active construction and post-construction sites, as well as various roadside channel stabilization practices for future analysis and implementation. The controlled testing methodology outlined in Chapter 2 is repeatable for other manufacturers and regulatory agencies. This methodology is also applicable to other skimmer designs and sizes to compare flow rate and hydraulic performance with those evaluated in this research. In addition, engineers and designers can utilize the engineer’s or estimator’s calculator to facilitate proper skimmer sizing using flow rate models derived from experimental results. The outline of existing roadside channel stabilization practices in Chapter 3 aimed to provide a foundation for future field monitoring studies to determine the most feasible and effective practices for application in rural conveyance channels throughout Alabama. Several stabilization measures were defined, and their design concepts were described. These concepts will be used to determine which practices to design for the field monitoring study. Findings from this research can be utilized by ALDOT and other regulatory agencies.

4.7 Acknowledgements

Chapter 2 of this thesis was funded by J.W. Faircloth and Son, Inc. Chapter 3 of this thesis was funded by the Auburn University Highway Research Center. The author is grateful for the support and funding from these organizations.

References

Alabama Department of Transportation. 2022. *Hydraulic Manual*. Montgomery, AL.

Álvarez-Mozos, J., E. Abad, R. Giménez, M. A. Campo, M. Goñi, M. Arive, J. Casalí, J. Díez, and I. Diego. 2014. “Evaluation of Erosion Control Geotextiles on Steep Slopes. Part 1: Effects on Runoff and Soil Loss.” *Catena*, 118: 168–178. Elsevier. https://doi.org/10.1016/j.catena.2013.05.018.

Armstrong, M., M. A. Perez, W. N. Donald, and X. Fang. 2023. *Optimization of Sediment Basin Configurations*. Auburn, AL.

Arnold, C., and J. Gibbons. 1994. *Impacts of Development on Waterways*. Storrs, CT.

ASTM D8107. 2018. *Standard Practice for Determining Sediment Pond Skimmer Flow Rate*. West Conshohocken, PA: ASTM International.

ASWCC. 2022. *Alabama Handbook for Erosion Control, Sediment Control and Stormwater Management on Construction Sites and Urban Areas Volume 1 Developing Plans and Designing Best Management Practices*. Montgomery, AL.

Atlanta Regional Commission. 2016. *Georgia Stormwater Management Manual*. Atlanta, GA.

Babcock, D. L., and R. A. McLaughlin. 2013. “Erosion Control Effectiveness of Straw, Hydromulch, and Polyacrylamide in a Rainfall Simulator.” *Journal of Soil and Water Conservation*, 68 (3): 221–227. https://doi.org/10.2489/jswc.68.3.221.

Babcock, D., and R. McLaughlin. 2019. “Mulch Options for Erosion Control on Construction Sites.” *North Carolina State University Extension Publications*. Accessed July 22, 2025. https://content.ces.ncsu.edu/mulch-options-for-erosion-control-on-construction-sites.

Bhattacharyya, R., T. Smets, M. A. Fullen, J. Poesen, and C. A. Booth. 2010. “Effectiveness of Geotextiles in Reducing Runoff and Soil Loss: A Synthesis.” *Catena*, 81 (3): 184–195. Elsevier B.V. https://doi.org/10.1016/j.catena.2010.03.003.

Burns, S. E., H. Choo, and J. Muk. 2013. *Categorization Of Erosion Control Matting For Slope Applications*. Atlanta, GA.

Chamberlin, R. W. 1992. *Geosynthetics for Erosion Control of Slopes. Local Road Research Board Research Implementation Series Number*. St. Paul, MN.

Clampitt, J. E., M. A. Perez, J. Blake Whitman, W. N. Donald, J. J. LaMondia, and A. J. Craig. 2023. “Hydraulic Evaluation of Wattle Encasement Materials.” *Transportation Research Record*, 2677 (7): 249–264. SAGE Publications Ltd. https://doi.org/10.1177/03611981231152255.

Connecticut Department of Transportation. 2000. *ConnDOT Drainage Manual*. Newington, CT.

Crimmins, A. R., C. W. Avery, D. R. Easterling, K. E. Kunkel, B. C. Stewart, and T. K. Maycock. 2023. *Fifth National Climate Assessment*. Washington, D.C., USA.

Donald, W. N., W. C. Zech, M. A. Perez, and X. Fang. 2016. “Evaluation and Modification of Wire-Backed Nonwoven Geotextile Silt Fence for Use As a Ditch Check.” *Journal of Irrigation and Drainage Engineering*, 142 (2). American Society of Civil Engineers (ASCE). https://doi.org/10.1061/(asce)ir.1943-4774.0000959.

Donaldson, B. M., and M. S. Rossetti. 2026. *Evaluation of Rolled Erosion Control Products and Seed Mixes for Vegetation Establishment on Slopes*. Charlottesville, VA.

Edwards, C. L., R. D. Shannon, and A. R. Jarrett. 1999. “Sedimentation Basin Retention Efficiencies for Sediment, Nitrogen, and Phosphorus from Simulated Agricultural Runoff.” *American Society of Agricultural Engineers*, 42 (2): 403–409. St. Joseph, Michigan.

Elzarka, H., C. Gao, J. Matos, and D. Chakraborty. 2017. *Manual of Temporary Erosion Control Products for Roadside Ditches*. Cincinnati, OH.

Erosion Control Technology Council. 2020. *Fact Sheet: Temporary Rolled Erosion Control Products (RECPs)*.

Fang, X., W. C. Zech, and C. P. Logan. 2015. “Stormwater Field Evaluation and Its Challenges of a Sediment Basin with Skimmer and Baffles at a Highway Construction Site.” *Water (Switzerland)*, 7 (7): 3407–3430. MDPI AG. https://doi.org/10.3390/w7073407.

Fay, L., M. Akin, and X. Shi. 2012. *Cost-Effective and Sustainable Road Slope Stabilization and Erosion Control*. Washington, D.C.

Fennessey, L. A. J., and A. R. Jarrett. 1997. “Influence of Principal Spillway Geometry and Permanent Pool Depth on Sediment Retention of Sedimentation Basins.” *American Society of Agricultural and Biological Engineers*, 40 (1): 53–59.

Harris County Flood Control District. 2001. *Design Manual for Articulating Concrete Block Systems*. Fort Collins, CO.

Hill, A. V. 1910. “The Combinations of Haemoglobin with Oxygen and with Carbon Monoxide. I.” *The Journal of Physiology*, 40: iv–vii.

Hoechst, L. M. 1997. “Evaluating the Effectiveness of the Skimmer Versus the Perforated Riser in Sedimentation Basins.” Master’s Thesis, Virginia Polytechnic Institute and State University.

IECA. 2021. *Temporary Sediment Basin Standard*.

Innovative Applied Sol. 2014. *IAS Water Quality Skimmer for Sediment and Erosion Control Applications*.

Iowa Statewide Urban Design & Specifications. 2013. *Design Manual 7E-23 Grass Channel*. Ames, IA.

Jarrett, A. R. 1993. “Design of Perforated Risers to Control Dewatering of Sedimentation Basins.” *American Society of Agricultural and Biological Engineers*, 9 (1): 37–42. St. Joseph, MI.

Jarrett, A. R. 2001. *Designing Sedimentation Basins for Better Sediment Capture*. *Soil Erosion Research for the 21st Century*. Honolulu, HI: Proceedings of the American Society of Agricultural Engineers International Symposium.

J.W Faircloth & Son Inc., and T. R. Evans. 2024. “Faircloth Skimmer® Discharge System with Embankment.” Hillsborough, NC.

Kelderman, K., A. Phillips, T. Pelton, E. Schaeffer, P. MacGillis-Falcon, and C. Bernhardt. 2022. *The Clean Water Act at 50: Promises Half Kept at the Half-Century Mark*. Washington, D.C.

Kilgore, R., A. T. Atayee, and G. Herrmann. 2024. *Urban Drainage Design: Fourth Edition*. Washington, D.C.

Kilgore, R. T., and G. K. Cotton. 2005. *Design of Roadside Channels with Flexible Linings*. Washington, D.C.

Lagasse, P. F., P. E. Clopper, J. E. Pagán-Ortiz, L. W. Zevenbergen, L. A. Arneson, J. D. Schall, and L. G. Girard. 2009. *Bridge Scour and Stream Instability Countermeasures: Experience, Selection, and Design Guidance-Third Edition*. Washington, D.C.

Li, M. H. 2014. “Evaluating erosion control performance of crimped straw mulch in comparison with RECPs on simulated highway roadsides.” *International Journal of Geotechnical Engineering*, 8 (3): 307–314. Maney Publishing. https://doi.org/10.1179/1939787913Y.0000000036.

Liu, L. 2020. “Design Guidance and Development of Construction Stormwater Technologies.” Dissertation, Auburn University.

Mahler, B. J. 2018. “Sediment-Associated Contaminants.” U.S. Geological Survey: Water Resource Mission Area.

Markiewicz, A., E. Koda, M. Kiraga, G. Wrzesiński, K. Kozanka, M. Naliwajko, and M. D. Vaverková. 2024. “Polymeric Products in Erosion Control Applications: A Review.” *Polymers*. Multidisciplinary Digital Publishing Institute (MDPI).

McCaleb, M. M., and R. A. McLaughlin. 2008. “Sediment Trapping by Five Different Sediment Detention Devices on Construction Sites.” *American Society of Agricultural and Biological Engineers*, 51 (5): 1613–1621.

McLaughlin, R. A., S. A. Hayes, D. L. Clinton, M. S. McCaleb, and G. D. Jennings. 2009. “Water Quality Improvements Using Modified Sediment Control Systems on Construction Sites.” *American Society of Agricultural and Biological Engineers*, 52 (6): 1859–1867.

Millen, J. A., A. R. Jarrett, and J. W. Faircloth. 1997. “Experimental Evaluation of Sedimentation Basin Performance for Alternative Dewatering Systems.” *American Society of Agricultural Engineers*, 40 (4): 1087–1095. https://doi.org/10.13031/2013.21361.

Minnesota Pollution Control Agency. 2025. “Minnesota Stormwater Manual.”

Nelsen, R. J. 2005. “Research Quantifies Performance of TRM Reinforced Vegetation.” In: *Erosion of Soils and Scour of Foundations*, 1–11. Austin, TX.

Oregon Department of Transportation. 2023. *Erosion Control Manual: Guidelines for Developing and Implementing Erosion and Sediment Controls*. Salem, OR.

Osouli, A., M. Grinter, J. Zhou, L. Ahiablame, and T. Stark. 2017. *Effective Post-Construction Best Management Practices (BMPs) to Infiltrate and Retain Stormwater Run-Off*. Edwardsville, IL.

Perez, M. A. 2016. “Improvements in the Design and Application of Erosion and Sediment Control Technologies for the Construction Industry.” Dissertation, Auburn University.

Perez, M. A., and W. N. Donald. 2023. *Faircloth Skimmer AU-SRF Post Construction Detention Pond Performance Test*. Auburn, AL.

Perez, M. A., W. C. Zech, W. N. Donald, and X. Fang. 2016. “SEDspread: Sediment-Basin Design Tool for Construction Sites.” *Journal of Irrigation and Drainage Engineering*, 142 (12). International Erosion Control Association. https://doi.org/10.1061/(ASCE)IR.1943-4774.0001099.

Perez, M., X. Fang, W. C. Zech, and J. Vasconcelos. 2015. *Design and Construction of a Large-Scale Sediment Basin and Preliminary Testing Results*. Auburn, AL.

Pitt, Robert., S. E. Clark, and D. W. Lake. 2020. *Construction Site Erosion and Sediment Controls: Planning, Design, and Performance*. 2nd ed. DEStech Publications, Inc.

Ricks, M. D., W. T. Wilson, W. C. Zech, X. Fang, and W. N. Donald. 2020. "Evaluation of Hydromulches as an Erosion Control Measure Using Laboratory-Scale Experiments." *Water (Switzerland)*, 12 (2). MDPI AG. https://doi.org/10.3390/w12020515.

Roche, B., M. A. Perez, W. N. Donald, and X. Fang. 2025. *Evaluation of Rock Check Dam Performance using Large-Scale Testing Techniques*. Auburn, AL.

Schall, J. D., E. V. Richardson, and J. L. Morris. 2001. *Introduction to Highway Hydraulics*. Washington, D.C.

Schall, J. D., E. V. Richardson, and J. L. Morris. 2008. *Introduction to Highway Hydraulics*. Washington, D.C.

Schussler, J. C., B. Kazaz, M. A. Perez, J. B. Whitman, and B. Cetin. 2021. "Field evaluation of wattle and silt fence ditch checks." *Transportation Research Record*, 2675 (6): 281–293. SAGE Publications Ltd. https://doi.org/10.1177/0361198121992073.

Sharpe, C. D. 2022. "Two-Part Master's Thesis Part One: Evaluation of Cool Roof Reflectivity Impacts Part Two: Surface Skimmer Flow Rates." Auburn University. https://etd.auburn.edu//handle/10415/8222.

Sharpe, C., M. A. Perez, and W. N. Donald. 2023. "Evaluation of Surface Skimmer Flow Rates and Size Selection." *Transportation Research Record*, 2677 (9): 199–211. SAGE Publications Ltd. https://doi.org/10.1177/03611981231158624.

Smith, J. L., and S. K. Bhatia. 2009. "Bioimprovement of Soils for Highway Applications Using Rolled Erosion Control Products." *Transportation Research Record*, 2108 (1): 117–126. National Research Council. https://doi.org/10.3141/2108-13.

Solinst Canada Ltd. 2025. "Solinst Levelogger 5 Series: Model 3001 Data Sheet."

Song, G., S. He, X. Song, Z. Duan, Y. Zhang, D. Kong, and M. Huang. 2021. "The Use of Geocell as Soil Stabilization and Soil Erosion Countermeasures." *Geomatics, Natural Hazards and Risk*, 12 (1): 2155–2169. Taylor and Francis Ltd. https://doi.org/10.1080/19475705.2021.1954555.

Temple, D. M., K. M. Robinson, R. M. Ahring, and A. G. Davis. 1987. *Stability Design of Grass-Lined Open Channels*. Washington, D.C.

Thaxton, C. S., J. Calantoni, and R. A. McLaughlin. 2004. "Hydrodynamic Assessment of Various Types of Baffles in a Sediment Retention Pond." *Transactions of the ASAE*, 47 (3): 741–749.

Travis, Q. B., and L. W. Mays. 2008. "Optimizing Retention Basin Networks." *Journal of Water Resources Planning and Management*, 134 (5). https://doi.org/10.1061/ASCE0733-94962008134:5432.

United States Department of Agriculture. 1986. *Urban Hydrology for Small Watersheds: TR-55*. Washington, D.C.

United States Department of Agriculture. 2012. *Water Quality Degradation - Sediment*. Washington, D.C.

United States Department of Agriculture, S. C. S. 2021. "Chapter 7: Grassed Waterways." *National Engineering Handbook, Part 650*. 2nd ed. Washington, D.C.

United States Federal Highway Administration. 2023. "Highway Statistics Series: Selected Measures For Identifying Peer States." Washington, D.C.

USEPA. 2005. *National Management Measures to Control Nonpoint Source Pollution from Urban Areas*. Washington, D.C.

USEPA. 2007. *Developing Your Stormwater Pollution Prevention Plan*. Washington, D.C.

USEPA. 2021a. *Dry Detention Ponds*. Washington, D.C.

USEPA. 2021b. *Check Dams*. Washington, D.C.

USEPA. 2022. "2022 Construction General Permit – Fact Sheet." Washington D.C.

USEPA. 2023a. *Stormwater Phase II Rule Construction Site Runoff Control Minimum Control Measure*. Washington, D.C.

USEPA. 2023b. *Small MS4 Stormwater Program Overview*. Washington, D.C.

USEPA. 2026a. *Impaired Waters and Stormwater*. Washington, D.C.

USEPA. 2026b. "About NPDES."

USEPA. 2026c. "Stormwater Discharges from Construction Activities."

Vaughan, B. T., and A. R. Jarrett. 2001. *Experimental Evaluation of Alternative Configurations for Floating Riser Sedimentation Basin Dewatering Devices*. *2001 ASAE Annual Meeting*. Sacramento, CA: American Society of Agricultural Engineers.

Whitman, J. B., J. C. Schussler, S. M. Asce, M. A. Perez, A. M. Asce, and L. Liu. 2021. "Hydraulic Performance Evaluation of Wattles Used for Erosion and Sediment Control." https://doi.org/10.1061/(ASCE)IR.1943.

Wisconsin Department of Transportation. 2012. *Facilities Development Manual 13-30-1: Channel Types and Characteristics*. Madison, WI.

Zech, W. C., J. L. Halverson, T. P. Clement, and A. M. Asce. 2008. "Intermediate-Scale Experiments to Evaluate Silt Fence Designs to Control Sediment Discharge from Highway Construction Sites." *ASCE Journal of Hydraulic Engineering*, 13 (6): 497–504. https://doi.org/10.1061/ASCE1084-0699200813:6497.

Zech, W. C., C. P. Logan, and X. Fang. 2014. "State of the Practice: Evaluation of Sediment Basin Design, Construction, Maintenance, and Inspection Procedures." *Practice Periodical on Structural Design and Construction*, 19 (2). American Society of Civil Engineers (ASCE). https://doi.org/10.1061/(asce)sc.1943-5576.0000172.